PROPRIETARY INFORMATION – WITHHOLD UNDER 10 CFR 2.390

Exelon Generation®

200 Exelon Way
Kennett Square, PA 19348

www.exeloncorp.com

10 CFR 50.90

NMP1L3188

February 9, 2018

U.S. Nuclear Regulatory Commission
ATTN: Document Control Desk
Washington, DC 20555-0001

Nine Mile Point Nuclear Station, Unit 1
Renewed Facility Operating License No. DPR-63
NRC Docket No. 50-220

Subject: License Amendment Request - Proposed Change to Remove Boraflex Credit from Spent Fuel Racks

In accordance with 10 CFR 50.90, "Application for amendment of license, construction permit, or early site permit," Exelon Generation Company, LLC (Exelon) requests an amendment to Renewed Facility Operating License No. DPR-63 for Nine Mile Point Nuclear Station, Unit 1 (NMP1). The proposed change would remove the Boraflex credit from the two remaining Boraflex storage racks located in the Spent Fuel Pool (SFP).

The proposed change will eliminate reliance on Boraflex for SFP reactivity control. A new criticality analysis was performed to support the proposed change. NMP1 will install permanent cell blockers in pre-determined spent fuel rack cells that will prevent the placement of spent fuel assemblies within the blocked cells. The cell blockers will be arranged in the spent fuel racks such that an analyzed geometric pattern will be created for the placement of spent fuel assemblies. Therefore, continued performance of the Boraflex Monitoring Program and the License Renewal commitment to enhance the program will no longer be necessary and will terminate with implementation of the approved license amendment.

The following attachments are included in support of the proposed change:

Attachment 1: Evaluation of Proposed Changes

Attachment 2: Markup of Technical Specifications Page

Attachment 3: Holtec International Report No. HI-2178001, Revision 0, "Proprietary LAR for the Criticality Analysis for the Nine Mile Point Unit 1 Boraflex Racks without Boraflex Credit and with Cell Blockers"

Attachment 4: Holtec International Report No. HI-2178001, Revision 0, "Non-Proprietary LAR for the Criticality Analysis for the Nine Mile Point Unit 1 Boraflex Racks without Boraflex Credit and with Cell Blockers"

Attachment 3 transmitted herewith contains Proprietary Information.
When separated from Attachment 3, this document is decontrolled.

Attachment 5: Holtec International Affidavit, "Affidavit to Withhold Proprietary HI-2178001"

The proposed change has been reviewed by the NMP Plant Operations Review Committee in accordance with the requirements of the Exelon Quality Assurance Program.

Exelon requests approval of the proposed amendment by May 31, 2019. Once approved, the amendment shall be implemented during the Spent Fuel Pool Clean-Up Plan scheduled to begin after the 2019 refuel outage.

In accordance with 10 CFR 50.91, "Notice for public comment; State consultation," paragraph (b), Exelon is notifying the State of New York of this application for license amendment by transmitting a copy of this letter and its attachments to the designated State Official.

There are no regulatory commitments contained in this letter.

If you have any questions or require additional information, please contact Ron Reynolds at (610) 765-5247.

I declare under penalty of perjury that the foregoing is true and correct. Executed on the 9th day of February 2018.

Respectfully,

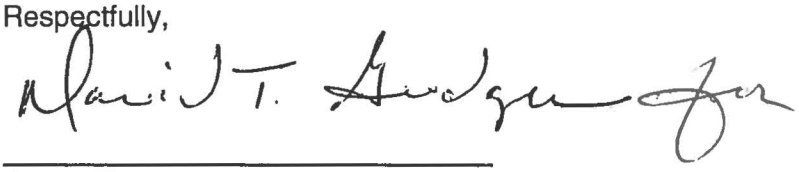

James Barstow
Director - Licensing & Regulatory Affairs
Exelon Generation Company, LLC

Attachment 1: Evaluation of Proposed Changes

Attachment 2: Markup of Technical Specifications Page

Attachment 3: Holtec International Report No. HI-2178001, Revision 0, "Proprietary LAR for the Criticality Analysis for the Nine Mile Point Unit 1 Boraflex Racks without Boraflex Credit and with Cell Blockers"

Attachment 4: Holtec International Report No. HI-2178001, Revision 0, "Non-Proprietary LAR for the Criticality Analysis for the Nine Mile Point Unit 1 Boraflex Racks without Boraflex Credit and with Cell Blockers"

Attachment 5: Holtec International Affidavit, "Affidavit to Withhold Proprietary HI-2178001"

cc:	Regional Administrator - NRC Region I	w/ attachments
	NRC Senior Resident Inspector - NMP	"
	NRC Project Manager, NRR - NMP	"
	A. L. Peterson, NYSERDA	"

ATTACHMENT 1

License Amendment Request

Nine Mile Point Nuclear Station, Unit 1

Docket No. 50-220

EVALUATION OF PROPOSED CHANGES

Subject: Proposed Changes to Remove Boraflex Credit from Spent Fuel Racks

1.0 SUMMARY DESCRIPTION

In accordance with 10 CFR 50.90, "Application for amendment of license, construction permit, or early site permit," Exelon Generation Company, LLC (Exelon) requests an amendment to Renewed Facility Operating License No. DPR-63 for Nine Mile Point Nuclear Station, Unit 1 (NMP1). The proposed change would revise NMP1 Technical Specification (TS) Section 5.5, "Storage of Unirradiated and Spent Fuel," to reflect the current spent fuel storage rack configuration and to eliminate reliance on Boraflex as a neutron absorber in the two remaining Boraflex storage racks located in the southwest portion of the Spent Fuel Pool (SFP). A new criticality analysis was performed to support the proposed change.

Nuclear industry experience has demonstrated that Boraflex material undergoes gamma radiation-induced degradation in the SFP environment (Generic Letter (GL) 96-04 (Reference 1) and GL 2016-01 (Reference 2)). NMP1 has an existing Boraflex Monitoring Program to manage degradation of the Boraflex material in the NMP1 SFP storage racks resulting from radiation exposure and possible water ingress. In its License Renewal Application, NMP1 committed to enhance the Boraflex Monitoring Program to provide reasonable assurance that aging effects will be effectively managed. A summary description of the Boraflex Monitoring Program and the commitment to enhance the program are contained in Appendix C, Section C.1.5, Item 16, to the NMP1 Updated Final Safety Analysis Report (UFSAR) (Reference 3).

2.0 DETAILED DESCRIPTION

2.1 Description of Proposed Change

The proposed change will eliminate reliance on Boraflex for SFP reactivity control. NMP1 will install 108 permanent cell blockers in pre-determined spent fuel rack cells that will prevent the placement of spent fuel assemblies within the blocked cells. The cell blockers will be arranged in the spent fuel racks such that an analyzed geometric pattern will be created for the placement of spent fuel assemblies. Therefore, continued performance of the Boraflex Monitoring Program and the License Renewal commitment to enhance the program will no longer be necessary and will terminate with implementation of the approved license amendment.

The following TS Section 5.5 changes are proposed:

The reference to 1710 spent fuel storage assemblies that can be stored in Boraflex racks in the south half of the SFP is revised to 306 assemblies.

The reference to 1066 spent fuel assemblies with up to 15.6 grams (3.0 weight percent) of Uranium-235 per axial centimeter of assembly that can be stored in non-poison flux trap racks in the north half of the SFP is deleted as these racks were previously removed (Reference 5).

TS Section 5.5 is further revised to state that both types of storage racks will maintain a k_{eff} of less than 0.95 under normal, abnormal and accident conditions.

Attachment 2 contains TS page 346 marked up to show the proposed changes to TS Section 5.5.

2.2 Background

As discussed in UFSAR Section X-J.2.1, there are currently two types of spent fuel storage racks in the SFP: (1) high-density storage racks that use Boral neutron absorbing material; and (2) storage racks that use Boraflex neutron absorbing material. Both types of racks are designed to maintain adequate subcriticality margin (k_{eff} less than 0.95) under all storage conditions.

In License Amendment No. 54 (Reference 4), the NRC approved the installation of Boraflex storage racks in the south half of the SFP. Following installation of the Boraflex racks, the total licensed spent fuel storage pool capacity was 2776 spent fuel assemblies. Specifically, the north half of the SFP contained eight storage racks of the non-poison flux trap (water box) design providing 1066 storage locations, and the south half of the SFP contained eight storage racks fabricated using Boraflex neutron absorbing material providing 1710 storage locations. Detailed analyses and evaluations were performed to demonstrate the acceptability of installing the Boraflex racks. Those analyses and evaluations, summarized in the safety evaluation that accompanied the NRC letter issuing License Amendment No. 54, included the following topical areas: criticality, SFP cooling, materials compatibility, storage rack and SFP structural integrity, installation and heavy load handling, and occupational radiation exposure.

In License Amendment No. 167 (Reference 5), the NRC approved re-racking the SFP with high-density fuel storage racks that use Boral neutron absorbing material. The re-racking was to be accomplished in two phases. In the first phase, the non-poison flux trap storage racks in the north half of the SFP were replaced with Boral storage racks after the 1999 refueling outage. The second phase was to replace the Boraflex racks in the south half of the SFP with Boral storage racks; however, only six of the eight Boraflex storage racks have been replaced. Two Boraflex storage racks remain in the southwest portion of the SFP.

The proposed changes to TS Section 5.5 retain the existing requirements that were based on completely re-racking the SFP with Boral storage racks. Detailed analyses and evaluations were performed to demonstrate the acceptability of installing these high-density storage racks, with a total of 4086 storage locations. Those analyses and evaluations, summarized in the safety evaluation that accompanied the NRC letter issuing License Amendment No. 167, included the following topical areas: criticality, SFP cooling, materials compatibility, storage rack and SFP structural integrity, occupational radiation exposure, solid radioactive waste, and fuel handling accident dose consequences. Also considered were interim configurations that could exist during the re-racking activity.

Replacement of the last two Boraflex racks in the south half of the SFP has been deferred for the foreseeable future. The Boraflex material will remain in place in these two storage racks; however, because nuclear industry experience has demonstrated that the Boraflex material undergoes gamma radiation-induced degradation in the SFP environment, NMP1 proposes to eliminate reliance on Boraflex for reactivity control in those spent fuel storage racks. A new criticality analysis was performed for these two Boraflex racks that do not credit neutron absorption by the Boraflex material. The new criticality analysis provides the technical basis for the proposed changes to TS 5.5. With the elimination of reliance on Boraflex for SFP reactivity control, the Boraflex Monitoring Program and the License Renewal commitment to enhance the program will no longer be necessary and will terminate with implementation of the approved license amendment. Benefits associated with termination of the Boraflex Monitoring Program include: (1) reductions in occupational radiation exposure that would otherwise be incurred during in-situ Boraflex testing and coupon retrieval; and (2) reductions in risk associated with lifting of the work platform (a heavy load) that is currently installed over a portion of the Boraflex spent fuel racks to allow access for in-situ Boraflex testing.

3.0 TECHNICAL EVALUATION

3.1 Criticality Analysis

A new criticality analysis was performed to support the storage of the spent fuel in the two remaining Boraflex racks located in the NMP1 SFP with permanent cell blockers installed in the pre-determined spent fuel rack cells. The criticality analysis (summarized in Attachment 3) demonstrates that, for a fuel assembly with a maximum lattice average enrichment of 4.6 wt% U-235 or less and a maximum k-inf in the Standard Cold Core Geometry (SCCG) for each lattice of 1.31 or less, the effective neutron multiplication factor, k_{eff}, is less than 0.95 with:

1. 108 Permanent[1] cell blockers installed in the pre-determined spent fuel rack cells as shown in Figure 1.1 of Attachment 3;
2. No negative reactivity credit taken for the residual amount of Boraflex;
3. The SFP rack cells loaded with the design basis fuel assembly that bounds any fuel assemblies in the NMP1 SFP;
4. The most limiting moderator temperature condition (100 °C); and
5. No burnup credit (peak reactivity isotopic composition is considered) taken in the analysis.

The permanent cell blockers are summarized in Section 3.2.

The design basis fuel assembly, as determined in Section 2.3.2 of Attachment 3, consists of a design basis lattice that has a uniform enrichment of 4.6 wt% U-235 and some Gadolinium loading that yields a SCCG k-inf conservatively greater than 1.31. The design basis lattice is

[1] "Permanent" means hereby and thereafter that the function of the cell blockers will be maintained at least until the end of the license life of the NMP1 SFP.

developed from the super lattices that are created based on the set of most reactive actual lattices in the NMP1 SFP. The details of the design basis development are included in Section 2.3.2 of Attachment 3.

CASMO-5 and MCNP5 are the computer codes used for the criticality analyses. CASMO-5 was used as the depletion code for the peak reactivity evaluations, i.e., to determine the isotopic composition of the depleted fuel for a given lattice. CASMO-5 is a multigroup two-dimensional transport theory code for burnup calculations of BWR and PWR fuel assemblies. CASMO-5 has been accepted and is currently in use for commercial reactor operations. MCNP5 is a three-dimensional Monte Carlo code and has a long history of successful use in fuel storage criticality analyses. MCNP5 was used with CASMO-5 pin-specific isotopic composition to compute reactivity. Validation and verification of MCNP5 were discussed in Section 2.2.2 of Attachment 3 and documented in Holtec International Report No HI-2104790, Revision 3, "Nuclear Group Computer Code Benchmark Calculations."

Accident conditions, including the maximum SFP temperature condition (100 °C), a dropped fuel assembly, mislocated fuel bundle outside the storage racks and rack movement due to seismic activity, were also evaluated. A misloaded fuel bundle within the storage racks is not a consequential accident since the design basis model evaluates the storage rack locations fully loaded with the most reactive lattices and the permanent cell blockers do not allow a misplaced bundle. The analysis demonstrates that the k_{eff}, is less than 0.95 with a 95% probability at a 95% confidence level for all normal and accident conditions (see Table 7.1 of Attachment 3).

The two remaining Boraflex racks in the NMP1 SFP are located in the southwest corner of the SFP adjacent to the south and west pool walls. The two remaining Boraflex racks are adjacent to the Boral racks to the east and the north. The removal of the Boraflex credit by using cell blockers creates a very low reactivity system. The further detailed technical justification of the interface between Boraflex and Boral racks are included in Supplement 1 of Attachment 3.

NEI 12-16, "Guidance for Performing Criticality Analyses of Fuel Storage at Light-Water-Reactor Power Plants," was reviewed and addressed, as applicable, in the criticality analysis (Attachment 3). The criticality analysis checklist was completed to indicate that the applicable subject areas conform to the guidance in NEI 12-16. The criticality analysis checklist is included in Appendix C of Attachment 3.

3.2 Cell Blockers Design

To ensure that fuel assemblies are not inadvertently placed into the designated unusable location (or unusable cell) in each 2x2 array of storage locations, the unusable cells will be 'blocked' by installing a structure that occupies the space and physically prevents placement of a fuel assembly. These structures are referred to as cell blockers (see Figure 1 for simplified sketch of a cell blocker).

Figure 1

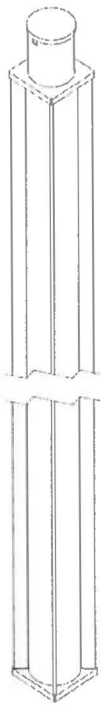

RACK CELL BLOCKER ASSEMBLY

Cell Blocker Functional Requirements:

1. The cell blocker is dimensionally sized to (1) prevent insertion of a fuel assembly in a fuel storage location, (2) fit within a fuel storage rack cell with sufficient clearance on all sides to ensure ease of insertion and the free movement of water into and out of the cell, but without such large clearances that it can be significantly tilted within the cell.

2. The cell blocker is equipped with flow holes on its top and bottom surfaces to permit displacement of air by water during installation in the SFP and to permit the free movement of water through the fuel storage rack cell.

3. The cell blocker has a unique lift lug to provide a means of engaging and handling the cell blocker using a specially designed long-handled tool.

4. The cell blocker length is set such that the lift lug or other handling appurtenance extends above the top of the fuel storage rack so it can be easily engaged by a specially designed long-handled tool. The top of the cell blocker is approximately 2 inches below the top of the fuel assemblies in the SFP racks.

5. The cell blocker is designed (1) to require specialized tools to install in a storage location and (2) so that it cannot be engaged and lifted by the normal fuel handling tool.

6. The cell blocker is equipped with a baseplate that will support its weight on the fuel storage rack baseplate.

7. The cell blocker is equipped with a locking cap feature to prevent inadvertent removal of the blocker from the fuel storage rack. This locking feature prevents the lift lug or other handling appurtenance on the cell blocker from being engaged by a handling tool and thereby operationally resists separation of the blocker and the rack.

8. The cell blocker locking feature is designed such that proper deployment of the feature can be confirmed.

9. The cell blocker is designed such that it will not be dislodged from its intended rack storage cell during normal operating conditions.
10. The cell blocker is designed to support a load which would cause the fuel handling machine underload trip sensor to activate.

Cell Blocker Material Requirements:

1. The cell blocker is fabricated entirely from austenitic stainless steel.
2. All cell blocker materials are supplied in accordance with ASME B&PV Section II or corresponding ASTM specifications.
3. All cell blocker materials are supplied with Certified Material Test Reports (CMTRs).

Structural Criteria:

1. The limiting normal condition for a cell blocker is handling. This condition is evaluated with stress design factors for non-critical lifts from NUREG-0612. A hoist load factor of 0.15 shall be assumed consistent with a low speed lift operation.

   Strength of material evaluations are performed for cell blocker. All NUREG-0612 stress design factors are satisfied for the cell blocker. Thus, it is concluded that the cell blocker meets all the requirements under the normal condition and will remain structurally adequate to support its self-weight during lifting.

2. The limiting upset condition for a cell blocker is a static vertical compressive load onto the top of the cell blocker equal to the load that would cause the fuel handling machine underload trip sensor to activate (700 lb). The acceptance criterion for this evaluation is that no component of the cell blocker shall experience a stress exceeding 80% of the material yield strength.

   Under the upset condition, the static vertical compressive load of 700 lb is assumed to act as a concentrated load on the center of the cell blocker lock-out cap top plate. Strength of material and ANSYS evaluations are performed for the cell blocker. The results from these evaluations show that the stainless steel lock-out cap plate is structurally adequate to support the load and the cell blocker does not experience stresses exceeding 80% of the material yield strength. In addition to the above evaluation, a conservative buckling check of the cell blocker neglecting the stiffener plates, is performed. The results from the buckling evaluation further confirm that the cell blocker under the postulated upset condition is structurally adequate. Thus, it is concluded that the cell blocker meets all the requirements under the upset condition and will remain structurally adequate to support a 700 lb. compressive load.

3. The limiting accident condition for a cell blocker is impact from above by a dropped fuel assembly. This condition is evaluated using the LS-DYNA based finite element impact analysis method used by Holtec in previous spent fuel and dry fuel storage analyses reviewed by NRC. The acceptance criterion for this evaluation is that no portion of the active length of the dropped fuel assembly may be axially-positioned adjacent to any portion of the active length of a fuel assembly stored in any neighboring fuel storage cell.

   LS-DYNA finite element analyses are performed for the postulated fuel assembly drop on to the cell blockers in the NMP1 SFP. The results of the LS-DYNA analyses demonstrate that the maximum vertical deflection of the cell blocker is 3 inches. The maximum deflection is less than the established limit of 13.375 inches. Therefore, under the postulated accident condition, the active length of a dropped fuel assembly will not be axially-positioned adjacent to any portion of active fuel assembly stored in any neighboring storage cell.

4. Rack Qualification:

   The cell blocker weight is significantly lower than the weight of the fuel assembly (approximately 160 lbs. versus approximately 700 lbs.). While the rack base plate cell loading is changed for the cell blocker which does not have a fuel assembly nose piece, the loads on the cell wall are expected to be lower than the loads when the rack cell wall is impacted by the fuel assembly. The loaded weight of the rack with the fuel assemblies and the cell blockers will be much lower than the loaded weight of the rack with fuel assemblies. Therefore, the rack seismic analysis will bound the rack seismic analysis with fuel assemblies and cell blockers. Additionally, the vertical center of gravity of the cell blocker is comparable with that of the fuel assembly, therefore the stability is not a concern. Thus, it is concluded that the stresses in the rack under the loaded weight of fuel assemblies and the cell blockers will remain within the allowable limits, and will be bounded by the rack seismic analysis.

<u>NEI 12-16 Cell Blocker Guidelines:</u>

The cell blocker design satisfies all recommendations proposed in NEI 12-16, Section 6.3.3.4, as reproduced (italicized) below; design adherence is described for each recommendation.

To ensure the maximum benefit and flexibility of these devices, the following criteria are recommended for blocking devices:

- *Physically configured to prevent insertion of a fuel assembly in a fuel storage location*
  - Cell blocker is fabricated from austenitic stainless steel pipes and plates and inserted into the storage cells, creating a physical barrier preventing insertion of a fuel assembly into the occupied cell.

- *Requires specialized tools to install or remove the blocking device from a storage location*
  - The lift point of the cell blocker is designed such that it cannot be engaged by any traditional or readily available tooling on the refuel bridge (i.e. j-hooks, fuel grapples, etc.). Holtec is designing a proprietary specialized handling tool, which will be supplied to NMP1 as the sole instrument possessed by NMP1 capable of engaging and installing/removing the cell blocker.
- *Designed to preclude falling inside a storage location or being dislodged from its position during normal operation*
  - The cell blocker is sized to largely fill the diameter and height of the storage cell such that it will not move or dislodge from its position during normal operation.
- *Contain a lock-in-place feature to prevent inadvertent movement*
  - The cell blocker shall be locked-in-place using a lock-out cap which will be installed over top of the lift point, creating a physical barrier preventing any engagement of the lift point using the specialized handling tool or any other tool.
- *Support a load which will cause the underload trip sensor to activate. This is typically the load of one fuel assembly plus the handling tool*
  - The cell blockers are structurally adequate to support not only the weight of a fuel assembly plus handling tool, but also can withstand accident drops as described below.
- *Allow for continued water flow through the storage cell.*
  - The interior of the cell blocker assembly is not sealed under the proposed design. The flow holes in the base and top plates are sufficient to allow continued flow through the assembly. The lock-out cap has been designed such that water may flow freely through the holes in the top plate, the annulus of the cap, and the flow holes under the cap's top plate. Additionally, the cell blocker plates do not form a seal between cell blocker and cell, and so will allow continued water flow around the cell blocker.
- *Blocking devices do not need to be designed to prevent a dropped fuel assembly from entering the storage cell. However, the accident analysis must consider a single dropped fuel assembly in a storage cell with the blocking device.*
  - The analyses demonstrate that the cell blockers can accept the load of a design basis fuel assembly drop direct hit onto the cell blocker, and will prevent any portion of the active fuel length of the dropped fuel assembly from overlapping any portion of the active fuel length of fuel assemblies in the surrounding rack cells.

4.0 REGULATORY EVALUATION

4.1 Applicable Regulatory Requirements/Criteria

10 CFR 50.68, "Criticality accident requirements," paragraph (b)(4) states that if no credit for soluble boron is taken, the k_{eff} of the spent fuel storage racks loaded with fuel of the maximum fuel assembly reactivity must not exceed 0.95, 95% confidence level, if flooded with unborated water. The cell blocker criticality analysis provided as Attachment 3 to this submittal demonstrate that this requirement is met.

Paragraph (b)(7) of 10 CFR 50.68 states that the maximum nominal U-235 enrichment of the fresh fuel assemblies is limited to 4.6 percent by weight. NMP1 new fuel is below 4.6 percent by weight U-235 enrichment.

Criterion 24, All fuel storage and waste handling systems must be contained if necessary to prevent the accidental release of radioactivity in amounts which could affect the health and safety of the public.

Criterion 25, The fuel handling and storage facilities must be designed to prevent criticality and to maintain adequate shielding and cooling for spent fuel under all anticipated normal and abnormal conditions, and credible accident conditions. Variables upon which health and safety of the public depend must be monitored.

4.2 Precedent

- Peach Bottom Units 2 and 3 (License Amendments 287 and 290, respectively, issued by NRC letter dated May 21, 2013 – TAC No. ME7538 and ME7539). Credit for Boraflex for reactivity control was eliminated. Instead, credit was taken for installation of NETCO-SNAP-IN rack inserts.

- Turkey Point Units 3 and 4 (License Amendment Nos. 234 and 229, respectively, issued by NRC letter dated July 17, 2007 – TAC No. MC9740 and MC9741). Credit for Boraflex for reactivity control was eliminated. Instead, credit was taken for a combination of rod cluster control assemblies, Metamic rack inserts, and administrative controls on fuel loading patterns to maintain required criticality margins.

The NMP1 license amendment request is similar to the above license amendments with regard to eliminating credit for Boraflex for reactivity control, crediting controlled fuel loading patterns, and eliminating the Boraflex monitoring program. The NMP1 request differs from the above license amendments in that NMP1 will incorporate the use of cell blockers to mandate fuel loading patterns in the Boraflex racks in lieu of NETCO-SNAP-IN rack inserts or rod cluster control assemblies and Metamic rack inserts.

4.3 No Significant Hazards Consideration

In accordance with 10 CFR 50.90, "Application for amendment of license, construction permit, or early site permit," Exelon Generation Company, LLC (Exelon) requests an amendment to Renewed Facility Operating License No. DPR-63 for Nine Mile Point Nuclear Station, Unit 1

(NMP1). The proposed changes would reflect the current spent fuel storage rack configuration and would eliminate reliance on Boraflex as a neutron absorber in the two remaining Boraflex storage racks located in the spent fuel storage pool. A new criticality analysis was performed to support the proposed change. The analysis credits existing administrative controls to assure that these two storage racks (re-characterized as non-poison racks) are loaded with fuel of a specified reactivity such that acceptable margins of subcriticality are maintained.

According to 10 CFR 50.92, "Issuance of amendment," paragraph (c), a proposed amendment to an operating license involves no significant hazards consideration if operation of the facility in accordance with the proposed amendment would not:

(1) Involve a significant increase in the probability or consequences of any accident previously evaluated; or

(2) Create the possibility of a new or different kind of accident from any accident previously evaluated; or

(3) Involve a significant reduction in a margin of safety.

Exelon has evaluated the proposed change, using the criteria in 10 CFR 50.92, and has determined that the proposed change does not involve a significant hazards consideration. The following information is provided to support a finding of no significant hazards consideration.

1. Does the proposed change involve a significant increase in the probability or consequences of an accident previously evaluated?

   Response: No.

   The proposed change does not make any change to the systems, structures or components in the Nine Mile Point Unit 1 (NMP1) Spent Fuel Pool (SFP) except for the installation of cell blockers in pre-determined Boraflex rack cells. The change is necessary to ensure that, with continued Boraflex degradation over time, the effective neutron multiplication factor, k_{eff}, is less than 0.95, if the SFP is fully flooded with unborated water. The proposed change does not change the manner in which spent fuel is handled, moved or stored in the storage rack cells. The installation of the cell blockers does not impact the fuel source terms, therefore, there is no adverse radiological impact. The installation of the cell blockers does not change the decay heat and the cell blockers meet the criterion to allow for continued water flow through the storage cell; thus, there is no

   adverse thermal-hydraulic impact. Therefore, the proposed change does not involve a significant increase in the probability or consequences of an accident previously evaluated.

2. Does the proposed change create the possibility of a new or different kind of accident from any accident previously evaluated?

   Response: No.

   Onsite storage of spent fuel assemblies in the NMP1 SFP is a normal activity for which NMP1 has been designed and licensed. As part of assuring that this normal activity can be performed without endangering public health and safety, the ability to safely accommodate different possible accidents in the SFP, such as dropping a fuel bundle or misloading a fuel bundle, have been analyzed. The proposed SFP storage configuration using cell blockers does not change the methods of fuel movement or spent fuel storage. The proposed change of using cell blockers in pre-determined Boraflex rack cells allows for continued use of SFP storage rack cells with degraded Boraflex while assuring the effective neutron multiplication factor, keff, is less than 0.95.

   The proposed use of cell blockers in the pre-determined Boraflex rack cells does not create a possible new or different kind of accident from any accident previously evaluated. The displacement of the SFP water by the cell blockers is small and hence has an insignificant impact on the heat transfer from fuel assemblies to the SFP water, the time-to-boil and boil-off rate in the SFP. The stresses in the storage rack under the loaded weight of fuel assemblies and the cell blockers will remain within the allowable limits and will be bounded by the rack seismic analysis. The accident condition, where a fuel assembly is dropped onto the cell blocker, will not cause loss of the cell blocker function. Therefore, the proposed change does not create the possibility of a new or different kind of accident from any accident previously evaluated.

3. Does the proposed change involve a significant reduction in a margin of safety?

   Response: No.

   The proposed change will maintain, per Attachment 3, the k_{eff} to be less than 0.95 and thus preserve the required safety margin of 5%. The installation of the cell blockers does not impact the fuel source terms and decay heat and hence has no adverse radiological impact. In addition, the radiological consequences of a dropped fuel bundle are unchanged because the event involving a dropped fuel bundle onto a spent fuel storage rack cell containing a cell blocker is bounded by the radiological consequences of a dropped fuel bundle onto a spent fuel storage rack cell containing a stored fuel bundle. Therefore, the proposed change does not involve a significant reduction in a margin of safety.

Based on the above evaluation, Exelon concludes that the proposed amendment presents no significant hazards consideration under the standards set forth in 10 CFR 50.92, paragraph (c), and accordingly, a finding of no significant hazards consideration is justified.

4.4 Conclusion

In conclusion, based on the considerations discussed above, (1) there is reasonable assurance that the health and safety of the public will not be endangered by operation in the proposed manner, (2) such activities will be conducted in compliance with the Commission's regulations, and (3) the issuance of the amendment will not be inimical to the common defense and security or the health and safety of the public.

5.0 ENVIRONMENTAL CONSIDERATION

Exelon has determined that the proposed amendment would change a requirement with respect to installation or use of a facility component located within the restricted area, as defined in 10 CFR 20, "Standards for Protection Against Radiation." However, the proposed amendment does not involve: (i) a significant hazards consideration, (ii) a significant change in the types or significant increase in the amounts of any effluent that may be released offsite, or (iii) a significant increase in individual or cumulative occupational radiation exposure. Accordingly, the proposed amendment meets the eligibility criterion for categorical exclusion set forth in 10 CFR 51.22, "Criterion for categorical exclusion; identification of licensing and regulatory actions eligible for categorical exclusion or otherwise not requiring environmental review," paragraph (c)(9). Therefore, pursuant to 10 CFR 51.22, paragraph (b), no environmental impact statement or environmental assessment needs to be prepared in connection with the proposed amendment.

6.0 REFERENCES

1. Generic Letter 96-04, "Boraflex Degradation in Spent Fuel Pool Storage Racks," dated June 26, 1996

2. Generic Letter 2016-01, "Monitoring of Neutron-Absorbing Materials in Spent Fuel Pools," dated April 7, 2016

3. Nine Mile Point Unit 1 Final Safety Analysis Report (Updated), Revision 25

4. Letter from R. A. Hermann (NRC) to G. K. Rhode (NMPC), dated February 1, 1984, issuing Amendment No. 54 to Facility Operating License No. DPR-63 for the Nine Mile Point Nuclear Station, Unit No. 1

5. Letter from D. S. Hood (NRC) to J. H. Mueller (NMPC), dated June 17, 1999, Issuance of Amendment for Nine Mile Point Nuclear Station, Unit No. 1 to Reflect a Planned Modification to Increase the Storage Capacity of the Spent Fuel Pool (TAC No. MA1945)

ATTACHMENT 2

License Amendment Request

Nine Mile Point Nuclear Station, Unit 1

Docket No. 50-220

MARKUP OF TECHNICAL SPECIFICATIONS PAGE

5.5 Storage of Unirradiated and Spent Fuel

Unirradiated fuel assemblies will normally be stored in critically safe new fuel storage racks in the reactor building storage vault. Even when flooded with water, the resultant k_{eff} is less than 0.95. Fresh fuel may also be stored in shipping containers. The unirradiated fuel storage vault is designed and shall be maintained with a storage capacity limited to no more than 200 fuel assemblies.

1066 spent fuel assemblies with up to 15.6 grams (3.0 weight percent) of Uranium-235 per axial centimeters of assembly can be stored in non-poison flux trap racks in the north half of the spent fuel pool. 1710 spent fuel assemblies with up to 18.13 grams (3.75 weight percent) of Uranium-235 per axial centimeters of assembly can be stored in Boraflex racks in the south half of the pool. These racks have been designed to maintain a k_{eff} less than 0.95 under conditions of optimum water moderation. The north and south half of the pool are analyzed to store 1840 and 2246 fuel assemblies, respectively, using racks containing the neutron absorber material Boral. The Boral racks will maintain a k_{eff} of less than 0.95 under abnormal and accident conditions. The spent fuel stored in the Boral racks must have a peak lattice enrichment of 4.6 % or less and the k-inf in the standard cold core geometry must be less than or equal to 1.31.

5.6 (Deleted)

Replace with insert

Insert

The north and south half of the spent fuel pool is analyzed to store 1840 and 2246 spent fuel assemblies, respectively, in storage racks containing the neutron absorber material Boral. The spent fuel pool is analyzed to store a total of 306 spent fuel assemblies in storage racks containing Boraflex. Both types of storage racks will maintain a k_{eff} of less than 0.95 under normal, abnormal and accident conditions. The spent fuel stored in both types of storage racks must have a peak lattice enrichment of 4.6 % or less and the k-inf in the standard cold core geometry must be less than or equal to 1.31.

ATTACHMENT 4

License Amendment Request

Nine Mile Point Nuclear Station, Unit 1

Docket No. 50-220

Holtec International Report No. HI-2178001, Revision 0,
"Non-Proprietary LAR for the Criticality Analysis for the Nine Mile Point Unit 1
Boraflex Racks without Boraflex Credit and with Cell Blockers."

HOLTEC INTERNATIONAL

Holtec Technology Center, One Holtec Boulevard, Camden, NJ 08104
Telephone (856) 797-0900
Fax (856) 797-0909

NONPROPRIETARY LAR for the Criticality Analysis for the Nine Mile Point Unit 1 Boraflex Racks without Boraflex Credit and with Cell Blockers

FOR

Exelon

Holtec Report No: HI-2178001

Holtec Project No: 2698

Sponsoring Holtec Division: NPD

Report Class : SAFETY RELATED

HOLTEC INTERNATIONAL

DOCUMENT ISSUANCE AND REVISION STATUS[1]

DOCUMENT NAME:	LAR for the Criticality Analysis for the Nine Mile Point Unit 1 Boraflex Racks without Boraflex Credit and with Cell Blockers - Non-Proprietary
DOCUMENT NO.:	HI-2178001
PROJECT NO.:	2698

CATEGORY: ☐ GENERIC ☑ PROJECT SPECIFIC

Rev. No.[2]	Date Approved	Author's Initials	VIR #
0	12/20/2017	B.Brickner	211481

DOCUMENT CATEGORIZATION

In accordance with the Holtec Quality Assurance Manual and associated Holtec Quality Procedures (HQPs), this document is categorized as a:

☐ Calculation Package[3] (Per HQP 3.2)
☑ Technical Report (Per HQP 3.2) (Such as a Licensing Report)
☐ Design Criterion Document (Per HQP 3.4)
☐ Design Specification (Per HQP 3.4)
☐ Other (Specify):

DOCUMENT FORMATTING

The formatting of the contents of this document is in accordance with the instructions of HQP 3.2 or 3.4 except as noted below:

DECLARATION OF PROPRIETARY STATUS

☑ Nonproprietary ☐ Holtec Proprietary ☐ Privileged Intellectual Property (PIP)

Notes

1. This document has been subjected to review, verification and approval process set forth in the Holtec Quality Assurance Procedures Manual. Password controlled signatures of Holtec personnel who participated in the preparation, review, and QA validation of this document are saved on the company"s network. The Validation Identifier Record (VIR) number is a random number that is generated by the computer after the specific revision of this document has undergone the required review and approval process, and the appropriate Holtec personnel have recorded their password-controlled electronic concurrence to the document.

2. A revision to this document will be ordered by the Project Manager and carried out if any of its contents including revisions to references is materially affected during evolution of this project. The determination as to the need for revision will be made by the Project Manager with input from others, as deemed necessary by him.

3. Revisions to this document may be made by adding supplements to the document and replacing the "Table of Contents", this page and the "Revision Log".

Summary of Revisions:

Revision 0: Original Issue

Table of Contents

1. Introduction

This report documents the spent fuel pool (SFP) criticality calculations performed for Exelon for the Nine Mile Point Unit 1 (NMP1) facility BORAFLEX™ racks without BORAFLEX™ credit using cell blockers in a checkerboard configuration (1 of 4 locations is blocked with a cell blocker assumed to be permanently installed). The NMP1 SFP is designed for storage of Boiling Water Reactor (BWR) fuel and contains two distinct fuel storage rack designs: multiple BORAL™ racks and two BORAFLEX™ racks (designated as racks 198 and 216 for the number of storage locations) [1]. The purpose of this analysis is to qualify the two BORAFLEX™ storage racks with the same Technical Specification (TS) requirements as the BORAL™ racks while also removing the credit for BORAFLEX™. The criticality safety analysis is performed such that the effective neutron multiplication factor (k_{eff}) in the BORAFLEX™ racks while fully loaded (one of four locations blocked with a cell blocker) with fuel of the highest anticipated reactivity, at a temperature corresponding to the highest reactivity, is less than 0.95 with a 95% probability at a 95% confidence level. Reactivity effects of abnormal and accident conditions are also evaluated to assure that under all credible abnormal and accident conditions, the reactivity will not exceed the regulatory limit.

The NMP1 SFP currently has the following two relevant TS requirements [2]:

- Each lattice must have a Standard Cold Core Geometry (SCCG) reactivity less than or equal to 1.31.
- Each lattice must have an initial maximum planar average enrichment (IMPAE) less than 4.6 wt% U-235.

The basis of the methodology for the two TS requirements is [3] and [4]. Based on the analysis in [3] and [4], all fuel bundle lattices that are shown to meet these two relevant TS requirements are also shown to meet the regulatory requirement of $k_{eff} < 0.95$ when stored in the BORAL™ racks. The criticality safety evaluations documented in this analysis will also show that all fuel bundle lattices to be stored in the BORAFLEX™ storage racks with cell blockers (credit for BORAFLEX™ removed) meet the two TS requirements and the regulatory requirement of $k_{eff} < 0.95$.

As a result of this analysis, criticality control in the BWR BORAFLEX™ storage racks DOES rely on the following:

- Cell blockers installed in a fixed configuration (see Figure 1.1).
- SCCG limit of $k_{inf} \leq 1.31$.
- IMPAE less than 4.6 wt% U-235.

Criticality control in the BWR BORAFLEX™ storage racks DOES NOT rely on:

- Residual amount of BORAFLEX™.

- Burnup (peak reactivity isotopic compositions are considered).

2. Methodology

2.1 General Approach

The analysis is performed in a manner such that the results are below the regulatory limit of $k_{eff} < 0.95$ with a 95% probability at a 95% confidence level. The calculations are performed using either the worst case bounding approach or the statistical analysis approach with respect to the various calculation parameters. The approach considered for each parameter is discussed further below.

2.2 Computer Codes and Cross Section Libraries

2.2.1 MCNP

MCNP5-1.51 [5] is used for the criticality analyses. MCNP is a three-dimensional Monte Carlo code developed at the Los Alamos National Laboratory. MCNP was selected because it has a long history of successful use in fuel storage criticality analyses and has all of the necessary features for the analysis to be performed for NMP1. MCNP calculations use continuous energy cross-section data predominantly based on ENDF/B-VII [6]. The default ENDF/B-VII cross sections are adjusted for temperature dependence using the appropriate continuous energy cross-section data processed with NJOY 99.396 code [7, 8].

The convergence of a Monte Carlo criticality problem is sensitive to the following parameters: (1) number of histories per cycle, (2) the number of cycles skipped before averaging, (3) the total number of cycles and (4) the initial source distribution. [Proprietary data removed].The initial source is specified over the fueled regions (assemblies) and confirmed to converge. It is a well-known fact [9] that k_{eff} (eigenvalue), which is an integral quantity, converges much faster than the fission source spatial distribution (eigenfunction). However, a convergence of the spatial source distribution is important for estimating local quantities, such as pin power. To assist users in assessing the convergence of the fission source spatial distribution, MCNP5 computes a quantity called the Shannon entropy of the fission source distribution, H_{src} [5]. The Shannon entropy convergence has been checked for each calculation.

2.2.2 MCNP Validation

Benchmarking of MCNP for criticality calculations is documented in [10]. The benchmarking is based on the guidance in [11], and includes calculations for a total of 562 critical experiments with fresh UO_2 fuel, fresh MOX fuel, and fuel with simulated actinide composition of spent fuel (HTC experiments [10]). The benchmarking area of applicability is presented in Table 2.1. The results of the benchmarking calculations for the full set of all 562 experiments are presented in Table 2.2 along with trending analysis. The statistical treatment used to determine those values considered

the variance of the population about the mean and used appropriate confidence factors and trend analysis.

Trend analyses are also performed in [10], and the significant trends determined for various subsets and parameters are presented in Table 2.2. In order to determine the maximum bias that is applicable to the calculations in this report, the trend equations from [10] are evaluated for the specific parameters of the current analyses in Table 2.3. The results presented in Table 2.3 show the maximum bias and bias uncertainty associated with the benchmark subsets. This maximum bias and bias uncertainty is applied to all analysis calculations that are used to determine k_{eff}.

2.2.3 CASMO-5

CASMO-5 version 2.08.00 [12] with the ENDF/B-VII library is used as the depletion code for the peak reactivity evaluations, i.e. to determine the isotopic composition of the depleted fuel for a given lattice. CASMO-5 version 2.08.00 is a multigroup two-dimensional transport theory code for burnup calculations of BWR and PWR fuel assemblies and is currently in use for commercial reactor operations. It allows modeling of a planar cross section of an individual fuel bundle, including all relevant details such as individual pellet and cladding diameters, locations of guide tubes and instrument tube, and material compositions of all materials. The calculations assume a planar and axially infinite array of fuel assemblies. CASMO-5 requires the fuel and absorber dimensions, the operating parameters, an initial enrichment and a maximum burnup. CASMO-5 performs core depletion calculations and calculates the reactivity of the bundle in both the core configuration and SFP configuration as desired. Depletion isotopic compositions are available both as planar average and as pin specific. Additional functional options exist for Gd rods to provide radial pin depletion differences. Over 700 nuclides are available although not all of these are concurrently available in MCNP. While CASMO-5 allows for SFP reactivity calculations, any studies done with CASMO-5 are for sensitivity or trending purposes only. Thus, CASMO-5 is used directly in the final criticality safety analysis for the determination of isotopic compositions for spent fuel only. The uncertainty associated with the CASMO-5 isotopic compositions for spent fuel is accounted for with a 5% depletion uncertainty [18].

2.3 Analysis Methods

The overall analysis approach is to show by evaluation that each fuel design lattice has a maximum reactivity including all biases and uncertainties of less than the regulatory limit of 0.95. For BWR fuel with Gd, the approach is to evaluate all lattices to determine the most reactive lattice(s). The most reactive lattice(s) is then either used to perform the analysis to show compliance with the regulatory limits or it is used to develop a more reactive super lattice(s) which is then used to perform the analysis to show compliance with the regulatory limits. The methodology to determine the most reactive lattice(s) (and super lattice(s)) is called a peak reactivity methodology (see below). The peak reactivity methodology is how compliance with regulatory requirements is shown. The methodology for future lattice qualification is called a standard cold core geometry (SCCG) methodology. The SCCG methodology does not show compliance with the regulatory limits but is used solely for qualification of future lattices. The SCCG methodology shows that future lattices are bounded by the lattices developed and used in the peak reactivity methodology.

Thus, this current criticality safety analysis approach provides technical justification for how the peak reactivity methodology and the SCCG methodology are related and may be combined to support the TS requirements for storage of fuel in the NMP1 SFP. In this manner, all fuel, both legacy and current fuel design, as well as future lattices within the current fuel design, are qualified for storage in the NMP1 SFP.

2.3.1 Peak Reactivity and SCCG Reactivity

The BWR fuel designs used at the NMP1 Station use Gd as an integral burnable absorber. Initially, the Gd in the fuel lattice holds down the fresh fuel lattice reactivity and then, as core depletion occurs, the Gd begins to burnout until it is essentially fully depleted. The Gd in the fuel rods depletes from the outside to the inside of the rod. As the Gd depletes the reactivity of the fuel lattices increases until it reaches a peak. This peak reactivity is the fuel bundle's most reactive condition and usually occurs at low burnup for lower Gd loading and/or lower numbers of Gd rods and at high burnup for higher Gd loadings and/or a higher number of Gd rods. The burnup at which a lattice with Gd reaches peak reactivity is called the peak reactivity burnup and is dependent on the number of Gd rods and the Gd rod loading. Note that the peak reactivity burnup is not directly related to the fuel assembly average burnup and it should not be directly compared to the fuel assembly average burnup.

Once located in the SFP, the peak reactivity burnup of a lattice is also dependent upon the SFP geometry and neutronic environment.

For the purpose of this analysis the term "peak reactivity" is defined as:

- The peak reactivity is the maximum reactivity of the lattice at its most reactive burnup when located in the SFP storage rack geometry. This is determined by MCNP (using CASMO depletion calculation isotopic compositions which include residual Gd). The peak reactivity is typically called a "k_{calc}" value because the MCNP reactivity is the maximum reactivity used to determine "k_{eff}" to show compliance with the regulatory limits.

The SCCG reactivity is very similar. The SCCG reactivity is defined as:

- The SCCG reactivity is the maximum reactivity at the most reactive burnup of the lattice in an uncontrolled, in-core geometry (i.e. 6 inches pitch) at 20°C. The SCCG reactivity is typically called a "k_{inf}" value because the calculations are performed using an infinite array (i.e. no neutron leakage).

Thus, the SCCG k_{inf} is determined in an in-core configuration while the peak reactivity k_{calc} is determined in a SFP in-rack configuration. Both involve the most reactive state of the depleted lattice.

The SCCG k_{inf} is a fuel vendor characterization of the fuel lattice and is determined using fuel vendor specific codes and methods. Historically, the fuel vendor SCCG k_{inf} has been used by criticality analysis vendors as fuel lattice qualification limits for SFP storage. Typically, some

maximum lattice SCCG k_{inf} value is determined such that the same lattice also meets the in-rack regulatory requirements. The approach includes some bias to account for the fuel vendor codes and criticality analysis vendor codes (and methods) being different. The fuel vendor maximum SCCG k_{inf} (plus the vendor bias) is then used to ensure that all future lattices with a SCCG k_{inf} less than this limit are automatically qualified for storage in the SFP.

While both the fuel vendor and the criticality analysis vendor use depletion codes to determine the most reactive burnup of the lattice, there are specific differences that must be addressed:

- The depletion parameters, or core operating parameters (COP), used in the fuel vendor methodology to determine the most reactive burnup may or may not be the same COP which yield the peak reactivity in the SFP in-rack geometry as determined by the criticality analysis vendor.
    - The reactivity impact of the COP will also vary between fuel designs and within fuel designs for various lattice configurations.
- The criticality analysis vendor determines the bounding (over all COP) peak reactivity used to demonstrate compliance with regulatory requirements while the fuel vendor considers a range of values that may or may not coincide with the criticality analysis vendor's set of bounding COP.
- In order to show compliance with the regulatory requirements that $k_{eff} < 0.95$, the peak reactivity methodology determines the most reactive conditions possible for each lattice and also includes various considerations for uncertainties and biases.
- The SCCG methodology does not consider any considerations for uncertainties or biases, thus is cannot demonstrate compliance with regulatory requirements that $k_{eff} < 0.95$.

The peak reactivity in the storage rack and the k_{inf} in SCCG are two different methodologies which are used for two different purposes. In this criticality safety analysis, the peak reactivity lattice that is used to show compliance with regulatory requirements is also used to show compliance with the TS SCCG k_{inf} limit. This is accomplished by using the same bounding CASMO isotopic compositions for both MCNP calculations (in-rack and SCCG).

2.3.2 Analysis Methodology Using Peak Reactivity and SCCG

There are various fuel design and depletion related parameters which directly impact peak reactivity and therefore should be carefully evaluated for the peak reactivity methodology and SCCG methodology. The fuel design related parameters are related to the complex geometry of the 3D BWR fuel bundle. The 3D BWR fuel bundle is composed of various axial sections (i.e. blankets, full length rods, part length rods, plenum regions etc.) Each axial lattice section along the fuel bundle axial length may have variations of the following design parameters which can impact peak reactivity:

- Variation in fuel rod enrichment.
- Gd rod number, location and loading.
- Normal fuel rods (full length).
- Empty fuel rods (plenum).

- Vanished rods (water).

Additionally, the orientation of the fuel bundle in the core with respect to the control blade as well as the orientation of the fuel bundle in the storage rack with respect to the other fuel assemblies (and their orientation) in the storage rack also impact in-rack reactivity. The SFP geometry and material compositions, the various fuel, rack and storage configurations also have a smaller but not insignificant impact on peak reactivity.

Typically, a spent fuel bundle is characterized by its bundle average burnup (over all lattices or nodes). In the peak reactivity methodology the fuel bundle average burnup is of no concern and is not credited for reactivity control. Rather, the methodology credits the residual Gd and other depletion isotopic compositions at the fuel bundle peak reactivity burnup. While the peak reactivity occurs at some specific *lattice burnup*, the peak reactivity lattice burnup varies from lattice to lattice within a fuel design and at different times for each lattice since burnup is axially dependent. Therefore, independent calculations with MCNP using pin specific compositions are performed for *every lattice* over a range of burnups to determine the peak reactivity burnup for all relevant analysis studies and conditions. Since each lattice is considered at its peak reactivity (and therefore the lattice or nodal burnup at which that occurs), the fuel bundle average burnup or fuel bundle burnup profile is not applicable because the analysis already considers each lattice at its most reactive composition, independent of the fuel bundle average burnup. The peak reactivity methodology is therefore inherently conservative because the actual lattice burnup is at some point determined by the bundle average burnup and the fuel bundle's axial burnup profile and axial void profile. Thus, while it is possible that some nodes along the axial length of the fuel bundle may be at the peak reactivity burnup for that lattice, most if not all nodes are either approaching or have passed the peak reactivity burnup for that lattice. Furthermore, the peak reactivity methodology is inherently conservative because depletion calculations are performed to determine the most reactive set of COP while the actual in-core operation is composed of variations in COP. For example, control blade use is the most dominant COP, along with void fraction. No lattice is likely to experience full control blade insertion while concurrently experiencing maximum void fraction, yet, this combination may yield the most reactive condition for the lattice. Rather, the actual fuel bundle may be controlled for certain periods of reactor operation, but not continuously and the bounding lattice may be the full length rods design, which resides at the lower end of the fuel bundle and experiences much lower void fractions. Thus, the overall methodology has several very significant inherent conservatisms.

The criticality safety analysis combines the peak reactivity methodology and the SCCG methodology in the following manner:

- Evaluation of every lattice in the NMP1 SFP, either by CASMO k_{inf} screening calculations or engineering judgement (i.e. low enriched axial blankets are not considered). Note that screening calculations are simplified versions of the design basis calculations. Where applicable, the phrase "design basis" is used to signify an important attribute of the methodology that is needed for the design basis calculations but not necessarily needed for the screening calculations.
    - Screening calculations consider four sets of COP (see Table 5.6) to determine the set that are among the most reactive.

    - The default CASMO isotopic compositions are used.
    - Zero hours cooling time is considered (i.e. 10^{-6} hours).
    - CASMO depletion calculations consider the only possible control blade orientation in the core.
    - A CASMO k_{inf} is calculated over a range of burnup for both SCCG and in-rack models so that comparisons can be made between the two sets of results with respect to selection of bounding actual lattices.
    - The set of actual lattices that have the highest peak reactivity in either SCCG or in-rack configurations is selected for the design basis analysis.
- Design basis CASMO depletion calculations with the set of most reactive actual lattices from the screening calculations.
    - Design basis CASMO depletion calculations resulting in pin specific isotopic compositions with radial Gd depletion using the RAD card are now considered.
    - Zero hours cooling time is also considered (i.e. 10^{-6} hours).
    - CASMO depletion calculations covering four sets of COP (see Table 5.6) to determine the bounding set of COP (i.e. the set that yields the maximum peak reactivity).
    - CASMO depletion calculations consider the only possible control blade orientation in the core.
    - The CASMO depletion isotopic compositions are obtained in 0.5 GWd/MTU increments. The isotopic compositions from CASMO include the following:
        - Xe-135 is not included.
        - Np-239 is added to any residual Pu-239 (since the half-life of Np-239 is 2.355 days and Np-239 decays to fissile Pu-239 via beta emission).
    - The most reactive set of COP is then determined from:
        - CASMO depletion calculations to determine the isotopic compositions for MCNP.
        - Design basis MCNP in-rack calculations. The MCNP model is a fully loaded rack model (i.e. no empty location).
        - Design basis MCNP SCCG calculations. The MCNP SCCG calculations with the set of most reactive lattices considers the following conditions:
            - Infinite array of the lattice at the in-core pitch.
            - Moderator is at 20 °C (all materials are at the same temperature)
            - No control blades.
        - The bounding set of COP is confirmed to be consistent between the MCNP SCCG and MCNP in-rack calculations.
        - The bounding COP is selected and used for all further analysis calculations.
- Combination of the peak reactivity methodology and the SCCG methodology to allow future lattice qualification under the TS requirement that k_{inf} in the SCCG be less than or equal to 1.31 and also to support the second TS requirement that the maximum allowed lattice average enrichment is 4.6 wt% U-235.
    - Super lattices are developed that are based on the set of most reactive actual lattices. A super lattice is a lattice which is developed from an actual lattice by changing the fuel enrichment and/or Gd loading to increase its reactivity. Thus, super lattices bound actual lattices.
    - For each of the actual bounding lattices a super lattice is developed by:

- The lattice enrichment of each fuel pin is increased to 4.6%.
- Variations on Gd loading are then considered by reducing the loading of the Gd rods in increments of 0.5 wt% Gd.
    - Additional calculations are performed with increments of 0.1 wt% Gd over a smaller range once the bounding Gd loading is determined.
- Design basis CASMO depletion calculations for each of the super lattice variations at the bounding COP.
- MCNP calculations are performed to determine the SCCG k_{inf} for the super lattice variations over the range of Gd loadings considered. From the results the Gd loading which yields a SCCG of 1.31 is interpolated.
- The MCNP SCCG calculations with the super lattice variations considers the following conditions:
    - Infinite array of the lattice at the in-core pitch.
    - Moderator is at 20 °C (all materials are at the same temperature)
    - No control blades.
- MCNP calculations are performed with a 2x2 array model with one location empty (for the cell blocker (empty location)) to determine the peak reactivity burnup for each of the super lattice variations over the range of Gd loadings considered. From the results the k_{calc} is interpolated to the Gd loading which was interpolated from the SCCG results discussed above.
- The results of the design basis rack model MCNP calculations and the results of the SCCG MCNP calculations are used to show the reactivity trend between in-rack and SCCG reactivity for each of the actual lattice and super lattice variations and select the bounding super lattice.
- From this set of calculations and comparisons a final Gd loading is determined (by interpolation) for each of the bounding super lattice such that each super lattice has a SCCG k_{inf} of at least 1.31.
- Confirmation studies are performed using the increments of 0.1 wt% Gd CASMO depletion isotopic compositions discussed above. These confirmation studies are performed to show that the interpolation of the Gd wt% is conservative.
- The final super lattice (i.e. the most reactive super lattice Gd variation which yields a SCCG > 1.31) is then used to perform the criticality safety analysis and show compliance with the regulatory requirement that $k_{eff} < 0.95$ at the 95/95 level.

The methodology described above yields the following results:

- Design basis lattice(s) has a uniform enrichment of 4.6% and some Gd loading that yields a SCCG reactivity conservatively greater than 1.31.
- The design basis super lattice(s) is used to perform the full criticality safety analysis to show compliance with regulatory limits.
- This approach shows that the design basis lattice(s) has a SCCG k_{inf} greater than the TS limit yet has a k_{eff} less than the regulatory limit.

2.3.3 SCCG Methodology Bias

As previously discussed in Section 2.3.1, the fuel vendor SCCG methodology has various differences from the criticality safety analysis vendor's SCCG methodology. For NMP1, the fuel vendor includes a 0.01 bias with the k_{inf} values reported for each lattice [24]. This bias is intended to account for the differences between the fuel vendor SCCG methodology and the criticality safety analysis vendor's SCCG methodology.

2.3.4 Design Basis MCNP Calculations to Determine Maximum k_{eff}

The studies performed in Section 2.3.2 provide the maximum in-rack MCNP reactivity (k_{calc}) for each of the most reactive actual lattices and the developed super lattices. The depletion analysis parameters which directly impact peak reactivity have already been evaluated in the design basis CASMO depletion calculations. The in-rack analysis parameters which impact peak reactivity are evaluated in this section using the design basis MCNP model. The design basis MCNP model includes the following features:

- A 2x2 infinite array of the BORAFLEX™ rack model (see Figure 5.2) except for specific evaluations which require a full rack model.
- All BORAFLEX™ is replaced by water.
- Periodic boundary conditions are considered, thus creating a laterally infinite array.
- The cell blockers cell is full of water (i.e. the cell blocker is not modeled).
- The fuel and storage rack design parameters are nominal values.
- The SFP moderator is at the maximum shown in Table 5.5 (see also Section 2.3.4.1).
- All materials in the model have the same temperature as the SFP moderator.
- The fuel is channeled and cell centered.
- The lattice radial orientation in the storage cell the with respect to the lattice corner which is adjacent to the control blades in the core are the same, i.e. all lattices in the model have the same orientation.

In order to determine the final maximum k_{eff}, additional studies are required to either confirm the design basis model assumptions or to determine the reactivity effect of the following parameters:

- Confirmation study to show the most reactive SFP moderator temperature and density (see Section 2.3.4.1) has been considered.
- Reactivity effect of the presence of the fuel channel or a missing fuel channel in the storage rack. The effect is treated as a bias.
- The most reactive condition related to the radial position (eccentric positioning) of the lattice in the SFP storage rack cell for fuel with and without a channel. These two parameters are treated together because each impacts the other (see Section 2.3.4.2). The effect is treated as a bias and bias uncertainty.
- Reactivity effect of the lattice radial orientation (see Section 2.3.4.3). The effect is treated as a bias and bias uncertainty.

- Reactivity effect of the fuel design and storage rack design manufacturing tolerances (see Section 2.3.4.4). The fuel manufacturing tolerances are treated in both CASMO and MCNP. The effect is treated as an analysis uncertainty.
- Reactivity effect determination of the depletion related fuel geometry changes (see Section 2.3.4.5). The fuel depletion related geometry changes are treated in both CASMO and MCNP. The effect is treated as a bias and bias uncertainty.
- Depletion related uncertainties related to spent fuel isotopic compositions [14], [15] (i.e. the "5% depletion uncertainty", see Section 2.3.4.6). The effect is treated as an analysis uncertainty.
- Reactivity effect determination of the cooling time variations (see Section 2.3.5). The cooling time variations are treated in both CASMO and MCNP. The effect is treated as a bias and bias uncertainty.
- Confirmation studies to show that the COP selected are appropriate by changing one parameter at a time (see Section 2.3.5).
- Evaluation of the fuel vendor SCCG bias to determine if an additional bias is appropriate.

Additional analysis biases that are also considered include:

- MCNP code bias and bias uncertainty from benchmarking (see Section 2.2.2).
- MCNP code calculation uncertainty (2 sigma from design basis calculations, 0.0008).

The reactivity effects of the various studies are evaluated in the following manner:

reactivity effect = delta-k_{calc} + 95/95 uncertainty

where delta-k_{calc} = ($k_{calc2} - k_{calc1}$)

where 95/95 uncertainty = $2 * \sqrt{\sigma_1^2 + \sigma_2^2}$

Each of the studies listed above, as well as the analysis biases and uncertainties, are discussed further in the sub-sections below.

2.3.4.1 Reactivity Effect of Spent Fuel Pool Water Temperature

The criticality analysis should be performed at the most reactive temperature and density [14], [15]. The effects of water temperature on both density and cross section need to be considered. In general, both density and cross section effects are not necessarily the same for all storage rack scenarios, since configurations with strong neutron absorbers typically show a higher reactivity at lower water temperature, while configurations without such neutron absorbers typically show a higher reactivity at a higher water temperature. For the NMP1 SFP BORAFLEX^{TM} storage racks with cell blockers and no credit for the BORAFLEX^{TM}, the maximum reactivity condition therefore is expected to be the maximum SFP water temperature and associated density.

Additionally there may be temperature-dependent cross section effects in MCNP that need to be

considered. The standard cross section temperature in MCNP is 300 K. Cross sections are also available at other temperatures, however not usually at the desired temperature for SFP criticality analysis. MCNP has the ability to automatically adjust the cross sections to the specified temperature when using the TMP card. Additionally, MCNP has the ability to make a molecular energy adjustment for select materials (such as water) by using the S(α,β) card; however, the S(α,β) card is provided for certain fixed temperatures which are not always applicable to SFP criticality analysis. Rather, there are limited temperature options, i.e. 300 K and 350 K, etc. Additionally, MCNP does not have the ability to adjust the S(α,β) card for temperatures as it does for the TMP card discussed above. Therefore, the cross sections and S(α,β) card are adjusted using NJOY [7], [8] and these adjusted cross sections use a temperature that is reasonably close to the SFP specific values. This approach is acceptable because the system is non-poisoned and the reactivity trend is well known.

The NMP1 SFP has the maximum normal water temperature operating range shown in Table 5.5. Temperatures above and below this range are considered accidents.

Studies are performed to demonstrate the reactivity effect of the moderator temperature and density over the range 4.0 °C through 100 °C using temperature adjusted cross sections and S(α,β) cards. The bounding temperature is determined using the same MCNP design basis rack model as discussed in Section 2.3.4 with the bounding lattice(s) determined in Section 2.3.2 with the exception for the variations in temperature, density and cross sections required by the studies.

The following studies are performed for the super lattice(s):

- Case 25: Reference case. Maximum accident temperature of 100 °C (NJOY cross sections are 100 °C). Same model as discussed in Section 2.3.4.
- Case 20: 0.0 °C (NJOY cross sections are at 0.0 °C).
- Case 21: 4.0 °C (NJOY cross sections are at 4.0 °C).
- Case 22: 20.45 °C (NJOY cross sections are at 20.45 °C).
- Case 23: 65.55 °C (NJOY cross sections are at 65.55 °C).
- Case 24: 82.25 °C (NJOY cross sections are at 82.25 °C).

All design basis calculations consider the bounding normal condition moderator temperature and density using temperature adjusted cross sections and S(α,β) cards.

2.3.4.2 Fuel Bundle Eccentric Positioning and Fuel Bundle De-Channeling

The BWR fuel that is loaded in the NMP1 SFP racks may not rest exactly in the center of the storage cell, therefore the potential reactivity effect of this eccentric positioning should be evaluated. The fuel bundle may also be de-channeled and therefore the potential reactivity effect of de-channeling should be evaluated. These two parameters, storage cell eccentric positioning and the fuel bundle de-channeling, may occur simultaneously and may impact the reactivity effect of each other. Therefore the two parameters should be evaluated together. Evaluations are therefore performed to determine the most limiting fuel radial location for fuel with and without a channel.

The bounding configuration is determined using a similar model to the design basis MCNP model discussed in Section 2.3.4 with the bounding lattice(s) determined in Section 2.3.2 with the exception that the model considers a rack array. This rack model is the reference case for the studies in this section.

The following cases with the fuel bundle channel present are analyzed for the super lattice(s):

- Case 10: Every lattice is cell centered (see Figure B.4).
- Case 11: Every lattice is positioned toward the rack center (see Figure B.5).
- Case 12: Every lattice is positioned away from the rack center (see Figure B.6).
- Case 13: Every 2x2 array of lattices within the rack is positioned at their closest approach (see Figure B.7).

The following cases with the fuel bundle channel NOT present are analyzed for the super lattice(s):

- Case 00: Every lattice is cell centered.
- Case 01: Every lattice is positioned toward the rack center.
- Case 02: Every lattice is positioned away from the rack center.
- Case 03: Every 2x2 array of lattices within the rack is positioned at their closest approach.

2.3.4.3 Fuel Bundle Orientation in SFP Rack Cell

As described in Section 2.3.2, fuel assemblies have various radial fuel enrichments and gadolinium distribution. Also, one corner of each fuel bundle is adjacent to the control blade during the depletion in the core. As a result, the fuel depletion is not uniform and therefore one fuel bundle corner may be more reactive than other corners and the fuel bundle orientation in the SFP storage cell may have an impact on reactivity.

Five cases are analyzed to assess the fuel bundle orientation variations and to determine the most limiting fuel orientation in SFP rack cell.

The following cases are considered for the super lattice(s):

- Case 00: Reference case (see Figure B.8).
- Case 01: The control blade corners in each 2x2 array all align (see Figure B.9).
- Case 02: Rotation variation 1 for the control blade corners in each 2x2 array (see Figure B.10).
- Case 03: Rotation variation 2 for the control blade corners in each 2x2 array (see Figure B.11).
- Case 04: Rotation variation 3 for the control blade corners in each 2x2 array (see Figure B.12).

2.3.4.4 Evaluation of the Fuel and Storage Rack Manufacturing Tolerances

The reactivity effect of the various fuel and storage rack manufacturing tolerances are evaluated to determine which parameters are bounding. The calculations are performed with the same design basis MCNP model as discussed in Section 2.3.4 except for the variations in fuel and rack parameters as discussed below. For the fuel bundle parameter evaluations, separate design basis CASMO depletion calculations are performed for each change to include the depletion related impacts of the manufacturing tolerance.

The following BWR fuel tolerances [19] are considered for the super lattice(s):

- Case 00: Nominal dimensions.
- Case 01: Minimum cladding thickness.
- Case 02: Maximum cladding thickness.
- Case 03: Minimum fuel rod pitch.
- Case 04: Maximum fuel rod pitch. This is case is not considered because the fuel vendor data indicates a tolerance of 0.0 inches [19].
- Case 05: Minimum water rod thickness.
- Case 06: Maximum water rod thickness.
- Case 07: Minimum fuel channel thickness.
- Case 08: Maximum fuel channel thickness.
- Case 09: Minimum fuel channel inner diameter.
- Case 10: Maximum fuel channel inner diameter.
- Case 25: Increase pellet density.
- Case 26: Decrease pellet outer diameter.
  Case 27: Increase pellet outer diameter

The following BORAFLEX™ rack manufacturing tolerances [16] are considered for the super lattice(s):

The following tolerances are considered:

- Case 11: Nominal dimensions.
- Case 12: Storage cell north-south inner diameter maximum.
- Case 13: Storage cell west-east inner diameter minimum.
- Case 14: Storage cell west-east inner diameter maximum.
- Case 15: Storage cell wall thickness minimum.
- Case 16: Storage cell wall thickness minimum.
- Case 17: BORAFLEX™ box inner diameter minimum.
- Case 18: BORAFLEX™ box inner diameter maximum.

2.3.4.5 Depletion Related Fuel Bundle Geometry Changes

During irradiation the BWR fuel assembly may experience depletion related fuel geometry changes. The important changes to consider are fuel rod growth and cladding creep, crud buildup, the fuel channel may bow and bulge and the grid straps may grow or shrink. These fuel assembly geometry changes can affect the neutron spectrum during depletion by changing the fuel to moderator ratio. In the spent fuel pool, there are two potential impacts from the depletion related fuel geometry changes: first, the effect during depletion may lead to a different isotopic composition, second, the fuel geometry change itself can also impact reactivity by the change in the fuel to moderator ratio. The effect of these possible fuel geometry changes on the reactivity of the fuel in the SFP are discussed below.

Information related to fuel geometry changes was provided by the GNF2 fuel vendor in [20] for nominal beginning of life conditions (BOL), low exposure conditions (up to about 20 GWd/MTU) and high exposure conditions (up to about 50 GWd/MTU). Information was provided for minimum fuel rod gaps, fuel cladding creep, fuel rod growth, channel bulge and channel bow. No information was provided with respect to grid strap growth or shrinkage. See Table 5.1.

Note that since the peak reactivity for the design basis fuel assembly is well below 20 GWd/MTU, i.e. is between 7.5 and 9.5 GWd/MTU for all super lattices there is no expected significant reactivity impact associated with any minimal fuel geometry changes which occur below that exposure value. However, for conservatism, the values for low exposure we used for the evaluations discussed below.

In the case of the fuel rod gap shrinkage, the bounding value was used in an overly conservative manner for the fuel rod tolerance calculations (see Section 2.3.4.4) by also reducing the water rod size such that the fuel rods did not impinge on the water rods due to the large gap shrinkage. Thus, the effect is vastly overestimated. The result of that calculation, if positive, will be used as a bias for the fuel geometry change.

In the case of the fuel channel effects, the change in the channel bulge is nearly twice that for the channel bow. Since the approach is to modify the channel dimensions along the entire length (an overly conservative approach), the channel bulge dimension is used to account for both impacts.

In the case of the grid strap dimensional changes, information found in [21] indicates that the change in grid strap dimensions is temperature driven during depletion, with the greatest change at end of life (EOL). Since the super lattice(s) peak reactivity burnup is at BOL, and the bounding COP are expected to be minimum temperature conditions, the conclusion can be made that this impact may be neglected.

The following BWR fuel geometry changes [20] are considered for the super lattice(s):

- Case gc: Nominal dimensions.
- Case cc: Fuel rod growth and cladding creep. The creep model considers the pellet to clad gap essentially closed and the clad thinning based on the rod growth provided in Table 5.1. The change in clad thickness and outer diameter is considered in both design basis CASMO calculations and in the design basis MCNP model.
- Case cb: Fuel channel bulging and bowing. The fuel channel model considers the change in

channel thickness along the entire length of the channel. The change in channel thickness provided in Table 5.1is considered in both design basis CASMO calculations and in the design basis MCNP model.

2.3.4.6 Depletion Uncertainty

There is some uncertainty associated with the design basis CASMO depletion calculation isotopic compositions. CASMO is a depletion code which has a long history of use in commercial nuclear depletion calculations, including the version in use for this safety analysis. Thus, it is acceptable to apply a 5% reactivity decrement as an uncertainty [18].

The following depletion uncertainty evaluations are considered for the super lattice(s):

- Case 25: Reference case from Section 2.3.4.1.
- Case duc: The fuel in the model is considered fresh 4.6 wt% with no Gd. A 5% reactivity decrement is taken between the reactivity of this case and Case 25 with the 95/95 uncertainty included.

2.3.5 Additional Studies with Design Basis Model

The following studies are performed with the design basis MCNP model:

- The COP are varied one parameter at a time to show that the bounding value has been selected. These cases require new design basis CASMO depletion calculations. These cases are:
  - Case 01: Same COP as "mnr" variation but with maximum fuel temperature.
  - Case 02: Same COP as "mnr" variation but with maximum moderator temperature.
  - Case 03: Same COP as "mnr" variation but with maximum void fraction.
- Cooling time studies. Variations with cooling times to show that 0 hours (i.e. 0 represents a very small time of 10^{-6} hours which is used) is conservative. These cases require new design basis CASMO depletion calculations. These cases are:
  - Case 01: Cooling time of 48 hours.
  - Case 02: Cooling time of 72 hours.
  - Case 03: Cooling time of 100 hours.
  - Case 04: Cooling time of 500 hours.
- Fuel vendor SCCG comparison. The fuel vendor provided SCCG values for the nine most reactive lattices, according to their own evaluations in SCCG [24]. A comparison is made between the SCCG k_{inf} calculated for the 10a63 lattice (used to create the bounding super lattice) and the fuel vendor supplied SCCG k_{inf} for the same lattice.

2.3.6 Storage Rack Interfaces

The NMP1 SFP contains two BORAFLEX™ storage racks and 14 BORAL™ racks. The two BORAFLEX™ storage racks are positioned in the south half of the pool such that the rack 216 is in the pool's southwest corners adjacent the south and west pool wall and adjacent to BORAL™

rack J2 to the east and BORAFLEX™ rack 198 to the north. The rack 198 is adjacent to the BORAL™ rack J1 to the east, the pool wall to the west, BORAFLEX™ rack 216 to the south and BORAL™ rack G to the north. The gaps between these racks, and between the racks and the SFP walls is presented in Table 5.4.

The removal of the BORAFLEX™ credit by using cell blockers creates a very low reactivity system. The results presented in Appendix B, Table B.3 show that the actual fuel lattices (i.e. not the super lattices) have a reactivity in the BORAFLEX™ racks more than 10% delta-k below the regulatory limit. Thus, the BORAFLEX™ racks cannot impact the reactivity of the BORAL™ racks. To preclude neutron coupling between the BORAFLEX™ racks and the BORAL™ racks from the BORAL™ side, an administrative restriction is imposed to require a row of cell blockers along the interface between the two rack designs. That restriction, along with the BORAL™ neutron absorber between the fuel in the two rack designs, and the reduction in the reactivity from using the lowest temperatures, preclude the need to perform further evaluations of the interface. See also Supplement 1.

2.3.7 Accident Conditions

The credible accidents to be evaluated are:

- The effect of SFP temperature outside the normal range.
- A dropped fuel bundle.
- A misloaded fuel bundle (a fuel bundle in the wrong location within the storage rack).
- A mislocated fuel bundle (a fuel bundle in the wrong location outside the storage rack).
- Rack movement due to seismic activity.

These accident conditions are discussed in detail in the sub-sections below.

2.3.7.1 Temperature and Water Density Effects

The SFP water temperature accident conditions for consideration are the decrease and increase in SFP water temperature below and above the nominal SFP temperature range. The decrease and increase in temperature is evaluated in Section 2.3.4.1.

2.3.7.2 Dropped Bundle – Horizontal

For the case in which a fuel bundle is assumed to be dropped on top of a rack, the fuel bundle will come to rest horizontally on top of the rack if the rack is empty or on top of the fuel bail handles which stick out of the top of the rack. The distance from the dropped bundle which is on top of fuel to the active length of the fuel in the cell is more than 12 inches [19], which is sufficient to preclude neutron coupling (i.e., an effectively infinite separation). Consequently, the horizontal fuel bundle drop accident will not result in a significant increase in reactivity. Furthermore, even if some combination of empty and filled cells resulted in the dropped fuel being closer than 12

inches, the case is bounded by the mislocated accident which aligns the dropped bundle along the entire active length of the fuel in the rack. Therefore, no further evaluations are required.

2.3.7.3 Dropped Bundle – Vertical into a Storage Cell

It is also possible to vertically drop a bundle into a location that might be occupied by another bundle or that might be occupied by a cell blocker. Such a vertical impact would at most cause a small compression of the stored bundle, if present, or result in a small deformation of the baseplate for an empty cell if the cell is empty. The damage to the cell blocker would be minimal [1] and not result in an increase in reactivity.

2.3.7.4 Misloaded Fresh Fuel Bundle

As discussed in Section 1, various cells contain permanent cell blockers. Also, as discussed in Section 4, it is assumed that the cell blockers are designed to withstand a fuel drop accident. Since the design basis model evaluates the storage rack locations fully loaded with the most reactive lattice(s) and the blocked cells do not allow a misplaced bundle, the misload accident is not a credible accident. Additionally, the results of various studies may also be considered to estimate the impact of fuel in a location which should be blocked. For example, the results of the studies presented in Appendix B, Table B.2.

2.3.7.5 Mislocated Fuel Bundle

The two BORAFLEX^{TM} racks are located in the south west corner of the SFP. The gap between the rack and south wall is too small to fit a bundle. The gap between the larger BORAFLEX^{TM} and the west SFP wall is large enough to fit a rack, however, there is a sparger pipe a few inches away from the rack and therefore that gap is also too small. The location where the two BORAFLEX^{TM} racks meet, along the west wall, creates an open location where a bundle could fit. To evaluate the possible reactivity effect of the mislocated fuel bundle accident outside of the BORAFLEX^{TM} racks a new MCNP model is constructed with both BORAFLEX^{TM} racks, with the corresponding rack to rack gap between them, a concrete wall along the south and west (40 inches thick) and water reflectors (12 inches thick) along the east and north. The mislocated fuel bundle is the same fuel as is within the BORAFLEX^{TM} racks.

Note that as discussed in Section 2.3.6, the cell blocker configuration is fixed so that there is a cell blocker in every other location along the interface with the BORAL^{TM} racks. However, for the accident case both configurations are considered, i.e. a cell blocker row along the rack edge and a fully loaded row along the rack edge. In that manner both configurations are covered for the accident conditions.

The following cases are considered:

- Case 010: Reference case. Variation of the reference case consider the same eccentric positions of the fuel within the rack as in Section 2.3.4.2 and variations for cell blocker position (case 011-015).

- Case 110: Mislocated fuel included. Variations consider the cell blocker configuration in Figure 1.1 in conjunction with the same eccentric positions of the fuel within the rack as in Section 2.3.4.2 (cases 110-112) and also a variation of the cell blocker configuration with the no cell blockers along the interface with the BORAL™ racks so that the mislocated fuel is face adjacent to two fuel assemblies while also in conjunction with the same eccentric positioning variations (cases 113-115).

2.3.7.6 Rack Movement

As discussed in Section 2.3.7.5, the two BORAFLEX™ racks are located in the south west corner of the SFP. The gaps between the rack and south wall is fixed [25] and therefore minimum gaps exist. These minimum gaps are presented in Table 5.4.

Note that as discussed in Section 2.3.6, the cell blocker configuration is fixed so that there is a cell blocker in every other location along the interface with the BORAL™ racks. However, for the accident case both configurations are considered, i.e. a cell blocker row along the rack edge and a fully loaded row along the rack edge. In that manner both configurations are covered for the accident conditions.

The following cases are considered:

- Case 010: Reference case. Variation of the reference case consider the same eccentric positions of the fuel within the rack as in Section 2.3.4.2 and variations for cell blocker position (case 011-015).
- Case 400: Rack to wall gap at minimum. Variations consider the same eccentric positions of the fuel within the rack as in Section 2.3.4.2 and variations for cell blocker position (cases 411-415).

2.3.8 Determination of Final k_{eff} Values

The maximum k_{eff} is determined using the following equation:

$$k_{eff} = k_{calc} + \sqrt{\sum \text{uncertainty}^2} + \sum \text{bias}$$

where k_{calc} includes:

- Maximum reactivity normal case k_{calc} or,
- Maximum reactivity accident case.

where uncertainty includes:

- Uncertainty from eccentric position of the fuel bundle in the storage cell and fuel channel presence bias (see Section 2.3.4.2).

- Uncertainty from orientation of the lattice with respect to the other lattices in the rack bias (see Section 2.3.4.3).
- BWR fuel and BORAFLEX^{TM} storage rack manufacturing tolerances (see Section 2.3.4.4).
- Uncertainty from depletion related fuel geometry change bias (see Section 2.3.4.5).
- Depletion uncertainty (see Section 2.3.4.6).
- Cooling time bias uncertainty (see Section 2.3.5).
- MCNP benchmarking bias uncertainty (95% probability at a 95% confidence level).
- MCNP calculations statistics (95% probability at a 95% confidence level, 2σ).

and the bias includes

- Bias from eccentric position of the fuel bundle in the storage cell and fuel channel presence (see Section 2.3.4.2).
- Bias from orientation of the lattice with respect to the other lattices in the rack (see Section 2.3.4.3).
- Depletion related fuel geometry change bias (see Section 2.3.4.5).
- Cooling time bias (see Section 2.3.5).
- MCNP benchmarking bias.
- Administrative bias (1% delta-k).
- SCCG bias (2% delta-k)

The purpose of the 1% administrative margin that may be used to account for minor uncertainties or other items that are not already explicitly covered.

3. Acceptance Criteria

Codes, standard, and regulations or pertinent sections thereof that are applicable to these analyses include the following:

- Code of Federal Regulations, Title 10, Part 50, Appendix A, General Design Criterion 62, "Prevention of Criticality in Fuel Storage and Handling."

- Code of Federal Regulations, Title 10, Part 50, Section 68, "Criticality Accident Requirements"

- USNRC Standard Review Plan, NUREG-0800, Section 9.1.1, Criticality Safety of Fresh and Spent Fuel Storage and Handling, Rev. 3 – March 2007.

- L. Kopp, "Guidance on the Regulatory Requirements for Criticality Analysis of Fuel Storage at Light-Water Reactor Power Plants," NRC Memorandum from L. Kopp to T. Collins, August 19, 1998.

- ANSI ANS-8.17-1984, Criticality Safety Criteria for the Handling, Storage and Transportation of LWR Fuel Outside Reactors.

- USNRC, NUREG/CR-6698, Guide for Validation of Nuclear Criticality Safety Calculational Methodology, January 2001.

- DSS-ISG-2010-01, Revision 0, Staff Guidance Regarding the Nuclear Criticality Safety Analysis for Spent Fuel Pools.

- Guidance for Performing Criticality Analyses of Fuel Storage at Light-Water-Reactor Power Plants, NEI 12-16, latest revision, Nuclear Energy Institute.

Consistent with the requirements in 10CFR50.68(b)(4), the objective of this analysis is to ensure that the effective neutron multiplication factor (k_{eff}) is less than or equal to 0.95 for all normal and accident conditions with 95% probability at a 95% confidence level.

4. Assumptions

The analyses apply a number of assumptions, either for conservatism or to simplify the calculation approach. Each assumption is appropriately discussed and justified in the text. The assumptions are summarized below:

- The fuel pellet is modeled as a solid right cylinder. This is acceptable because neglecting the dishing and chamfering increases the amount of fuel in the model.
- The fuel pellet to clad gap is modeled as a void. This is acceptable since a void has no interactions with neutrons.
- The axial length of the fuel bundle is modeled as a single continuous lattice rather than as the as built combination of various lattices. This is acceptable to determine the maximum reactivity of the individual bundle lattices because the approach neglects potential neutron leakage from lattices with shorter lengths. It also forces the maximum reactivity location to the center of the fuel bundle length, thus eliminating the impact of leakage from the top and bottom of the fuel bundle.
- The structural components of the fuel bundle within the active length, i.e. water holes, channel, etc. are considered to be the same length as the fuel bundle active length. This is acceptable because each lattice is modeled as full length along the fuel bundle active length.
- Fuel bundle components above and below the active length are modeled as a 12-inch water reflector. This is acceptable because the regions above and below the active length are not considered neutronically important due to their distance from the middle of the active length.
- Fuel bundle grid straps are not modeled. This is acceptable because they are not neutronically important. Any impact that grid strap growth during depletion has on fuel rod pitch is addressed with specific depletion related fuel geometry changes calculations. Small changes in the fuel to moderator ratio due to the presence or absence of the grid straps is minimized or negligible due to their relative size compared to the overall active length with no grid straps.
- All legacy and current fuel design lattices at NMP1 have a SCCG < 1.31 and an IMPAE < 4.6 wt% U-235.

- All plenum regions are assumed to be a void.
- The BORAFLEX™ rack and BORAL™ rack models do not consider the rack baseplate or any structural components above and below the active length of the fuel. Those components are replaced by water. This is acceptable because the area of high neutron importance is the center of the fuel bundle active length.
- 12 inches of water is considered an infinite reflector.
- All materials in the model have the same temperature as the SFP moderator. This is acceptable because the most significant temperature related impacts, i.e. water and fuel, are considered in a conservative manner.
- The cell blockers are not considered and the empty locations are filled with water. This is acceptable because the cell blocker with dispel water and the storage racks are un-poisoned, meaning that the displacement of water is non-conservative.
- The cell blocker is assumed to be not capable of being crushed such that a fuel bundle dropped on top would not enter a storage location meant to be blocked [1].
- The SFP wall concrete is modeled using the most conservative material compositions from [22].
- The CASMO models for GNF2 fuel consider the variations along the channel edge as an average thickness. The thicker channel corners are also modeled explicitly. This method is supported by [12] for GNF2 fuel and properly accounts for the gaps between the detector and the control blade and the fuel during depletion. The impact that this approach has is to force the sum of the cell pitch to be 12 inches, which is the design objective [12].
- The MCNP models consider the fuel channel at the thickness presented in Table 5.1. This approach simplifies the MCNP model for the channel and therefore doesn't consider the variations in thickness along the sides or the thicker corners. This is acceptable as an approach because the reactivity effect of the channel thickness manufacturing tolerance is small while the maximum reactivity case for channel impacts is for fuel with no channel (see Section 7).
- The MCNP SCCG calculations consider a pitch of 6 inches. This approach is used to be consistent with CASMO built in requirements for GNF2 fuel [12] and fuel vendor SCCG calculations (a value of 6 inches is assumed to have been used by the fuel vendor).

5. Input Data

The evaluations in this report use validated input data from various sources. In some cases, simplifications or assumptions are used. The subsections below discuss the source of the various analysis parameters and any applicable simplifications or assumptions considered in the analysis evaluations.

5.1 Fuel Bundle Designs

The NMP1 contains various legacy fuel designs (7x7, 8x8 and 9x9) as well as the currently used fuel design the GNF2 (10x10). The BWR fuel bundle data used in the analysis is presented in Table 5.1. Note that all legacy fuel designs are well bounded in reactivity by the GNF2 fuel design and therefore only the GNF2 fuel design information is provided in Table 5.1 (see Appendix A). The legacy fuel design information may be found in [19].

For all fuel designs, the fuel bundle is explicitly modeled in terms of fuel pin, cladding, water holes and channel. A void is considered in the fuel pellet to cladding gap. The water holes and channels considered to be the same length as the active fuel length. Above and below the active fuel length is modeled as water. Space grids and other minor structural components are neglected.

5.2 Storage Rack Designs

The NMP1 SFP contains two BORAFLEX™ storage racks and 14 BORAL™ storage racks. The design of these two rack types is described in following sub-sections.

5.2.1 BORAFLEX™ Storage Racks

The BORAFLEX™ spent fuel storage racks are described as a rack type 198 and rack type 218 (i.e. rack type 198 has 198 usable locations and rack type 218 has 218 usable locations). The two BORAFLEX™ rack designs are constructed with two BORAFLEX™ panels encased in stainless steel cladding separated by a water gap, all within a stainless steel BORAFLEX™ box. Adjacent to the BORAFLEX™ box are two stainless steel fuel storage cells separated by a stainless steel wall. Thus, each row of BORAFLEX™ boxes separates rows of fuel storage cells. See Figure 5.1 and Figure 5.2. The BORAFLEX™ storage rack is specified in Table 5.2.

As discussed in Section 2, various BORAFLEX™ rack models are considered for the evaluations. For each evaluation, the storage rack model axial length is the same as the fuel design active length specified in Section 5.1. The BORAFLEX™ is replaced by water. The rack baseplate and construction above the active fuel length is not considered, thus above and below the active fuel length is considered water.

5.2.2 BORAL™ Storage Racks

The NMP1 SFP contains 14 BORAL™ racks of various sizes. The BORAL™ racks are high density racks constructed using formed and fabricated cells with a BORAL™ panel encased in stainless steel sheathing on each of the four sides of the fabricated cells. These storage racks credit the BORAL™ and have the same TS requirements as the BORAFLEX™ racks. The BORAL™ storage rack is specified in Table 5.3 for informational purposes only.

5.2.3 Rack to Rack Gaps

The NMP1 SFP rack to rack gaps and rack to SFP wall gaps are presented in Table 5.4.

5.3 Spent Fuel Pool Operating Conditions

The SFP has a normal maximum operating temperature shown in Table 5.5.

5.4 Depletion Parameters

The NMP1 Unit 1 reactor operates with the parameters shown in Table 5.6. The control blade parameters are shown in Table 5.7.

5.5 Material Composition

The material compositions for the various MCNP models are presented in Table 5.8.

6. Computer codes

The following computer code was used in this analysis. Note that the isotopic compositions from the depletion calculations performed in [10] are used directly in this analysis. See [10] for information regarding the depletion calculation code.

- MCNP [1-2] is a three-dimensional continuous energy Monte Carlo code developed at Los Alamos National Laboratory. This code offers the capability of performing full three-dimensional calculations for the loaded storage racks. MCNP was run on the PCs at Holtec.
- CASMO-5 [12] version 2.08.00 is a two-dimensional multigroup transport theory code developed by Studsvik of Sweden. This code is used to determining the isotopic composition of spent fuel for burnup credit only.

7. Analysis

As discussed in Section 2.0, the analysis is performed using a combination of bounding analysis parameters and statistical uncertainties. The use of bounding analysis parameters allows for simplicity and inclusion of analysis margin in the results. The following analysis parameters are treated in a bounding manner:

- Conservative COP (see Section 2.3.5)
- Peak reactivity method (see Section 2.3.2)
- SFP moderator temperature (see Section 2.3.4.1).
- A bias for radial positioning of fuel bundle and presence of fuel bundle channel (see Section 2.3.4.2).
- A bias for radial orientation of the lattice(s) in the storage rack (see Section 2.3.4.3).
- A bias for depletion related fuel geometry changes (see Section 2.3.4.5).
- A bias for cooling time variations (See Section 2.3.5).

Additional discussions are provided below.

7.1 Screening Evaluations for the Bounding Lattice(s)

As discussed in Section 2.3.2, screening calculations were performed using CASMO in both the SCCG and in-rack (no empty location) for all legacy and current fuel designs to determine the bounding COP and set of most reactive lattices. The results of those calculations are presented in Appendix A. The results showed that there are lattices with a reactivity higher than the other

lattices. These seven lattices selected are listed below by analysis nomenclature, fuel vendor bundle ID and axial location:

- 10a61, GNF2-P10DG2B375-11G5.0-100T2-145-T6-4313, lattice-1.
- 10a62, GNF2-P10DG2B375-11G5.0-100T2-145-T6-4313, lattice-2.
- 10a63, GNF2-P10DG2B375-11G5.0-100T2-145-T6-4313, lattice-3.
- 10a64, GNF2-P10DG2B375-11G5.0-100T2-145-T6-4313, lattice-4.
- 10a82, GNF2-P10DG2B377-12GZ-100T2-145-T6-4483, lattice-2.
- 10a83, GNF2-P10DG2B377-12GZ-100T2-145-T6-4483, lattice-3.
- 10a84, GNF2-P10DG2B377-12GZ-100T2-145-T6-4483, lattice-4.

Additionally, as discussed in Section 2.3.2, design basis MCNP calculations were performed using the set of seven lattices in both the SCCG configuration, the in-rack configuration with no empty location and the design basis model with an empty location. These calculations consider the expected bounding SFP moderator temperature (maximum). The studies are performed to confirm the results of the CASMO screening calculations to determine the bounding COP. The results of these calculations are presented in Appendix B, Table B.1 through Appendix B, Table B.3. The results of these calculations confirm the bounding COP determined by the screening calculation results presented in Appendix A.

Further, as discussed in Section 2.3.2, super lattices were developed from the set of seven actual lattices. The process for super lattice development is as follows:

- MCNP SCCG calculations were performed with Gd loading increments of 0.5 wt%.
    - The two results which yield SCCG values which envelope 1.31 are used to interpolate the Gd loading which yields a SCCG of 1.31. These calculation results are presented in Appendix B, Table B.4 and plotted in Figure B.1.
- MCNP in-rack calculations with the design basis model (includes the empty location for the cell blocker) were also performed for the same Gd loading increments as the SCCG calculations. The two Gd increment results which envelope the interpolated Gd loading are used to interpolate the in-rack reactivity. These calculation results are presented in Appendix B, Table B.5 and plotted in Figure B.2.
- The reactivity difference ($k_{inf} - k_{calc}$) is plotted in Figure B.3. This plot shows that there is little relative change in the difference between the reactivity values from SCCG and corresponding in-rack.

The results of the incremental Gd calculations show that there are two super lattices with a higher reactivity than the other super lattices. These two super lattices are 10a63 and 10a83. The 10a63 was selected as the bounding super lattice and was used to confirm the interpolations described above following the same process, i.e. SCCG and in-rack calculations. These evaluations involve additional Gd incremental calculations in much smaller 0.1 Gd loading wt% increments. The results of these confirmatory calculations are presented in Appendix B, Table B.6 and Appendix B, Table B.7 respectively. The results of the confirmatory calculations show that the interpolation process was conservative because the interpolation from the smaller Gd loading increments is higher than the larger Gd loading increments. Thus, the required Gd loading for a SCCG of 1.31

is more reactive than actually needed. For the bounding super lattices the required Gd loading is about 3.4%. However, for additional conservatism, a Gd loading of 3.0 wt% is used for the super lattice for the design basis calculations.

Thus, all further analysis calculations consider the bounding super lattice, 10a63, with a Gd loading of 3.0 wt%, bounding COP and maximum SFP moderator temperature.

The results for the super lattice evaluations in SCCG and in rack show that for each of the super lattices, the variation of lattice design and/or the location of the Gd rods has an impact on which Gd loading is required to meet a SCCG k_{inf} of 1.31. For example, in Appendix B, Figure B.1 the results show that the same lattices which reach the SCCG k_{inf} limit of 1.31 first (at the higher Gd loading) are not the most reactive in the SFP (Appendix B, Figure B.2). Thus, for this methodology, the lattices which are selected as the bounding super lattices are those which are the more reactive in the SFP at the SCCG k_{inf} limit of 1.31. It should be noted that these results show that the SCCG methodology is not an exact methodology since it cannot be concluded that all lattices with a SCCG k_{inf} of 1.31 correspondingly have the same reactivity in the SFP.

7.2 Reactivity Effect of SFP Water Temperature

As discussed in Section 2.3.4.1, the reactivity effect of SFP water temperature and density is evaluated so that the bounding values can be used in the design basis model. The results of the evaluations are presented in Appendix B, Table B.8. The results presented in Appendix B, Table B.8 show that the bounding temperature (and corresponding density) are the maximum temperature and associated density. This is expected because the BORAFLEX™ racks are un-poisoned. Therefore, these values are used in the design basis model.

7.3 Reactivity Effect of Eccentric Positioning and Fuel Bundle De-Channeling

As discussed in Section 2.3.4.2, the reactivity effect of the fuel bundles eccentric positioning in conjunction with fuel bundle de-channeling is evaluated. The results of the evaluations are presented in Appendix B, Table B.9. The results presented in Appendix B, Table B.9 show that the fuel with no channel and eccentric to the rack center is much more reactive than the other cases. While this configuration is very unlikely, i.e. all fuel to have no channel and eccentric to the rack center, the large reactivity increase is included in the analysis results as bias and bias uncertainty.

7.4 Reactivity Effect of Lattice Orientation in the SFP Rack Cell

As discussed in Section 2.3.4.3, the reactivity effect of the lattice orientation in the BORAFLEX™ rack storage cell with respect to the control blade corner in the core is evaluated to determine the bounding configuration. The results of the evaluations are presented in Appendix B, Table B.10. The maximum positive orientation impact is included in the analysis as a bias and bias uncertainty.

7.5 Reactivity Effect of the Fuel Bundle and BORAFLEX™ Rack Manufacturing Tolerances

As discussed in Section 2.3.4.4, evaluations are performed to determine the reactivity effect of the bounding lattice(s) manufacturing tolerances. The results of the evaluations for the bounding lattice(s) is presented in Appendix B, Table B.11.

Also, as discussed in Section 2.3.4.4 evaluations are performed to determine the reactivity effect of the BORAFLEX^{TM} rack manufacturing tolerances. The results of these evaluations are presented in Appendix B, Table B.12.

The maximum positive reactivity effect for each fuel and rack parameter is statistically combined and treated, along with its 95/95 uncertainty as an analysis uncertainty.

7.6 Reactivity Effect of Depletion Related Fuel Geometry Changes

As discussed in Section 2.3.4.5, the reactivity effect of the depletion related fuel geometry changes is evaluated for the bounding lattices(s). The results of the evaluations are presented in Appendix B, Table B.13. The results are treated as an analysis bias and bias uncertainty.

7.7 Depletion Uncertainty

As discussed in Section 2.3.4.6, the reactivity effect of the depletion uncertainty is evaluated for the bounding lattices(s). The results of the evaluations are presented in Appendix B, Table B.14. The results are treated as an analysis uncertainty.

7.8 Additional Studies with the Design Basis Model

As discussed in Section 2.3.5, additional studies are performed to determine the reactivity effect of: longer cooling times than used in the design basis calculations, alternative COP and to compare the analysis SCCG with the fuel vendor SCCG. The results of these studies are presented in Appendix B, Table B.15 and Table B.16 for the cooling time studies and the alternative COP, respectively, and Table B.18 for the SCCG comparison.

The results of the cooling time studies show that the design basis approach is acceptable. However, when applying the 95/95 uncertainty to the study delta-k, there may be some small impact. Thus, this small impact is added as an analysis bias uncertainty and the negative bias is truncated.

The results of the COP study show that when considering the bounding COP, “mnr”, if a maximum fuel temperature is applied there may be a slight increase in reactivity. The other two COP, i.e. maximum moderator temperature and maximum void fraction, both lead to decreases in reactivity. These studies are presented for information only since these combinations of COP are not physically realistic.

The results of the 10a63 lattice SCCG comparison presented in Table B.18 shows that the MCNP SCCG k_{inf} with bounding analysis COP is more than 1% delta-k higher in reactivity than the fuel vendor SCCG k_{inf} with the fuel vendor 1% bias included in the fuel vendor SCCG k_{inf} value. This difference in reactivity is due to differences in methodology. Since the MCNP reactivity is higher,

it is appropriate to include an additional bias to account for the difference in methodology. Therefore, a 2% bias is applied to the analysis results.

7.9 Storage Rack Interfaces

As discussed in Section 2.3.6, BORAL™ rack to BORAFLEX™ rack interface is a very low reactivity interface due to the restriction on cell blocker location along the interface. No additional evaluation is required. See also Supplement 1.

7.10 Accident Conditions

As discussed in Section 2.3.7, the following accident conditions have been evaluated:

- The effect of SFP temperature exceeding the normal range.
- A dropped fuel bundle.
- A misloaded fuel bundle (a fuel bundle in the wrong location within the storage rack).
- A mislocated fuel bundle (a fuel bundle in the wrong location outside the storage rack).
- Rack movement due to seismic activity.

The results of the accident condition evaluations are presented in Appendix B, Table B.17. The maximum reactivity case is used to determine k_{eff} for accident conditions (see Section 7.11).

7.11 Calculation of the Maximum k_{eff}

As discussed in Section 2.3.8, the maximum k_{eff} for both normal and accident conditions is determined. The results of the k_{eff} calculations are presented in Table 7.1.

8. Conclusion

The criticality calculations for the NMP1 SFP BORAFLEX™ racks with cell blockers and no credit for BORAFLEX™ have been performed while considering the two TS limits; SCCG $k_{inf} \leq 1.31$ and a maximum lattice average enrichment of 4.6 wt% U-235. The results show that the effective neutron multiplication factor (k_{eff}) is less than 0.95 with a 95% probability at a 95% confidence level as presented in Table 7.1 for all normal and accident conditions.

The analysis results show that for all actual lattices the reactivity of the BORAFLEX™ racks with cell blockers is very low, i.e. more than 10% delta-k below the regulatory limit (see Appendix B). This is expected due to the empty storage locations. The criticality safety analysis provides ample margin to the regulatory limit while also providing an additional 1% delta-k administrative margin that may be used to account for minor uncertainties or other items that are not already explicitly covered.

The analysis considers the maximum reactivity of both normal and accident conditions for the bounding super lattice (selected from the set of seven super lattices created from the set of seven bounding actual lattices). The bounding super lattice is also used to show agreement with the TS

limits. However, the analysis results also show that there is some variation in reactivity among the seven super lattices in terms of relationship between SCCG and in rack reactivity, i.e. the super lattices which reach k_{inf} in SCCG of 1.31 first due to incremental decreases in Gd loading are not the most reactive super lattices in rack. The analysis results suggest that the SCCG methodology may be inherently conservative because the TS limit of SCCG $k_{inf} \leq 1.31$ is met for some lattices before those same lattices have an in rack reactivity that is greater than the lattices used for the TCF calculations.

9. References

1. Contract 00581422, “2016 – NMP 3 out of 4 Criticality Analysis”, dated 6/20/2016.

2. Nine Mile Point Nuclear Station Unit 1 – Technical Specifications.

3. HI-92793, Revision 4, “Fuel Criticality Analysis for Nine Mile Unit 1”, dated 6/19/1992.

4. HI-2114838, Revision 1, “GNF2 Fuel Criticality Analysis for Nine Mile Point Unit 1 Spent Fuel Pool”, dated 3/18/2011.

5. “MCNP - A General Monte Carlo N-Particle Transport Code, Version 5,” Los Alamos National Laboratory, LA-UR-03-1987 (2003, Revised 2/1/2008).

6. ENDF/B-VII.0 Evaluated Nuclear Data Library, Release December 15, 2006.

7. NJOY99.0, Code System for Producing Pointwise and Multigroup Neutron and Photon Cross Section from ENDF/B Data, PSR-480, March 2000, ORNL.

8. HI-2156450, "MCNP5 Temperature Dependent Library Construction with NJOY", latest revision, Holtec International.

9. F. Brown, A Review of Monte Carlo Criticality Calculations – Convergence, Bias, Statistics, 2009 International Conference on Mathematics, Computational Methods and Reactor Physics, Saratoga Springs, NY, 2009.

10. "Nuclear Group Computer Code Benchmark Calculations", Holtec Report HI-2104790 Rev. 3.

11. Guide for Validation of Nuclear Criticality Safety Calculational Methodology, NUREG/CR-6698, January 2001.

12. CASMO-5/CASMO-5M, A Fuel Assembly Burnup Program”, SSP-07/431 Rev 0, Studsvik, 8/16/2007.

13. “ENDF/B-VII.0 586 Group Neutron Data Library for CASMO-5 and CASMO-5M”, SSP-07/402 Rev 5.

14. L.I. Kopp, “Guidance on the Regulatory Requirements for Criticality Analysis of Fuel Storage at Light-Water Reactor Power Plants,” NRC Memorandum from L. Kopp to T. Collins, August 19, 1998.

15. DSG-ISG-2010-01, Staff Guidance Regarding the Nuclear Criticality Safety Analysis for Spent Fuel Pools, Revision 0.

16. Transmittal of Design Information NF162302, Revision 0, “SFP Information for SFP Criticality Analysis Revision to Remove Boraflex Credit”, dated 10/5/2016.

17. ASME B&PV Code, Section II, Part A, SA-480

18. “Guidance for Performing Criticality Analyses of Fuel Storage at Light-Water-Reactor Power Plants”, NEI 12-16, Revision 2 draft, Nuclear Energy Institute.

19. Transmittal of Design Information NF162346, Revision 0, “Fuel Bundles and Core Operating Parameters for NMP1 SFP Criticality Analysis without Boraflex Credit”, dated 11/28/2016.

20. Transmittal of Design Information NF172732, Revision 0, “GNF2 and GE11 Fuel Depletion Related Geometry Change Parameters and Thermal Operating Parameters for NMP1 SFP Criticality Analysis without Boraflex Credit”, dated 2/22/2017.

21. “An Investigation on Irradiation-induced Grid Width Growth in Advanced Fuels”, Transactions of the Korean Nuclear Society Autumn Meeting Gyeongju, Korea, October 27-28, 2011.

22. EPRI Report 3002003073, “Sensitivity Analysis for Spent Fuel Pool Criticality,” 2014.

23. GE Hitachi Nuclear Energy Report 004N1484, Revision 0, “OYSTER CREEK ORIGINAL EQUIPMENT CONTROL ROD DIMENSIONS”, March 2017.

24. Transmittal of Design Information NF172732, Revision 0, “GNF2 Fuel Limiting Lattice K-infinity for NMP1 SFP Criticality Analysis without Boraflex Credit”, dated 01/19/2017.

25. Transmittal of Design Information NF172902, “Values of Gaps Between Boraflex Racks and the SFP walls for NMP1 SFP Criticality Analysis without Boraflex Credit”, dated 4/13/2017.

Table 2.1
Summary of the Area of Applicability of the MCNP Benchmark

Parameter	Design Application	Benchmarks	Validated
Fissionable Material	^{235}U, ^{239}Pu, ^{241}Pu	^{235}U, ^{239}Pu, ^{241}Pu	^{235}U, ^{239}Pu, ^{241}Pu
Isotopic Composition			
$^{235}U/U$	< 5.0wt%	1.57 – 10%	< 10wt%
Pu/(U+Pu)	n/a	1.104 - 20 %	< 20wt%
Physical Form	UO_2	UO_2, MOX	UO_2, MOX
Fuel Density (g/cm^3)	10.31 – 10.731	6.1 – 10.4	6.1 – 10.7[1]
Moderator Material (coolant)	H	H	H
Physical Form	H_2O	H_2O	H_2O
Density (g/cm^3)	around 1.0 g/cm^3	around 1.0 g/cm^3	around 1.0 g/cm^3
Reflector Material	H	H	H
Physical Form	H_2O	H_2O	H_2O
Density (g/cm^3)	around 1.0 g/cm^3	around 1.0 g/cm^3	around 1.0 g/cm^3
Interstitial Reflector Material			
Plate	Steel	Steel or Lead	Steel or Lead
Absorber Material			
Soluble	None	None	None
Separating Material			
Plate	Water, Boral	Water, B-SS, Boral, Boroflex, Zircaloy or Cadmium	Water, B-SS, Boral, Boroflex, Zircaloy or Cadmium
Geometry			
Lattice type	Square	Square, Triangle	Square, Triangle
Lattice Pitch (cm)	1.44 – 1.87 (BWR)	0.7 to 4.318	0.7 to 4.318
Neutron Energy	Thermal spectrum	Thermal spectrum	Thermal spectrum

[1] See Table 2.3 in [11].

Table 2.2
MCNP Benchmarking Bias and Bias Uncertainty and Trending Analysis [10]

Experiment Description	No. of exp.	Bias	Bias Uncertainty	Normality χ^2 ($P_d(\chi^2;d)$)	Linear Correlation	Residuals Normality, ($P_d(\chi^2;d)$)
All experiments	562	Proprietary data removed			None	-
All except those with Gadolinium, Cadmium and Lead[2]	389				None	-
All with Fresh Water	311				None	0.19%
Fresh UO2 Fuel with Fresh Water	178					
HTC + MOX Fuel with Fresh Water	133					

[2] Note: Critical experiments with Gadolinium, Cadmium and Lead were excluded from all subsequent subsets.

Table 2.3
Summary of MCNP Benchmarking Bias and Bias Uncertainty Significant Trending Analysis

Experiment Description	Linear Correlation	Analysis Parameter Value[3]	Analysis Parameter Trend Bias	Analysis Parameter Trend Bias Uncertainty	[10] Trend Table
Fresh UO2 Fuel with Fresh Water	Proprietary data removed.	0.22 eV (min)			D.3-16
HTC + MOX Fuel with Fresh Water		0.22 eV (min)			
		0 % (min)			

[3] The maximum or minimum parameter value that provides the maximum bias is used.

Table 5.1
Specification of the GNF2 Fuel Bundle Parameters used in Analysis [19], [20]

Parameter	Value
Fuel Rod Array	10x10
Fuel Bundle Overall Length, Inches	Proprietary data removed.
Distance from Bottom of Fuel Bundle to Beginning of Active Length, Inches	
Clad Outer Diameter, Inches	
Clad Inner Diameter, Inches	
Clad thickness	
Pellet Diameter, Inches	
Stack Density g/cc	
Maximum design IMPAE wt% U-235	4.6
Full Length Rods Active Length, Inches	
Part Length Rods Active Length (short/long), Inches	
Fuel Rod Pitch, Inches	
Number of Water Rods	2
Water Rod Outer Diameter, Inches	
Water Rod Inner Diameter, Inches	
Channel Inner Diameter, Inches	
Channel Side Thickness, Inches	
Channel Corner Radius, Inches	
Depletion related fuel rod growth, Inches	
Depletion related channel thickness, Inches	

Table 5.2
Specification of the Rack 198 and Rack 216 BORAFLEX™ Fuel Storage Racks [16]

Parameter	Value
BORAFLEX™ SS box cell wall thickness, inches	0.093 ± 0.008[4]
Storage cell north-south inner diameter, inches	11.834 ± 0.03
Storage cell east-west diameter, inches	5.899 ± 0.030
BORAFLEX™ SS box cell east-west inner diameter, inches	1.534 ± 0.030
BORAFLEX™ SS sheathing thickness (both sides), inches	0.031
BORAFLEX™ pocket thickness (modeled as water), inches	0.110 +0, -0.03
BORAFLEX™ panel width, inches	11.25
Distance from rack baseplate top to beginning of neutron absorber, inches	12
Rack height (top of baseplate to top of rack), inches	163

[4] All tolerances with 0.008 inches dimensions in this table are an assumed value.

Table 5.3
Specification of the BORAL™ Fuel Storage Racks[5] [12]

Description	Value
Storage cell inner diameter, inches	5.9
Storage cell wall thickness, inches	0.06
Storage cell pitch, inches	6.06
BORAL™ width, inches	5.125
BORAL™ thickness, inches	0.07
BORAL™ areal density, g/cm^2	0.0162 (0.015 min)

[5] The information in this Table is for information purposes only. The information is not used in the analysis.

Table 5.4
Rack to Rack Gaps [16], [25]

Parameter	Gap Size (inches)
Distance between Rack 198 and Rack 216	0.375
Distance between Rack 198and BORAL™ Rack G	2.00
Distance between Rack 198 and BORAL™ Rack J1	3.15
Distance between Rack 198 and SFP wall to the west	26.00
Distance between Rack 216 and BORAL™ Rack J2	3.15
Distance between Rack 216 and SFP wall to the west	19.10
Distance between Rack 216 and SFP wall to the south	5.25
Distance between Rack 216 and SFP wall to the west during a seismic accident	18.25
Distance between Rack 216 and SFP wall to the south during a seismic accident	4.38

Table 5.5
SFP Operating Parameters [16]

Parameter	Value
SFP moderator maximum temperature	140 °F

Table 5.6
Core Operating Parameters [19]

Parameter	Minimum Value (mnu)	Minimum Value with Control Blades Inserted (mnr)	Maximum Value (mxu)	Maximum Value with Control Blades Inserted (mxr)
Power density (kW/liter)	50	50	50	50
Fuel temperature (K)	1453.15	1453.15	1984.261	1984.261
Moderator temperature (K)	548.706	548.706	560.922	560.922
Void fraction (%)	0	0	76.6	76.6
Control blade	no	yes	no	yes

Table 5.7
Reactor Control Blade Data [19], [23]

Description (Unit)	Nominal Value
GE standard initial equipment	
Central support span (inches)	Proprietary data removed.
Wing tip to wing tip blade span (inches)	
Blade wing thickness (inches)	
Blade sheath thickness (inches)	
Poison tube Wall thickness (inches)	
Poison tube OD (inches)	
Number of B_4C tubes (per wing)	
B_4C density (g/cc)	

Table 5.8
Material Compositions

Element	MCNP ZAID[6] [5],[8]	Weight Fraction
Steel (density 7.92 g/cc) [10]		
Cr	24050.25c	0.00790496
	24052.25c	0.15852660
	24053.25c	0.01832179
	24054.25c	0.00464667
Mn	25055.25c	0.02001000
Fe	26054.25c	0.03898260
	26056.25c	0.63458000
	26057.25c	0.01491736
	26058.25c	0.00202002
Ni	28058.25c	0.06719768
	28060.25c	0.02677598
	28061.25c	0.00118336
	28062.25c	0.00383482
	28064.25c	0.00100815
Zr (density = 6.55 g/cc) [10]		
Zr	40090.25c	0.50706120
	40091.25c	0.11180900
	40092.25c	0.17278100
	40094.25c	0.17891100
	40096.25c	0.02943790

[6] The MCNP ZAID used is customized for ENDF/B-VII NJOY adjusted cross sections.

Table 5.8 (continued)
Material Compositions

Element	MCNP ZAID[7] [5],[8]	Weight Fraction
Concrete (density 2.9 g/cc) [22]		
Mg	12024.25c	0.058696310
	12025.25c	0.007740914
	12026.25c	0.008862759
O	8017.25c	0.001097938
C	6000.25c	0.140000000
Na	11023.25c	0.023200000
Al	13027.25c	0.027200000
Fe	26054.25c	2.540502e-04
	26056.25c	0.004135569
	26057.25c	9.721666e-05
	26058.25c	1.316451e-05
Si	14028.25c	0.247507000
	14029.25c	0.013016850
	14030.25c	0.008876131
Ca	20040.25c	0.034024950
	20042.25c	0.0002384304
	20043.25c	5.093569e-05
	20044.25c	0.0008053114
	20046.25c	1.614421e-06
	20048.25c	7.875700e-05

[7] The MCNP ZAID used is customized for ENDF/B-VII NJOY adjusted cross sections.

Table 7.1
Summary of the Analysis Results

Analysis Uncertainties	
BWR fuel eccentric positioning bias uncertainty (Appendix B, Table B.9)	0.0011
BWR fuel rotation bias uncertainty (Appendix B, Table B.10)	0.0011
BWR fuel tolerances (Appendix B, Table 11)	0.0040
BORAFLEXTM rack manufacturing tolerances (Appendix B, Table 12)	0.0087
Depletion related geometry changes bias uncertainty (Appendix B, Table 13)	0.0011
Depletion uncertainty (Appendix B, Table 14)	0.0041
Cooling time bias uncertainty (Appendix B, Table B.15)	0.0011
MCNP code bias uncertainty (Table 2.2)	Proprietary data removed.
MCNP calculation uncertainty (2 sigma)	0.0008
statistical combination of analysis uncertainties	0.0154
Analysis Biases	
BWR fuel eccentric positioning bias (Appendix B, Table B.9)	0.0182
BWR fuel rotation bias (Appendix B, Table B.10)	0.0007
Depletion related geometry changes bias (Appendix B, Table 13)	0.0036
Cooling time bias (Appendix B, Table B.15)	0.0000
MCNP code bias (Table 2.3)	
Administrative bias (Section 2.3.8)	0.0100
SCCG bias (Section 7.8)	0.0200
Sum of biases	0.0539
Total correction factor	0.0693
Maximum k_{calc} for normal conditions	0.8677
Maximum k_{eff} for normal conditions	0.9370
Maximum k_{calc} for accident conditions	0.8697
Maximum k_{eff} for accident conditions	0.9390
Margin to Regulatory Limit	0.0110

Figure 1.1

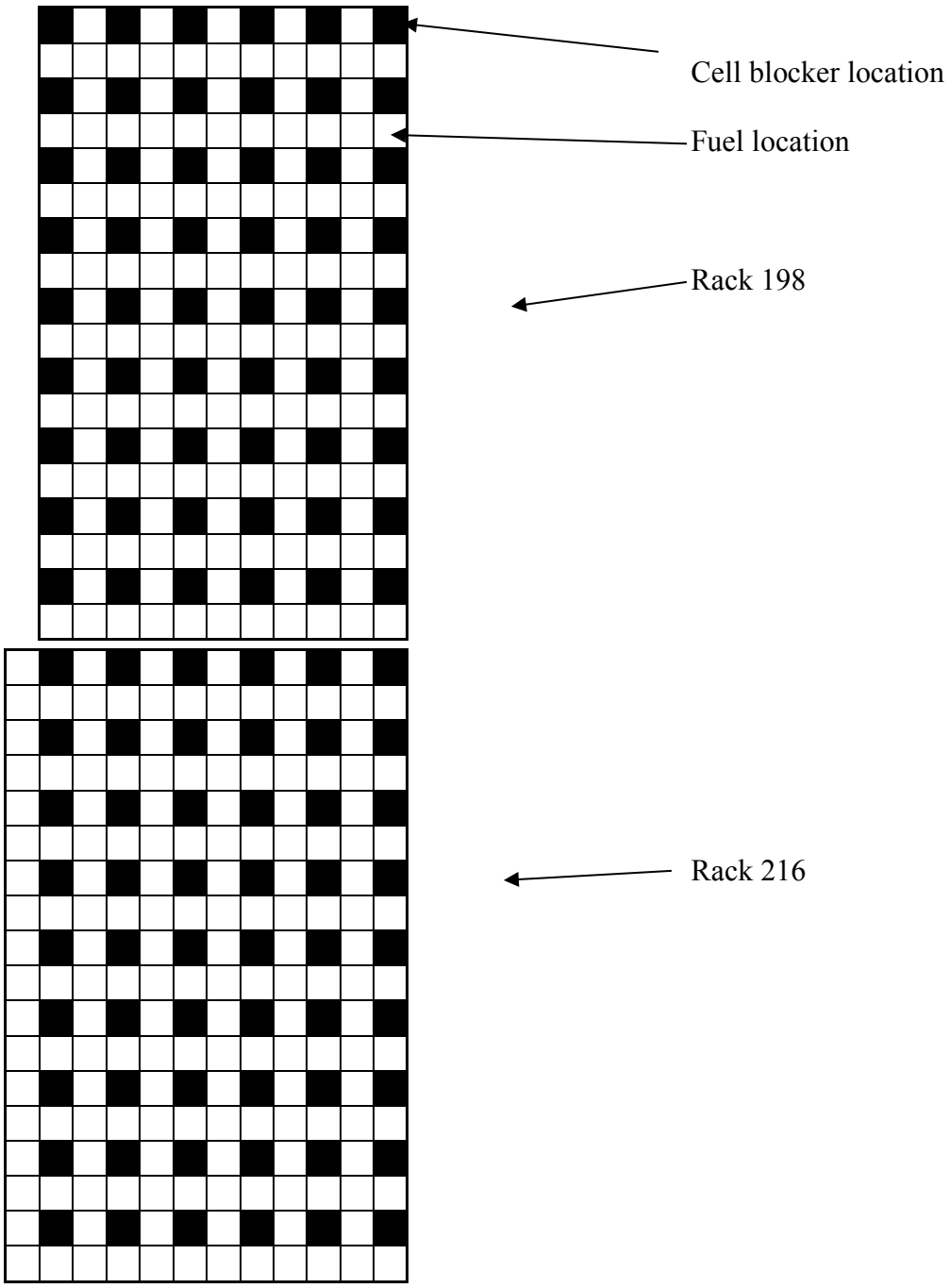

Figure 2.1
MCNP BWR BORAFLEX™ Design Basis Model

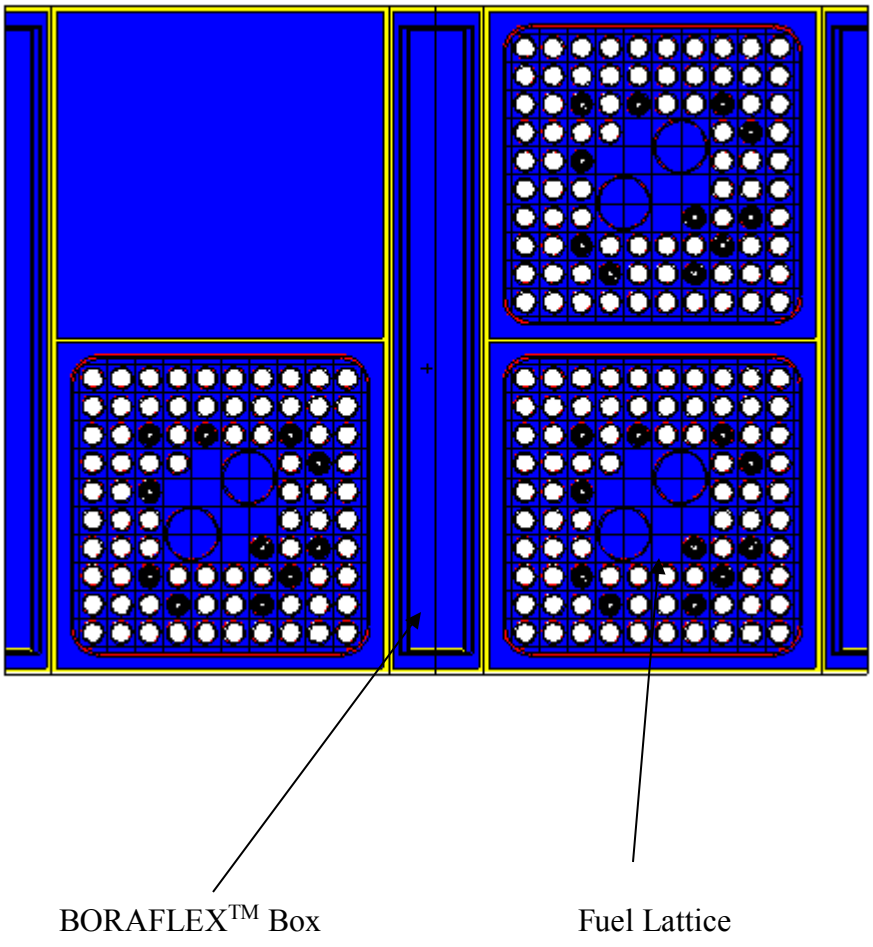

Figure 5.1
A Simplified Diagram of the BORAFLEX™ Rack Construction.

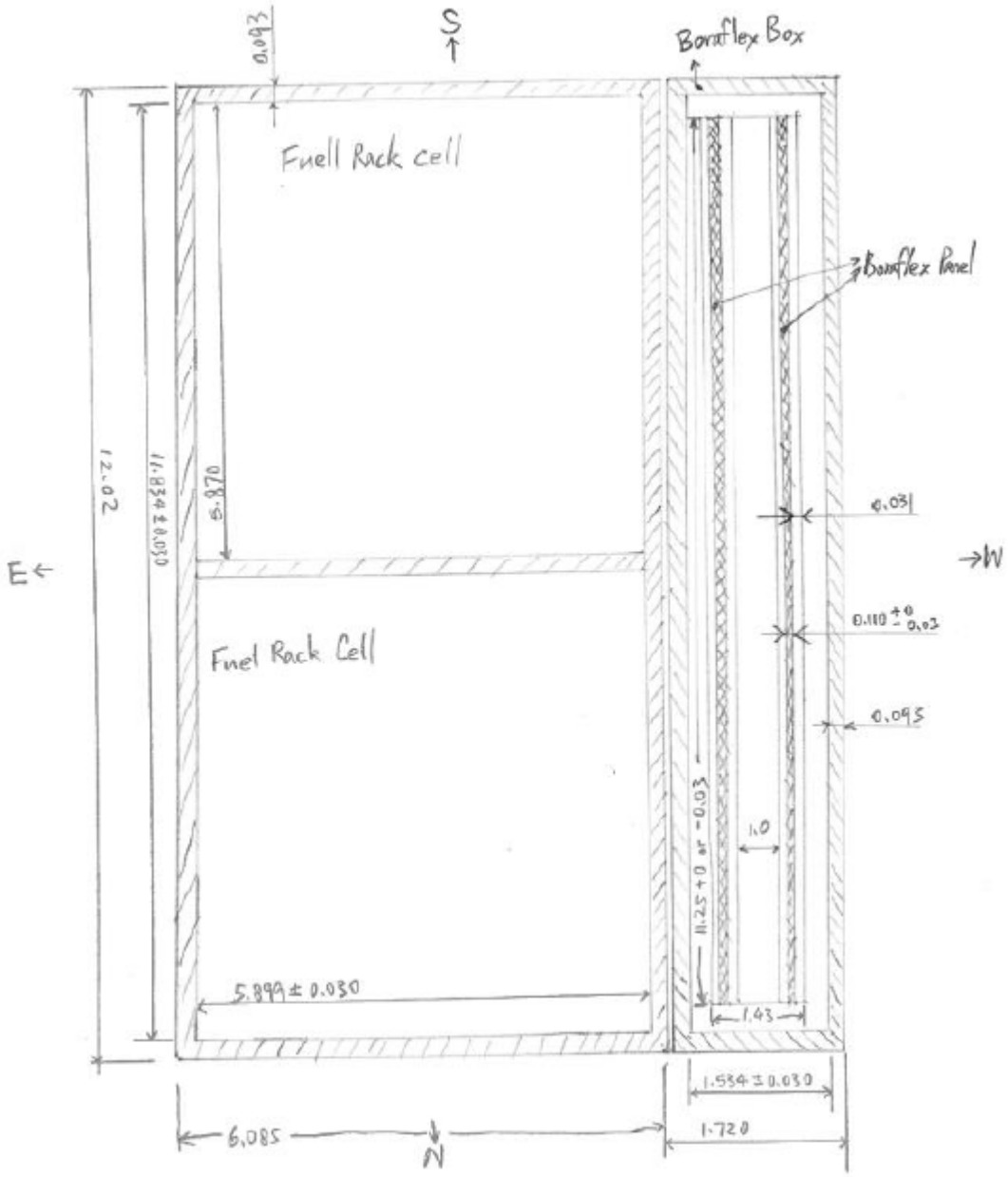

Figure 5.2
A Detailed Diagram of the Rack Type 198 BORAFLEX™ Rack.

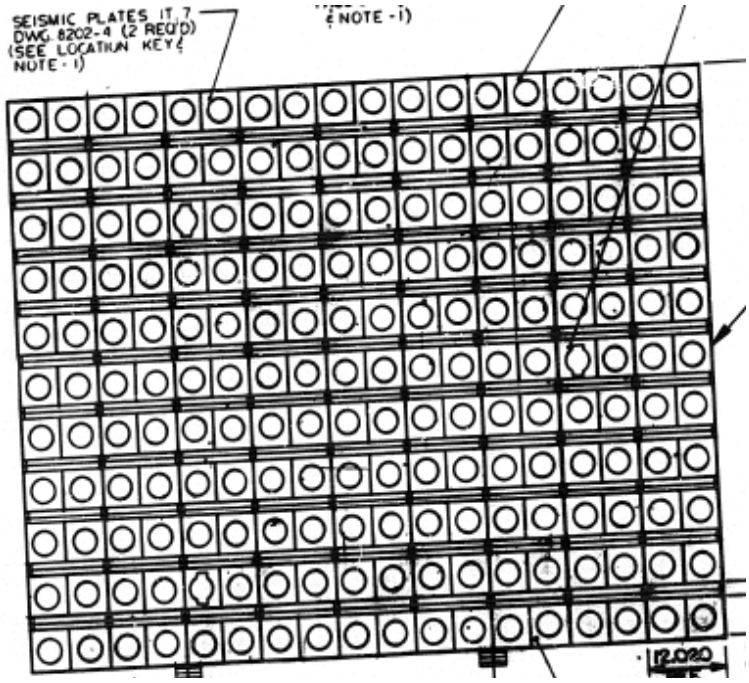

Appendix A
Screening Calculations

Appendix A contains results and other analysis information in the following tables:

Table A.1
Summary of Pre/Post Processor Nomenclature for Fuel Lattices

```
#
# class / idx / assembly / lattice
#
# ------------------------------------------------------------------------
# 7x7A
7a  00  7DKB210-NOG-80M-144                    initial
#
# 7x7B
7b  10  7DAB250-2G1.0_2G0.5-80M-144            reload-1
7b  20  7DAB230-3G2.5-80M-144                  reload-2
#
# 7x7C
7c  00  7DBB250-4G1.5-80M-144                  reload-3
#
# ------------------------------------------------------------------------
# 8x8A
8a  10  8DJB262-4G1.5-80M-144                  reload-4a
8a  20  8DJB250-4G1.5-80M-144                  reload-4b
8a  30  8DJB274-5G2.0-80M-144                  reload-6
8a  40  8DJB274-5G3.0-80M-144                  reload-6
#
# 8x8B
8b  11  8DNB277-6G3.0-1GZ4.0-80M-145           lattice-0
8b  12  8DNB277-6G3.0-1GZ4.0-80M-145           lattice-1
8b  13  8DNB277-6G3.0-1GZ4.0-80M-145           lattice-2
8b  20  GE7B-P8DRB299-7G4.0-80M-145.24          lattice-1
#
# 8x8C
8c  11  GE8B-P8DQB321-8GZ-80M-4WR-145-T        lattice-1
8c  12  GE8B-P8DQB321-8GZ-80M-4WR-145-T        lattice-2
8c  21  GE8B-P8DQB338-12GZ-80M-4WR-145-T       lattice-1
8c  22  GE8B-P8DQB338-12GZ-80M-4WR-145-T       lattice-2
8c  23  GE8B-P8DQB338-12GZ-80M-4WR-145-T       lattice-3
#
# ------------------------------------------------------------------------
# 9x9A
9a  11  GE11-P9HUB310-10GZ-100M-145-T          lattice-1
9a  12  GE11-P9HUB310-10GZ-100M-145-T          lattice-2
9a  13  GE11-P9HUB310-10GZ-100M-145-T          lattice-3
9a  21  GE11-P9HUB340-10GZ-100M-145-T          lattice-1
9a  22  GE11-P9HUB340-10GZ-100M-145-T          lattice-2
9a  23  GE11-P9HUB340-10GZ-100M-145-T          lattice-3
#
# 9x9B
```

```
9b  11  GE11-P9HUB340-12GZ1-100T-145-T              lattice-1
9b  12  GE11-P9HUB340-12GZ1-100T-145-T              lattice-2
9b  13  GE11-P9HUB340-12GZ1-100T-145-T              lattice-3
9b  21  GE11-P9DUB339-12GZ-100T-145-T               lattice-1
9b  22  GE11-P9DUB339-12GZ-100T-145-T               lattice-2
9b  23  GE11-P9DUB339-12GZ-100T-145-T               lattice-3
9b  31  GE11-P9DUB362-13GZ-100T-145-T-2414          lattice-1
9b  32  GE11-P9DUB362-13GZ-100T-145-T-2414          lattice-2
9b  33  GE11-P9DUB362-13GZ-100T-145-T-2414          lattice-3
9b  41  GE11-P9DUB376-12GZ-100T-145-T-2583          lattice-1
9b  42  GE11-P9DUB376-12GZ-100T-145-T-2583          lattice-2
9b  51  GE11-P9DUB376-12GZ-100T-145-T-2584          lattice-1
9b  52  GE11-P9DUB376-12GZ-100T-145-T-2584          lattice-2
9b  61  GE11-P9DUB382-13GZ-100T-145-T6-2831         lattice-1
9b  62  GE11-P9DUB382-13GZ-100T-145-T6-2831         lattice-2
9b  63  GE11-P9DUB382-13GZ-100T-145-T6-2831         lattice-3
9b  71  GE11-P9DUB381-13GZ-100T-145-T6-2945         lattice-1
9b  72  GE11-P9DUB381-13GZ-100T-145-T6-2945         lattice-2
9b  73  GE11-P9DUB381-13GZ-100T-145-T6-2945         lattice-3
9b  81  GE11-P9DUB381-14GZ-100T-145-T6-2946         lattice-1
9b  82  GE11-P9DUB381-14GZ-100T-145-T6-2946         lattice-2
9b  83  GE11-P9DUB381-14GZ-100T-145-T6-2946         lattice-3
9b  91  GE11-P9DUB380-13GZ-100T-145-T6-2948         lattice-1
9b  92  GE11-P9DUB380-13GZ-100T-145-T6-2948         lattice-2
9b  93  GE11-P9DUB380-13GZ-100T-145-T6-2948         lattice-3
9b  a1  GE11-P9DUB376-12GZ-100T-145-T6-2586         lattice-1
9b  a2  GE11-P9DUB376-12GZ-100T-145-T6-2586         lattice-2
#
# ------------------------------------------------------------------------------
# 10x10A
10a 11  GNF2-P10DG2B384-16GZ-100T2-145-T6-3351       lattice-1
10a 12  GNF2-P10DG2B384-16GZ-100T2-145-T6-3351       lattice-2
10a 13  GNF2-P10DG2B384-16GZ-100T2-145-T6-3351       lattice-3
10a 14  GNF2-P10DG2B384-16GZ-100T2-145-T6-3351       lattice-4
10a 15  GNF2-P10DG2B384-16GZ-100T2-145-T6-3351       lattice-5
10a 21  GNF2-P10DG2B386-13GZ-100T2-145-T6-3352       lattice-1
10a 22  GNF2-P10DG2B386-13GZ-100T2-145-T6-3352       lattice-2
10a 23  GNF2-P10DG2B386-13GZ-100T2-145-T6-3352       lattice-3
10a 24  GNF2-P10DG2B386-13GZ-100T2-145-T6-3352       lattice-4
10a 25  GNF2-P10DG2B386-13GZ-100T2-145-T6-3352       lattice-5
10a 31  GNF2-P10DG2B384-16GZ-100T2-145-T6-4133       lattice-1
10a 32  GNF2-P10DG2B384-16GZ-100T2-145-T6-4133       lattice-2
10a 33  GNF2-P10DG2B384-16GZ-100T2-145-T6-4133       lattice-3
10a 34  GNF2-P10DG2B384-16GZ-100T2-145-T6-4133       lattice-4
10a 35  GNF2-P10DG2B384-16GZ-100T2-145-T6-4133       lattice-5
10a 41  GNF2-P10DG2B386-13GZ-100T2-145-T6-4134       lattice-1
```

10a 42 GNF2-P10DG2B386-13GZ-100T2-145-T6-4134 lattice-2
10a 43 GNF2-P10DG2B386-13GZ-100T2-145-T6-4134 lattice-3
10a 44 GNF2-P10DG2B386-13GZ-100T2-145-T6-4134 lattice-4
10a 45 GNF2-P10DG2B386-13GZ-100T2-145-T6-4134 lattice-5
10a 51 GNF2-P10DG2B371-16GZ-100T2-145-T6-4312 lattice-1
10a 52 GNF2-P10DG2B371-16GZ-100T2-145-T6-4312 lattice-2
10a 53 GNF2-P10DG2B371-16GZ-100T2-145-T6-4312 lattice-3
10a 54 GNF2-P10DG2B371-16GZ-100T2-145-T6-4312 lattice-4
10a 55 GNF2-P10DG2B371-16GZ-100T2-145-T6-4312 lattice-5
10a 61 GNF2-P10DG2B375-11G5.0-100T2-145-T6-4313 lattice-1
10a 62 GNF2-P10DG2B375-11G5.0-100T2-145-T6-4313 lattice-2
10a 63 GNF2-P10DG2B375-11G5.0-100T2-145-T6-4313 lattice-3
10a 64 GNF2-P10DG2B375-11G5.0-100T2-145-T6-4313 lattice-4
10a 65 GNF2-P10DG2B375-11G5.0-100T2-145-T6-4313 lattice-5
10a 71 GNF2-P10DG2B371-12G5.0_4G4.0-100T2-145-T6-4482 lattice-1
10a 72 GNF2-P10DG2B371-12G5.0_4G4.0-100T2-145-T6-4482 lattice-2
10a 73 GNF2-P10DG2B371-12G5.0_4G4.0-100T2-145-T6-4482 lattice-3
10a 74 GNF2-P10DG2B371-12G5.0_4G4.0-100T2-145-T6-4482 lattice-4
10a 75 GNF2-P10DG2B371-12G5.0_4G4.0-100T2-145-T6-4482 lattice-5
10a 81 GNF2-P10DG2B377-12GZ-100T2-145-T6-4483 lattice-1
10a 82 GNF2-P10DG2B377-12GZ-100T2-145-T6-4483 lattice-2
10a 83 GNF2-P10DG2B377-12GZ-100T2-145-T6-4483 lattice-3
10a 84 GNF2-P10DG2B377-12GZ-100T2-145-T6-4483 lattice-4
10a 85 GNF2-P10DG2B377-12GZ-100T2-145-T6-4483 lattice-5
10a 91 GNF2-P10DG2B373-14GZ-100T2-145-T6-4484 lattice-1
10a 92 GNF2-P10DG2B373-14GZ-100T2-145-T6-4484 lattice-2
10a 93 GNF2-P10DG2B373-14GZ-100T2-145-T6-4484 lattice-3
10a 94 GNF2-P10DG2B373-14GZ-100T2-145-T6-4484 lattice-4
10a 95 GNF2-P10DG2B373-14GZ-100T2-145-T6-4484 lattice-5

Table A.2
Post Processing Summary for CASMO SCCG COP Screening Calculations[1]

* Peak Reactivity for 07a00 at mnu: 1.2374 / 07a00-mnu-sccg-5-Decay-0.0-0.00
* Peak Reactivity for 07a00 at mnr: 1.2374 / 07a00-mnr-sccg-5-Decay-0.0-0.00
* Peak Reactivity for 07a00 at mxu: 1.2374 / 07a00-mxu-sccg-5-Decay-0.0-0.00
* Peak Reactivity for 07a00 at mxr: 1.2374 / 07a00-mxr-sccg-5-Decay-0.0-0.00
* Final Peak Reactivity for 07a00: 1.2374 / 07a00-mxr-sccg-5-Decay-0.0-0.00
* Peak Reactivity for 07b10 at mnu: 1.2283 / 07b10-mnu-sccg-5-Decay-0.0-3.00
* Peak Reactivity for 07b10 at mnr: 1.2388 / 07b10-mnr-sccg-5-Decay-0.0-3.00
* Peak Reactivity for 07b10 at mxu: 1.2267 / 07b10-mxu-sccg-5-Decay-0.0-4.00
* Peak Reactivity for 07b10 at mxr: 1.2400 / 07b10-mxr-sccg-5-Decay-0.0-5.00
* Final Peak Reactivity for 07b10: 1.2400 / 07b10-mxr-sccg-5-Decay-0.0-5.00
* Peak Reactivity for 07b20 at mnu: 1.1586 / 07b20-mnu-sccg-5-Decay-0.0-6.00
* Peak Reactivity for 07b20 at mnr: 1.1770 / 07b20-mnr-sccg-5-Decay-0.0-5.50
* Peak Reactivity for 07b20 at mxu: 1.1676 / 07b20-mxu-sccg-5-Decay-0.0-7.50
* Peak Reactivity for 07b20 at mxr: 1.1939 / 07b20-mxr-sccg-5-Decay-0.0-9.00
* Final Peak Reactivity for 07b20: 1.1939 / 07b20-mxr-sccg-5-Decay-0.0-9.00
* Peak Reactivity for 07c00 at mnu: 1.2059 / 07c00-mnu-sccg-5-Decay-0.0-4.50
* Peak Reactivity for 07c00 at mnr: 1.2097 / 07c00-mnr-sccg-5-Decay-0.0-5.00
* Peak Reactivity for 07c00 at mxu: 1.2066 / 07c00-mxu-sccg-5-Decay-0.0-5.50
* Peak Reactivity for 07c00 at mxr: 1.2156 / 07c00-mxr-sccg-5-Decay-0.0-8.00
* Final Peak Reactivity for 07c00: 1.2156 / 07c00-mxr-sccg-5-Decay-0.0-8.00
* Peak Reactivity for 08a10 at mnu: 1.2244 / 08a10-mnu-sccg-5-Decay-0.0-4.00
* Peak Reactivity for 08a10 at mnr: 1.2311 / 08a10-mnr-sccg-5-Decay-0.0-4.00
* Peak Reactivity for 08a10 at mxu: 1.2253 / 08a10-mxu-sccg-5-Decay-0.0-5.00
* Peak Reactivity for 08a10 at mxr: 1.2340 / 08a10-mxr-sccg-5-Decay-0.0-6.00
* Final Peak Reactivity for 08a10: 1.2340 / 08a10-mxr-sccg-5-Decay-0.0-6.00
* Peak Reactivity for 08a20 at mnu: 1.2133 / 08a20-mnu-sccg-5-Decay-0.0-4.00
* Peak Reactivity for 08a20 at mnr: 1.2197 / 08a20-mnr-sccg-5-Decay-0.0-4.00
* Peak Reactivity for 08a20 at mxu: 1.2150 / 08a20-mxu-sccg-5-Decay-0.0-5.00
* Peak Reactivity for 08a20 at mxr: 1.2250 / 08a20-mxr-sccg-5-Decay-0.0-5.50
* Final Peak Reactivity for 08a20: 1.2250 / 08a20-mxr-sccg-5-Decay-0.0-5.50
* Peak Reactivity for 08a30 at mnu: 1.2208 / 08a30-mnu-sccg-5-Decay-0.0-5.00
* Peak Reactivity for 08a30 at mnr: 1.2175 / 08a30-mnr-sccg-5-Decay-0.0-5.50
* Peak Reactivity for 08a30 at mxu: 1.2219 / 08a30-mxu-sccg-5-Decay-0.0-6.00
* Peak Reactivity for 08a30 at mxr: 1.2208 / 08a30-mxr-sccg-5-Decay-0.0-8.50
* Final Peak Reactivity for 08a30: 1.2219 / 08a30-mxu-sccg-5-Decay-0.0-6.00
* Peak Reactivity for 08a40 at mnu: 1.1970 / 08a40-mnu-sccg-5-Decay-0.0-7.00
* Peak Reactivity for 08a40 at mnr: 1.1928 / 08a40-mnr-sccg-5-Decay-0.0-7.00
* Peak Reactivity for 08a40 at mxu: 1.2016 / 08a40-mxu-sccg-5-Decay-0.0-8.00
* Peak Reactivity for 08a40 at mxr: 1.2029 / 08a40-mxr-sccg-5-Decay-0.0-10.00
* Final Peak Reactivity for 08a40: 1.2029 / 08a40-mxr-sccg-5-Decay-0.0-10.00

[1] The data in this table is used solely for screening lattices. The reactivity of the lattices using CASMO-5 is not used for the design basis analysis.

* Peak Reactivity for 08b11 at mnu: 1.2035 / 08b11-mnu-sccg-5-Decay-0.0-0.00
* Peak Reactivity for 08b11 at mnr: 1.2035 / 08b11-mnr-sccg-5-Decay-0.0-0.00
* Peak Reactivity for 08b11 at mxu: 1.2035 / 08b11-mxu-sccg-5-Decay-0.0-0.00
* Peak Reactivity for 08b11 at mxr: 1.2035 / 08b11-mxr-sccg-5-Decay-0.0-0.00
* Final Peak Reactivity for 08b11: 1.2035 / 08b11-mxr-sccg-5-Decay-0.0-0.00
* Peak Reactivity for 08b12 at mnu: 1.1935 / 08b12-mnu-sccg-5-Decay-0.0-7.50
* Peak Reactivity for 08b12 at mnr: 1.1899 / 08b12-mnr-sccg-5-Decay-0.0-7.00
* Peak Reactivity for 08b12 at mxu: 1.1909 / 08b12-mxu-sccg-5-Decay-0.0-9.50
* Peak Reactivity for 08b12 at mxr: 1.1977 / 08b12-mxr-sccg-5-Decay-0.0-11.00
* Final Peak Reactivity for 08b12: 1.1977 / 08b12-mxr-sccg-5-Decay-0.0-11.00
* Peak Reactivity for 08b13 at mnu: 1.1967 / 08b13-mnu-sccg-5-Decay-0.0-7.50
* Peak Reactivity for 08b13 at mnr: 1.1968 / 08b13-mnr-sccg-5-Decay-0.0-7.00
* Peak Reactivity for 08b13 at mxu: 1.1974 / 08b13-mxu-sccg-5-Decay-0.0-9.00
* Peak Reactivity for 08b13 at mxr: 1.2060 / 08b13-mxr-sccg-5-Decay-0.0-10.50
* Final Peak Reactivity for 08b13: 1.2060 / 08b13-mxr-sccg-5-Decay-0.0-10.50
* Peak Reactivity for 08b20 at mnu: 1.1965 / 08b20-mnu-sccg-5-Decay-0.0-10.00
* Peak Reactivity for 08b20 at mnr: 1.1943 / 08b20-mnr-sccg-5-Decay-0.0-10.50
* Peak Reactivity for 08b20 at mxu: 1.1951 / 08b20-mxu-sccg-5-Decay-0.0-11.50
* Peak Reactivity for 08b20 at mxr: 1.2004 / 08b20-mxr-sccg-5-Decay-0.0-15.00
* Final Peak Reactivity for 08b20: 1.2004 / 08b20-mxr-sccg-5-Decay-0.0-15.00
* Peak Reactivity for 08c11 at mnu: 1.1868 / 08c11-mnu-sccg-5-Decay-0.0-12.50
* Peak Reactivity for 08c11 at mnr: 1.1914 / 08c11-mnr-sccg-5-Decay-0.0-13.50
* Peak Reactivity for 08c11 at mxu: 1.1863 / 08c11-mxu-sccg-5-Decay-0.0-14.50
* Peak Reactivity for 08c11 at mxr: 1.1944 / 08c11-mxr-sccg-5-Decay-0.0-17.50
* Final Peak Reactivity for 08c11: 1.1944 / 08c11-mxr-sccg-5-Decay-0.0-18.00
* Peak Reactivity for 08c12 at mnu: 1.2106 / 08c12-mnu-sccg-5-Decay-0.0-11.00
* Peak Reactivity for 08c12 at mnr: 1.2143 / 08c12-mnr-sccg-5-Decay-0.0-11.50
* Peak Reactivity for 08c12 at mxu: 1.2070 / 08c12-mxu-sccg-5-Decay-0.0-12.50
* Peak Reactivity for 08c12 at mxr: 1.2118 / 08c12-mxr-sccg-5-Decay-0.0-15.50
* Final Peak Reactivity for 08c12: 1.2143 / 08c12-mnr-sccg-5-Decay-0.0-11.50
* Peak Reactivity for 08c21 at mnu: 1.1999 / 08c21-mnu-sccg-5-Decay-0.0-13.00
* Peak Reactivity for 08c21 at mnr: 1.1873 / 08c21-mnr-sccg-5-Decay-0.0-14.50
* Peak Reactivity for 08c21 at mxu: 1.1957 / 08c21-mxu-sccg-5-Decay-0.0-15.00
* Peak Reactivity for 08c21 at mxr: 1.1875 / 08c21-mxr-sccg-5-Decay-0.0-19.00
* Final Peak Reactivity for 08c21: 1.1999 / 08c21-mnu-sccg-5-Decay-0.0-13.00
* Peak Reactivity for 08c22 at mnu: 1.2236 / 08c22-mnu-sccg-5-Decay-0.0-11.00
* Peak Reactivity for 08c22 at mnr: 1.2118 / 08c22-mnr-sccg-5-Decay-0.0-12.50
* Peak Reactivity for 08c22 at mxu: 1.2167 / 08c22-mxu-sccg-5-Decay-0.0-13.00
* Peak Reactivity for 08c22 at mxr: 1.2064 / 08c22-mxr-sccg-5-Decay-0.0-17.00
* Final Peak Reactivity for 08c22: 1.2236 / 08c22-mnu-sccg-5-Decay-0.0-11.00
* Peak Reactivity for 08c23 at mnu: 1.2040 / 08c23-mnu-sccg-5-Decay-0.0-12.50
* Peak Reactivity for 08c23 at mnr: 1.1975 / 08c23-mnr-sccg-5-Decay-0.0-13.50
* Peak Reactivity for 08c23 at mxu: 1.1920 / 08c23-mxu-sccg-5-Decay-0.0-15.50
* Peak Reactivity for 08c23 at mxr: 1.1859 / 08c23-mxr-sccg-5-Decay-0.0-19.50
* Final Peak Reactivity for 08c23: 1.2040 / 08c23-mnu-sccg-5-Decay-0.0-12.50
* Peak Reactivity for 09a11 at mnu: 1.1934 / 09a11-mnu-sccg-5-Decay-0.0-12.00

* Peak Reactivity for 09a11 at mnr: 1.1920 / 09a11-mnr-sccg-5-Decay-0.0-12.50
* Peak Reactivity for 09a11 at mxu: 1.1922 / 09a11-mxu-sccg-5-Decay-0.0-14.00
* Peak Reactivity for 09a11 at mxr: 1.1913 / 09a11-mxr-sccg-5-Decay-0.0-16.50
* Final Peak Reactivity for 09a11: 1.1934 / 09a11-mnu-sccg-5-Decay-0.0-12.00
* Peak Reactivity for 09a12 at mnu: 1.2008 / 09a12-mnu-sccg-5-Decay-0.0-12.00
* Peak Reactivity for 09a12 at mnr: 1.1913 / 09a12-mnr-sccg-5-Decay-0.0-12.50
* Peak Reactivity for 09a12 at mxu: 1.2006 / 09a12-mxu-sccg-5-Decay-0.0-13.50
* Peak Reactivity for 09a12 at mxr: 1.1929 / 09a12-mxr-sccg-5-Decay-0.0-16.00
* Final Peak Reactivity for 09a12: 1.2008 / 09a12-mnu-sccg-5-Decay-0.0-12.00
* Peak Reactivity for 09a13 at mnu: 1.1991 / 09a13-mnu-sccg-5-Decay-0.0-11.50
* Peak Reactivity for 09a13 at mnr: 1.1858 / 09a13-mnr-sccg-5-Decay-0.0-12.00
* Peak Reactivity for 09a13 at mxu: 1.1991 / 09a13-mxu-sccg-5-Decay-0.0-13.50
* Peak Reactivity for 09a13 at mxr: 1.1901 / 09a13-mxr-sccg-5-Decay-0.0-15.50
* Final Peak Reactivity for 09a13: 1.1991 / 09a13-mxu-sccg-5-Decay-0.0-13.50
* Peak Reactivity for 09a21 at mnu: 1.1859 / 09a21-mnu-sccg-5-Decay-0.0-14.50
* Peak Reactivity for 09a21 at mnr: 1.1922 / 09a21-mnr-sccg-5-Decay-0.0-15.50
* Peak Reactivity for 09a21 at mxu: 1.1860 / 09a21-mxu-sccg-5-Decay-0.0-16.50
* Peak Reactivity for 09a21 at mxr: 1.1853 / 09a21-mxr-sccg-5-Decay-0.0-20.00
* Final Peak Reactivity for 09a21: 1.1922 / 09a21-mnr-sccg-5-Decay-0.0-15.50
* Peak Reactivity for 09a22 at mnu: 1.1859 / 09a22-mnu-sccg-5-Decay-0.0-14.50
* Peak Reactivity for 09a22 at mnr: 1.2031 / 09a22-mnr-sccg-5-Decay-0.0-15.00
* Peak Reactivity for 09a22 at mxu: 1.1873 / 09a22-mxu-sccg-5-Decay-0.0-16.00
* Peak Reactivity for 09a22 at mxr: 1.1961 / 09a22-mxr-sccg-5-Decay-0.0-19.50
* Final Peak Reactivity for 09a22: 1.2031 / 09a22-mnr-sccg-5-Decay-0.0-15.00
* Peak Reactivity for 09a23 at mnu: 1.1851 / 09a23-mnu-sccg-5-Decay-0.0-14.00
* Peak Reactivity for 09a23 at mnr: 1.2049 / 09a23-mnr-sccg-5-Decay-0.0-14.50
* Peak Reactivity for 09a23 at mxu: 1.1863 / 09a23-mxu-sccg-5-Decay-0.0-16.50
* Peak Reactivity for 09a23 at mxr: 1.1972 / 09a23-mxr-sccg-5-Decay-0.0-19.50
* Final Peak Reactivity for 09a23: 1.2049 / 09a23-mnr-sccg-5-Decay-0.0-14.50
* Peak Reactivity for 09b11 at mnu: 1.1903 / 09b11-mnu-sccg-5-Decay-0.0-14.50
* Peak Reactivity for 09b11 at mnr: 1.1964 / 09b11-mnr-sccg-5-Decay-0.0-15.50
* Peak Reactivity for 09b11 at mxu: 1.1892 / 09b11-mxu-sccg-5-Decay-0.0-17.00
* Peak Reactivity for 09b11 at mxr: 1.1878 / 09b11-mxr-sccg-5-Decay-0.0-20.00
* Final Peak Reactivity for 09b11: 1.1964 / 09b11-mnr-sccg-5-Decay-0.0-15.50
* Peak Reactivity for 09b12 at mnu: 1.1902 / 09b12-mnu-sccg-5-Decay-0.0-14.50
* Peak Reactivity for 09b12 at mnr: 1.2072 / 09b12-mnr-sccg-5-Decay-0.0-15.00
* Peak Reactivity for 09b12 at mxu: 1.1905 / 09b12-mxu-sccg-5-Decay-0.0-16.50
* Peak Reactivity for 09b12 at mxr: 1.1987 / 09b12-mxr-sccg-5-Decay-0.0-19.50
* Final Peak Reactivity for 09b12: 1.2072 / 09b12-mnr-sccg-5-Decay-0.0-15.00
* Peak Reactivity for 09b13 at mnu: 1.1897 / 09b13-mnu-sccg-5-Decay-0.0-14.00
* Peak Reactivity for 09b13 at mnr: 1.2092 / 09b13-mnr-sccg-5-Decay-0.0-14.50
* Peak Reactivity for 09b13 at mxu: 1.1898 / 09b13-mxu-sccg-5-Decay-0.0-16.50
* Peak Reactivity for 09b13 at mxr: 1.2000 / 09b13-mxr-sccg-5-Decay-0.0-19.50
* Final Peak Reactivity for 09b13: 1.2092 / 09b13-mnr-sccg-5-Decay-0.0-14.50
* Peak Reactivity for 09b21 at mnu: 1.1852 / 09b21-mnu-sccg-5-Decay-0.0-15.50
* Peak Reactivity for 09b21 at mnr: 1.1793 / 09b21-mnr-sccg-5-Decay-0.0-15.50

* Peak Reactivity for 09b21 at mxu: 1.1827 / 09b21-mxu-sccg-5-Decay-0.0-18.50
* Peak Reactivity for 09b21 at mxr: 1.1756 / 09b21-mxr-sccg-5-Decay-0.0-21.00
* Final Peak Reactivity for 09b21: 1.1852 / 09b21-mnu-sccg-5-Decay-0.0-15.50
* Peak Reactivity for 09b22 at mnu: 1.1907 / 09b22-mnu-sccg-5-Decay-0.0-15.00
* Peak Reactivity for 09b22 at mnr: 1.1783 / 09b22-mnr-sccg-5-Decay-0.0-15.50
* Peak Reactivity for 09b22 at mxu: 1.1901 / 09b22-mxu-sccg-5-Decay-0.0-18.00
* Peak Reactivity for 09b22 at mxr: 1.1770 / 09b22-mxr-sccg-5-Decay-0.0-20.50
* Final Peak Reactivity for 09b22: 1.1907 / 09b22-mnu-sccg-5-Decay-0.0-15.00
* Peak Reactivity for 09b23 at mnu: 1.1894 / 09b23-mnu-sccg-5-Decay-0.0-14.50
* Peak Reactivity for 09b23 at mnr: 1.1740 / 09b23-mnr-sccg-5-Decay-0.0-16.00
* Peak Reactivity for 09b23 at mxu: 1.1912 / 09b23-mxu-sccg-5-Decay-0.0-17.00
* Peak Reactivity for 09b23 at mxr: 1.1742 / 09b23-mxr-sccg-5-Decay-0.0-20.50
* Final Peak Reactivity for 09b23: 1.1912 / 09b23-mxu-sccg-5-Decay-0.0-17.00
* Peak Reactivity for 09b31 at mnu: 1.1913 / 09b31-mnu-sccg-5-Decay-0.0-16.50
* Peak Reactivity for 09b31 at mnr: 1.1907 / 09b31-mnr-sccg-5-Decay-0.0-16.50
* Peak Reactivity for 09b31 at mxu: 1.1851 / 09b31-mxu-sccg-5-Decay-0.0-19.50
* Peak Reactivity for 09b31 at mxr: 1.1801 / 09b31-mxr-sccg-5-Decay-0.0-22.00
* Final Peak Reactivity for 09b31: 1.1913 / 09b31-mnu-sccg-5-Decay-0.0-16.50
* Peak Reactivity for 09b32 at mnu: 1.1986 / 09b32-mnu-sccg-5-Decay-0.0-16.00
* Peak Reactivity for 09b32 at mnr: 1.1901 / 09b32-mnr-sccg-5-Decay-0.0-16.50
* Peak Reactivity for 09b32 at mxu: 1.1938 / 09b32-mxu-sccg-5-Decay-0.0-19.00
* Peak Reactivity for 09b32 at mxr: 1.1820 / 09b32-mxr-sccg-5-Decay-0.0-21.50
* Final Peak Reactivity for 09b32: 1.1986 / 09b32-mnu-sccg-5-Decay-0.0-16.00
* Peak Reactivity for 09b33 at mnu: 1.1985 / 09b33-mnu-sccg-5-Decay-0.0-15.00
* Peak Reactivity for 09b33 at mnr: 1.1877 / 09b33-mnr-sccg-5-Decay-0.0-16.50
* Peak Reactivity for 09b33 at mxu: 1.1959 / 09b33-mxu-sccg-5-Decay-0.0-18.00
* Peak Reactivity for 09b33 at mxr: 1.1811 / 09b33-mxr-sccg-5-Decay-0.0-21.50
* Final Peak Reactivity for 09b33: 1.1985 / 09b33-mnu-sccg-5-Decay-0.0-15.50
* Peak Reactivity for 09b41 at mnu: 1.2049 / 09b41-mnu-sccg-5-Decay-0.0-17.00
* Peak Reactivity for 09b41 at mnr: 1.2015 / 09b41-mnr-sccg-5-Decay-0.0-17.00
* Peak Reactivity for 09b41 at mxu: 1.1971 / 09b41-mxu-sccg-5-Decay-0.0-19.50
* Peak Reactivity for 09b41 at mxr: 1.1888 / 09b41-mxr-sccg-5-Decay-0.0-22.00
* Final Peak Reactivity for 09b41: 1.2049 / 09b41-mnu-sccg-5-Decay-0.0-17.00
* Peak Reactivity for 09b42 at mnu: 1.2126 / 09b42-mnu-sccg-5-Decay-0.0-15.50
* Peak Reactivity for 09b42 at mnr: 1.1995 / 09b42-mnr-sccg-5-Decay-0.0-17.00
* Peak Reactivity for 09b42 at mxu: 1.2084 / 09b42-mxu-sccg-5-Decay-0.0-18.50
* Peak Reactivity for 09b42 at mxr: 1.1901 / 09b42-mxr-sccg-5-Decay-0.0-22.00
* Final Peak Reactivity for 09b42: 1.2126 / 09b42-mnu-sccg-5-Decay-0.0-15.50
* Peak Reactivity for 09b51 at mnu: 1.2049 / 09b51-mnu-sccg-5-Decay-0.0-17.00
* Peak Reactivity for 09b51 at mnr: 1.2015 / 09b51-mnr-sccg-5-Decay-0.0-17.00
* Peak Reactivity for 09b51 at mxu: 1.1971 / 09b51-mxu-sccg-5-Decay-0.0-19.50
* Peak Reactivity for 09b51 at mxr: 1.1888 / 09b51-mxr-sccg-5-Decay-0.0-22.00
* Final Peak Reactivity for 09b51: 1.2049 / 09b51-mnu-sccg-5-Decay-0.0-17.00
* Peak Reactivity for 09b52 at mnu: 1.2164 / 09b52-mnu-sccg-5-Decay-0.0-15.50
* Peak Reactivity for 09b52 at mnr: 1.1991 / 09b52-mnr-sccg-5-Decay-0.0-17.00
* Peak Reactivity for 09b52 at mxu: 1.2153 / 09b52-mxu-sccg-5-Decay-0.0-17.50

* Peak Reactivity for 09b52 at mxr: 1.1915 / 09b52-mxr-sccg-5-Decay-0.0-21.00
* Final Peak Reactivity for 09b52: 1.2164 / 09b52-mnu-sccg-5-Decay-0.0-15.50
* Peak Reactivity for 09b61 at mnu: 1.2084 / 09b61-mnu-sccg-5-Decay-0.0-17.00
* Peak Reactivity for 09b61 at mnr: 1.2021 / 09b61-mnr-sccg-5-Decay-0.0-17.00
* Peak Reactivity for 09b61 at mxu: 1.1980 / 09b61-mxu-sccg-5-Decay-0.0-20.00
* Peak Reactivity for 09b61 at mxr: 1.1868 / 09b61-mxr-sccg-5-Decay-0.0-22.50
* Final Peak Reactivity for 09b61: 1.2084 / 09b61-mnu-sccg-5-Decay-0.0-17.00
* Peak Reactivity for 09b62 at mnu: 1.2215 / 09b62-mnu-sccg-5-Decay-0.0-16.00
* Peak Reactivity for 09b62 at mnr: 1.2086 / 09b62-mnr-sccg-5-Decay-0.0-15.50
* Peak Reactivity for 09b62 at mxu: 1.2105 / 09b62-mxu-sccg-5-Decay-0.0-19.00
* Peak Reactivity for 09b62 at mxr: 1.1941 / 09b62-mxr-sccg-5-Decay-0.0-21.00
* Final Peak Reactivity for 09b62: 1.2215 / 09b62-mnu-sccg-5-Decay-0.0-16.00
* Peak Reactivity for 09b63 at mnu: 1.2260 / 09b63-mnu-sccg-5-Decay-0.0-15.00
* Peak Reactivity for 09b63 at mnr: 1.2043 / 09b63-mnr-sccg-5-Decay-0.0-16.50
* Peak Reactivity for 09b63 at mxu: 1.2192 / 09b63-mxu-sccg-5-Decay-0.0-18.00
* Peak Reactivity for 09b63 at mxr: 1.1936 / 09b63-mxr-sccg-5-Decay-0.0-20.50
* Final Peak Reactivity for 09b63: 1.2260 / 09b63-mnu-sccg-5-Decay-0.0-15.00
* Peak Reactivity for 09b71 at mnu: 1.2079 / 09b71-mnu-sccg-5-Decay-0.0-17.00
* Peak Reactivity for 09b71 at mnr: 1.2019 / 09b71-mnr-sccg-5-Decay-0.0-17.00
* Peak Reactivity for 09b71 at mxu: 1.1975 / 09b71-mxu-sccg-5-Decay-0.0-20.00
* Peak Reactivity for 09b71 at mxr: 1.1864 / 09b71-mxr-sccg-5-Decay-0.0-22.50
* Final Peak Reactivity for 09b71: 1.2079 / 09b71-mnu-sccg-5-Decay-0.0-17.00
* Peak Reactivity for 09b72 at mnu: 1.2169 / 09b72-mnu-sccg-5-Decay-0.0-16.00
* Peak Reactivity for 09b72 at mnr: 1.2100 / 09b72-mnr-sccg-5-Decay-0.0-16.00
* Peak Reactivity for 09b72 at mxu: 1.2084 / 09b72-mxu-sccg-5-Decay-0.0-19.00
* Peak Reactivity for 09b72 at mxr: 1.1947 / 09b72-mxr-sccg-5-Decay-0.0-21.00
* Final Peak Reactivity for 09b72: 1.2169 / 09b72-mnu-sccg-5-Decay-0.0-16.00
* Peak Reactivity for 09b73 at mnu: 1.2214 / 09b73-mnu-sccg-5-Decay-0.0-15.00
* Peak Reactivity for 09b73 at mnr: 1.2053 / 09b73-mnr-sccg-5-Decay-0.0-15.50
* Peak Reactivity for 09b73 at mxu: 1.2206 / 09b73-mxu-sccg-5-Decay-0.0-17.50
* Peak Reactivity for 09b73 at mxr: 1.1959 / 09b73-mxr-sccg-5-Decay-0.0-20.50
* Final Peak Reactivity for 09b73: 1.2214 / 09b73-mnu-sccg-5-Decay-0.0-15.00
* Peak Reactivity for 09b81 at mnu: 1.2279 / 09b81-mnu-sccg-5-Decay-0.0-15.00
* Peak Reactivity for 09b81 at mnr: 1.2234 / 09b81-mnr-sccg-5-Decay-0.0-15.50
* Peak Reactivity for 09b81 at mxu: 1.2136 / 09b81-mxu-sccg-5-Decay-0.0-18.00
* Peak Reactivity for 09b81 at mxr: 1.2022 / 09b81-mxr-sccg-5-Decay-0.0-20.50
* Final Peak Reactivity for 09b81: 1.2279 / 09b81-mnu-sccg-5-Decay-0.0-15.00
* Peak Reactivity for 09b82 at mnu: 1.2291 / 09b82-mnu-sccg-5-Decay-0.0-15.00
* Peak Reactivity for 09b82 at mnr: 1.2388 / 09b82-mnr-sccg-5-Decay-0.0-14.50
* Peak Reactivity for 09b82 at mxu: 1.2162 / 09b82-mxu-sccg-5-Decay-0.0-17.50
* Peak Reactivity for 09b82 at mxr: 1.2129 / 09b82-mxr-sccg-5-Decay-0.0-20.50
* Final Peak Reactivity for 09b82: 1.2388 / 09b82-mnr-sccg-5-Decay-0.0-14.50
* Peak Reactivity for 09b83 at mnu: 1.2364 / 09b83-mnu-sccg-5-Decay-0.0-14.00
* Peak Reactivity for 09b83 at mnr: 1.2387 / 09b83-mnr-sccg-5-Decay-0.0-14.00
* Peak Reactivity for 09b83 at mxu: 1.2275 / 09b83-mxu-sccg-5-Decay-0.0-16.50
* Peak Reactivity for 09b83 at mxr: 1.2180 / 09b83-mxr-sccg-5-Decay-0.0-19.50

* Final Peak Reactivity for 09b83: 1.2387 / 09b83-mnr-sccg-5-Decay-0.0-14.00
* Peak Reactivity for 09b91 at mnu: 1.1838 / 09b91-mnu-sccg-5-Decay-0.0-19.00
* Peak Reactivity for 09b91 at mnr: 1.1852 / 09b91-mnr-sccg-5-Decay-0.0-18.50
* Peak Reactivity for 09b91 at mxu: 1.1766 / 09b91-mxu-sccg-5-Decay-0.0-22.00
* Peak Reactivity for 09b91 at mxr: 1.1725 / 09b91-mxr-sccg-5-Decay-0.0-25.00
* Final Peak Reactivity for 09b91: 1.1852 / 09b91-mnr-sccg-5-Decay-0.0-18.50
* Peak Reactivity for 09b92 at mnu: 1.2055 / 09b92-mnu-sccg-5-Decay-0.0-17.00
* Peak Reactivity for 09b92 at mnr: 1.2193 / 09b92-mnr-sccg-5-Decay-0.0-16.50
* Peak Reactivity for 09b92 at mxu: 1.1956 / 09b92-mxu-sccg-5-Decay-0.0-20.00
* Peak Reactivity for 09b92 at mxr: 1.1970 / 09b92-mxr-sccg-5-Decay-0.0-22.50
* Final Peak Reactivity for 09b92: 1.2193 / 09b92-mnr-sccg-5-Decay-0.0-16.50
* Peak Reactivity for 09b93 at mnu: 1.2089 / 09b93-mnu-sccg-5-Decay-0.0-16.00
* Peak Reactivity for 09b93 at mnr: 1.2199 / 09b93-mnr-sccg-5-Decay-0.0-16.00
* Peak Reactivity for 09b93 at mxu: 1.2032 / 09b93-mxu-sccg-5-Decay-0.0-19.00
* Peak Reactivity for 09b93 at mxr: 1.2022 / 09b93-mxr-sccg-5-Decay-0.0-22.00
* Final Peak Reactivity for 09b93: 1.2199 / 09b93-mnr-sccg-5-Decay-0.0-16.00
* Peak Reactivity for 09ba1 at mnu: 1.2049 / 09ba1-mnu-sccg-5-Decay-0.0-16.50
* Peak Reactivity for 09ba1 at mnr: 1.2014 / 09ba1-mnr-sccg-5-Decay-0.0-16.50
* Peak Reactivity for 09ba1 at mxu: 1.1971 / 09ba1-mxu-sccg-5-Decay-0.0-19.50
* Peak Reactivity for 09ba1 at mxr: 1.1887 / 09ba1-mxr-sccg-5-Decay-0.0-22.00
* Final Peak Reactivity for 09ba1: 1.2049 / 09ba1-mnu-sccg-5-Decay-0.0-17.00
* Peak Reactivity for 09ba2 at mnu: 1.2193 / 09ba2-mnu-sccg-5-Decay-0.0-15.00
* Peak Reactivity for 09ba2 at mnr: 1.2298 / 09ba2-mnr-sccg-5-Decay-0.0-14.50
* Peak Reactivity for 09ba2 at mxu: 1.2197 / 09ba2-mxu-sccg-5-Decay-0.0-16.50
* Peak Reactivity for 09ba2 at mxr: 1.2159 / 09ba2-mxr-sccg-5-Decay-0.0-20.00
* Final Peak Reactivity for 09ba2: 1.2298 / 09ba2-mnr-sccg-5-Decay-0.0-14.50
* Peak Reactivity for 10a11 at mnu: 1.2132 / 10a11-mnu-sccg-5-Decay-0.0-16.50
* Peak Reactivity for 10a11 at mnr: 1.2002 / 10a11-mnr-sccg-5-Decay-0.0-16.00
* Peak Reactivity for 10a11 at mxu: 1.2021 / 10a11-mxu-sccg-5-Decay-0.0-19.00
* Peak Reactivity for 10a11 at mxr: 1.1818 / 10a11-mxr-sccg-5-Decay-0.0-21.00
* Final Peak Reactivity for 10a11: 1.2132 / 10a11-mnu-sccg-5-Decay-0.0-16.50
* Peak Reactivity for 10a12 at mnu: 1.2194 / 10a12-mnu-sccg-5-Decay-0.0-15.50
* Peak Reactivity for 10a12 at mnr: 1.2114 / 10a12-mnr-sccg-5-Decay-0.0-15.50
* Peak Reactivity for 10a12 at mxu: 1.2064 / 10a12-mxu-sccg-5-Decay-0.0-18.50
* Peak Reactivity for 10a12 at mxr: 1.1902 / 10a12-mxr-sccg-5-Decay-0.0-21.00
* Final Peak Reactivity for 10a12: 1.2194 / 10a12-mnu-sccg-5-Decay-0.0-15.50
* Peak Reactivity for 10a13 at mnu: 1.2166 / 10a13-mnu-sccg-5-Decay-0.0-15.50
* Peak Reactivity for 10a13 at mnr: 1.2087 / 10a13-mnr-sccg-5-Decay-0.0-15.00
* Peak Reactivity for 10a13 at mxu: 1.2041 / 10a13-mxu-sccg-5-Decay-0.0-18.50
* Peak Reactivity for 10a13 at mxr: 1.1885 / 10a13-mxr-sccg-5-Decay-0.0-20.50
* Final Peak Reactivity for 10a13: 1.2166 / 10a13-mnu-sccg-5-Decay-0.0-15.50
* Peak Reactivity for 10a14 at mnu: 1.2131 / 10a14-mnu-sccg-5-Decay-0.0-14.50
* Peak Reactivity for 10a14 at mnr: 1.2032 / 10a14-mnr-sccg-5-Decay-0.0-15.50
* Peak Reactivity for 10a14 at mxu: 1.2068 / 10a14-mxu-sccg-5-Decay-0.0-17.00
* Peak Reactivity for 10a14 at mxr: 1.1909 / 10a14-mxr-sccg-5-Decay-0.0-18.50
* Final Peak Reactivity for 10a14: 1.2131 / 10a14-mnu-sccg-5-Decay-0.0-14.50

* Peak Reactivity for 10a15 at mnu: 1.2065 / 10a15-mnu-sccg-5-Decay-0.0-14.50
* Peak Reactivity for 10a15 at mnr: 1.2005 / 10a15-mnr-sccg-5-Decay-0.0-15.00
* Peak Reactivity for 10a15 at mxu: 1.2009 / 10a15-mxu-sccg-5-Decay-0.0-17.00
* Peak Reactivity for 10a15 at mxr: 1.1866 / 10a15-mxr-sccg-5-Decay-0.0-18.50
* Final Peak Reactivity for 10a15: 1.2065 / 10a15-mnu-sccg-5-Decay-0.0-14.50
* Peak Reactivity for 10a21 at mnu: 1.2149 / 10a21-mnu-sccg-5-Decay-0.0-16.50
* Peak Reactivity for 10a21 at mnr: 1.2171 / 10a21-mnr-sccg-5-Decay-0.0-15.50
* Peak Reactivity for 10a21 at mxu: 1.2054 / 10a21-mxu-sccg-5-Decay-0.0-19.00
* Peak Reactivity for 10a21 at mxr: 1.2002 / 10a21-mxr-sccg-5-Decay-0.0-20.00
* Final Peak Reactivity for 10a21: 1.2171 / 10a21-mnr-sccg-5-Decay-0.0-16.00
* Peak Reactivity for 10a22 at mnu: 1.2202 / 10a22-mnu-sccg-5-Decay-0.0-16.00
* Peak Reactivity for 10a22 at mnr: 1.2386 / 10a22-mnr-sccg-5-Decay-0.0-15.00
* Peak Reactivity for 10a22 at mxu: 1.2116 / 10a22-mxu-sccg-5-Decay-0.0-18.50
* Peak Reactivity for 10a22 at mxr: 1.2133 / 10a22-mxr-sccg-5-Decay-0.0-20.50
* Final Peak Reactivity for 10a22: 1.2386 / 10a22-mnr-sccg-5-Decay-0.0-15.00
* Peak Reactivity for 10a23 at mnu: 1.2174 / 10a23-mnu-sccg-5-Decay-0.0-15.50
* Peak Reactivity for 10a23 at mnr: 1.2366 / 10a23-mnr-sccg-5-Decay-0.0-14.50
* Peak Reactivity for 10a23 at mxu: 1.2088 / 10a23-mxu-sccg-5-Decay-0.0-18.00
* Peak Reactivity for 10a23 at mxr: 1.2117 / 10a23-mxr-sccg-5-Decay-0.0-20.00
* Final Peak Reactivity for 10a23: 1.2366 / 10a23-mnr-sccg-5-Decay-0.0-14.50
* Peak Reactivity for 10a24 at mnu: 1.2308 / 10a24-mnu-sccg-5-Decay-0.0-13.50
* Peak Reactivity for 10a24 at mnr: 1.2389 / 10a24-mnr-sccg-5-Decay-0.0-13.00
* Peak Reactivity for 10a24 at mxu: 1.2233 / 10a24-mxu-sccg-5-Decay-0.0-15.50
* Peak Reactivity for 10a24 at mxr: 1.2171 / 10a24-mxr-sccg-5-Decay-0.0-17.50
* Final Peak Reactivity for 10a24: 1.2389 / 10a24-mnr-sccg-5-Decay-0.0-13.00
* Peak Reactivity for 10a25 at mnu: 1.2237 / 10a25-mnu-sccg-5-Decay-0.0-13.50
* Peak Reactivity for 10a25 at mnr: 1.2319 / 10a25-mnr-sccg-5-Decay-0.0-13.00
* Peak Reactivity for 10a25 at mxu: 1.2175 / 10a25-mxu-sccg-5-Decay-0.0-15.50
* Peak Reactivity for 10a25 at mxr: 1.2121 / 10a25-mxr-sccg-5-Decay-0.0-17.50
* Final Peak Reactivity for 10a25: 1.2319 / 10a25-mnr-sccg-5-Decay-0.0-13.00
* Peak Reactivity for 10a31 at mnu: 1.2131 / 10a31-mnu-sccg-5-Decay-0.0-16.50
* Peak Reactivity for 10a31 at mnr: 1.2028 / 10a31-mnr-sccg-5-Decay-0.0-17.00
* Peak Reactivity for 10a31 at mxu: 1.2014 / 10a31-mxu-sccg-5-Decay-0.0-19.00
* Peak Reactivity for 10a31 at mxr: 1.1809 / 10a31-mxr-sccg-5-Decay-0.0-21.50
* Final Peak Reactivity for 10a31: 1.2131 / 10a31-mnu-sccg-5-Decay-0.0-16.50
* Peak Reactivity for 10a32 at mnu: 1.2194 / 10a32-mnu-sccg-5-Decay-0.0-15.50
* Peak Reactivity for 10a32 at mnr: 1.2114 / 10a32-mnr-sccg-5-Decay-0.0-15.50
* Peak Reactivity for 10a32 at mxu: 1.2064 / 10a32-mxu-sccg-5-Decay-0.0-18.50
* Peak Reactivity for 10a32 at mxr: 1.1902 / 10a32-mxr-sccg-5-Decay-0.0-21.00
* Final Peak Reactivity for 10a32: 1.2194 / 10a32-mnu-sccg-5-Decay-0.0-15.50
* Peak Reactivity for 10a33 at mnu: 1.2166 / 10a33-mnu-sccg-5-Decay-0.0-15.50
* Peak Reactivity for 10a33 at mnr: 1.2087 / 10a33-mnr-sccg-5-Decay-0.0-15.00
* Peak Reactivity for 10a33 at mxu: 1.2041 / 10a33-mxu-sccg-5-Decay-0.0-18.50
* Peak Reactivity for 10a33 at mxr: 1.1885 / 10a33-mxr-sccg-5-Decay-0.0-20.50
* Final Peak Reactivity for 10a33: 1.2166 / 10a33-mnu-sccg-5-Decay-0.0-15.50
* Peak Reactivity for 10a34 at mnu: 1.2131 / 10a34-mnu-sccg-5-Decay-0.0-14.50

* Peak Reactivity for 10a34 at mnr: 1.2032 / 10a34-mnr-sccg-5-Decay-0.0-15.50
* Peak Reactivity for 10a34 at mxu: 1.2068 / 10a34-mxu-sccg-5-Decay-0.0-17.00
* Peak Reactivity for 10a34 at mxr: 1.1909 / 10a34-mxr-sccg-5-Decay-0.0-18.50
* Final Peak Reactivity for 10a34: 1.2131 / 10a34-mnu-sccg-5-Decay-0.0-14.50
* Peak Reactivity for 10a35 at mnu: 1.2065 / 10a35-mnu-sccg-5-Decay-0.0-14.50
* Peak Reactivity for 10a35 at mnr: 1.2005 / 10a35-mnr-sccg-5-Decay-0.0-15.00
* Peak Reactivity for 10a35 at mxu: 1.2009 / 10a35-mxu-sccg-5-Decay-0.0-17.00
* Peak Reactivity for 10a35 at mxr: 1.1866 / 10a35-mxr-sccg-5-Decay-0.0-18.50
* Final Peak Reactivity for 10a35: 1.2065 / 10a35-mnu-sccg-5-Decay-0.0-14.50
* Peak Reactivity for 10a41 at mnu: 1.2149 / 10a41-mnu-sccg-5-Decay-0.0-16.50
* Peak Reactivity for 10a41 at mnr: 1.2171 / 10a41-mnr-sccg-5-Decay-0.0-15.50
* Peak Reactivity for 10a41 at mxu: 1.2054 / 10a41-mxu-sccg-5-Decay-0.0-19.00
* Peak Reactivity for 10a41 at mxr: 1.2002 / 10a41-mxr-sccg-5-Decay-0.0-20.00
* Final Peak Reactivity for 10a41: 1.2171 / 10a41-mnr-sccg-5-Decay-0.0-16.00
* Peak Reactivity for 10a42 at mnu: 1.2198 / 10a42-mnu-sccg-5-Decay-0.0-16.00
* Peak Reactivity for 10a42 at mnr: 1.2322 / 10a42-mnr-sccg-5-Decay-0.0-15.50
* Peak Reactivity for 10a42 at mxu: 1.2105 / 10a42-mxu-sccg-5-Decay-0.0-18.50
* Peak Reactivity for 10a42 at mxr: 1.2073 / 10a42-mxr-sccg-5-Decay-0.0-20.50
* Final Peak Reactivity for 10a42: 1.2322 / 10a42-mnr-sccg-5-Decay-0.0-15.50
* Peak Reactivity for 10a43 at mnu: 1.2170 / 10a43-mnu-sccg-5-Decay-0.0-15.50
* Peak Reactivity for 10a43 at mnr: 1.2300 / 10a43-mnr-sccg-5-Decay-0.0-15.00
* Peak Reactivity for 10a43 at mxu: 1.2078 / 10a43-mxu-sccg-5-Decay-0.0-18.00
* Peak Reactivity for 10a43 at mxr: 1.2056 / 10a43-mxr-sccg-5-Decay-0.0-20.50
* Final Peak Reactivity for 10a43: 1.2300 / 10a43-mnr-sccg-5-Decay-0.0-15.00
* Peak Reactivity for 10a44 at mnu: 1.2310 / 10a44-mnu-sccg-5-Decay-0.0-13.50
* Peak Reactivity for 10a44 at mnr: 1.2293 / 10a44-mnr-sccg-5-Decay-0.0-13.50
* Peak Reactivity for 10a44 at mxu: 1.2226 / 10a44-mxu-sccg-5-Decay-0.0-15.50
* Peak Reactivity for 10a44 at mxr: 1.2098 / 10a44-mxr-sccg-5-Decay-0.0-18.00
* Final Peak Reactivity for 10a44: 1.2310 / 10a44-mnu-sccg-5-Decay-0.0-13.50
* Peak Reactivity for 10a45 at mnu: 1.2239 / 10a45-mnu-sccg-5-Decay-0.0-13.50
* Peak Reactivity for 10a45 at mnr: 1.2225 / 10a45-mnr-sccg-5-Decay-0.0-13.50
* Peak Reactivity for 10a45 at mxu: 1.2168 / 10a45-mxu-sccg-5-Decay-0.0-15.50
* Peak Reactivity for 10a45 at mxr: 1.2047 / 10a45-mxr-sccg-5-Decay-0.0-17.50
* Final Peak Reactivity for 10a45: 1.2239 / 10a45-mnu-sccg-5-Decay-0.0-13.50
* Peak Reactivity for 10a51 at mnu: 1.2040 / 10a51-mnu-sccg-5-Decay-0.0-15.50
* Peak Reactivity for 10a51 at mnr: 1.1994 / 10a51-mnr-sccg-5-Decay-0.0-16.50
* Peak Reactivity for 10a51 at mxu: 1.1945 / 10a51-mxu-sccg-5-Decay-0.0-18.00
* Peak Reactivity for 10a51 at mxr: 1.1784 / 10a51-mxr-sccg-5-Decay-0.0-21.00
* Final Peak Reactivity for 10a51: 1.2040 / 10a51-mnu-sccg-5-Decay-0.0-15.50
* Peak Reactivity for 10a52 at mnu: 1.2136 / 10a52-mnu-sccg-5-Decay-0.0-14.50
* Peak Reactivity for 10a52 at mnr: 1.2128 / 10a52-mnr-sccg-5-Decay-0.0-15.00
* Peak Reactivity for 10a52 at mxu: 1.2016 / 10a52-mxu-sccg-5-Decay-0.0-17.50
* Peak Reactivity for 10a52 at mxr: 1.1914 / 10a52-mxr-sccg-5-Decay-0.0-20.50
* Final Peak Reactivity for 10a52: 1.2136 / 10a52-mnu-sccg-5-Decay-0.0-14.50
* Peak Reactivity for 10a53 at mnu: 1.2110 / 10a53-mnu-sccg-5-Decay-0.0-14.50
* Peak Reactivity for 10a53 at mnr: 1.2103 / 10a53-mnr-sccg-5-Decay-0.0-15.00

* Peak Reactivity for 10a53 at mxu: 1.1993 / 10a53-mxu-sccg-5-Decay-0.0-17.50
* Peak Reactivity for 10a53 at mxr: 1.1898 / 10a53-mxr-sccg-5-Decay-0.0-20.00
* Final Peak Reactivity for 10a53: 1.2110 / 10a53-mnu-sccg-5-Decay-0.0-14.50
* Peak Reactivity for 10a54 at mnu: 1.2043 / 10a54-mnu-sccg-5-Decay-0.0-14.00
* Peak Reactivity for 10a54 at mnr: 1.2050 / 10a54-mnr-sccg-5-Decay-0.0-15.00
* Peak Reactivity for 10a54 at mxu: 1.1975 / 10a54-mxu-sccg-5-Decay-0.0-16.50
* Peak Reactivity for 10a54 at mxr: 1.1904 / 10a54-mxr-sccg-5-Decay-0.0-19.00
* Final Peak Reactivity for 10a54: 1.2050 / 10a54-mnr-sccg-5-Decay-0.0-15.00
* Peak Reactivity for 10a55 at mnu: 1.1976 / 10a55-mnu-sccg-5-Decay-0.0-14.00
* Peak Reactivity for 10a55 at mnr: 1.2003 / 10a55-mnr-sccg-5-Decay-0.0-14.50
* Peak Reactivity for 10a55 at mxu: 1.1914 / 10a55-mxu-sccg-5-Decay-0.0-16.50
* Peak Reactivity for 10a55 at mxr: 1.1859 / 10a55-mxr-sccg-5-Decay-0.0-18.50
* Final Peak Reactivity for 10a55: 1.2003 / 10a55-mnr-sccg-5-Decay-0.0-14.50
* Peak Reactivity for 10a61 at mnu: 1.2267 / 10a61-mnu-sccg-5-Decay-0.0-14.50
* Peak Reactivity for 10a61 at mnr: 1.2449 / 10a61-mnr-sccg-5-Decay-0.0-13.50
* Peak Reactivity for 10a61 at mxu: 1.2182 / 10a61-mxu-sccg-5-Decay-0.0-16.50
* Peak Reactivity for 10a61 at mxr: 1.2286 / 10a61-mxr-sccg-5-Decay-0.0-17.00
* Final Peak Reactivity for 10a61: 1.2449 / 10a61-mnr-sccg-5-Decay-0.0-13.50
* Peak Reactivity for 10a62 at mnu: 1.2329 / 10a62-mnu-sccg-5-Decay-0.0-14.00
* Peak Reactivity for 10a62 at mnr: 1.2536 / 10a62-mnr-sccg-5-Decay-0.0-13.00
* Peak Reactivity for 10a62 at mxu: 1.2222 / 10a62-mxu-sccg-5-Decay-0.0-16.50
* Peak Reactivity for 10a62 at mxr: 1.2337 / 10a62-mxr-sccg-5-Decay-0.0-17.50
* Final Peak Reactivity for 10a62: 1.2536 / 10a62-mnr-sccg-5-Decay-0.0-13.00
* Peak Reactivity for 10a63 at mnu: 1.2300 / 10a63-mnu-sccg-5-Decay-0.0-13.50
* Peak Reactivity for 10a63 at mnr: 1.2512 / 10a63-mnr-sccg-5-Decay-0.0-12.50
* Peak Reactivity for 10a63 at mxu: 1.2195 / 10a63-mxu-sccg-5-Decay-0.0-16.00
* Peak Reactivity for 10a63 at mxr: 1.2315 / 10a63-mxr-sccg-5-Decay-0.0-17.00
* Final Peak Reactivity for 10a63: 1.2512 / 10a63-mnr-sccg-5-Decay-0.0-12.50
* Peak Reactivity for 10a64 at mnu: 1.2232 / 10a64-mnu-sccg-5-Decay-0.0-13.50
* Peak Reactivity for 10a64 at mnr: 1.2411 / 10a64-mnr-sccg-5-Decay-0.0-12.50
* Peak Reactivity for 10a64 at mxu: 1.2161 / 10a64-mxu-sccg-5-Decay-0.0-15.50
* Peak Reactivity for 10a64 at mxr: 1.2253 / 10a64-mxr-sccg-5-Decay-0.0-16.50
* Final Peak Reactivity for 10a64: 1.2411 / 10a64-mnr-sccg-5-Decay-0.0-12.50
* Peak Reactivity for 10a65 at mnu: 1.2159 / 10a65-mnu-sccg-5-Decay-0.0-13.50
* Peak Reactivity for 10a65 at mnr: 1.2332 / 10a65-mnr-sccg-5-Decay-0.0-12.50
* Peak Reactivity for 10a65 at mxu: 1.2100 / 10a65-mxu-sccg-5-Decay-0.0-15.50
* Peak Reactivity for 10a65 at mxr: 1.2199 / 10a65-mxr-sccg-5-Decay-0.0-16.50
* Final Peak Reactivity for 10a65: 1.2332 / 10a65-mnr-sccg-5-Decay-0.0-12.50
* Peak Reactivity for 10a71 at mnu: 1.2139 / 10a71-mnu-sccg-5-Decay-0.0-14.50
* Peak Reactivity for 10a71 at mnr: 1.2298 / 10a71-mnr-sccg-5-Decay-0.0-14.50
* Peak Reactivity for 10a71 at mxu: 1.2027 / 10a71-mxu-sccg-5-Decay-0.0-17.00
* Peak Reactivity for 10a71 at mxr: 1.2064 / 10a71-mxr-sccg-5-Decay-0.0-19.50
* Final Peak Reactivity for 10a71: 1.2298 / 10a71-mnr-sccg-5-Decay-0.0-14.50
* Peak Reactivity for 10a72 at mnu: 1.2171 / 10a72-mnu-sccg-5-Decay-0.0-14.50
* Peak Reactivity for 10a72 at mnr: 1.2359 / 10a72-mnr-sccg-5-Decay-0.0-14.00
* Peak Reactivity for 10a72 at mxu: 1.2039 / 10a72-mxu-sccg-5-Decay-0.0-17.50

* Peak Reactivity for 10a72 at mxr: 1.2120 / 10a72-mxr-sccg-5-Decay-0.0-19.50
* Final Peak Reactivity for 10a72: 1.2359 / 10a72-mnr-sccg-5-Decay-0.0-14.00
* Peak Reactivity for 10a73 at mnu: 1.2148 / 10a73-mnu-sccg-5-Decay-0.0-14.50
* Peak Reactivity for 10a73 at mnr: 1.2339 / 10a73-mnr-sccg-5-Decay-0.0-13.50
* Peak Reactivity for 10a73 at mxu: 1.2012 / 10a73-mxu-sccg-5-Decay-0.0-17.00
* Peak Reactivity for 10a73 at mxr: 1.2105 / 10a73-mxr-sccg-5-Decay-0.0-19.00
* Final Peak Reactivity for 10a73: 1.2339 / 10a73-mnr-sccg-5-Decay-0.0-13.50
* Peak Reactivity for 10a74 at mnu: 1.2090 / 10a74-mnu-sccg-5-Decay-0.0-14.00
* Peak Reactivity for 10a74 at mnr: 1.2240 / 10a74-mnr-sccg-5-Decay-0.0-13.50
* Peak Reactivity for 10a74 at mxu: 1.1994 / 10a74-mxu-sccg-5-Decay-0.0-16.50
* Peak Reactivity for 10a74 at mxr: 1.2033 / 10a74-mxr-sccg-5-Decay-0.0-19.00
* Final Peak Reactivity for 10a74: 1.2240 / 10a74-mnr-sccg-5-Decay-0.0-13.50
* Peak Reactivity for 10a75 at mnu: 1.2010 / 10a75-mnu-sccg-5-Decay-0.0-14.00
* Peak Reactivity for 10a75 at mnr: 1.2191 / 10a75-mnr-sccg-5-Decay-0.0-13.50
* Peak Reactivity for 10a75 at mxu: 1.1933 / 10a75-mxu-sccg-5-Decay-0.0-16.50
* Peak Reactivity for 10a75 at mxr: 1.1989 / 10a75-mxr-sccg-5-Decay-0.0-18.50
* Final Peak Reactivity for 10a75: 1.2191 / 10a75-mnr-sccg-5-Decay-0.0-13.50
* Peak Reactivity for 10a81 at mnu: 1.2308 / 10a81-mnu-sccg-5-Decay-0.0-14.00
* Peak Reactivity for 10a81 at mnr: 1.2376 / 10a81-mnr-sccg-5-Decay-0.0-13.00
* Peak Reactivity for 10a81 at mxu: 1.2228 / 10a81-mxu-sccg-5-Decay-0.0-16.50
* Peak Reactivity for 10a81 at mxr: 1.2236 / 10a81-mxr-sccg-5-Decay-0.0-16.50
* Final Peak Reactivity for 10a81: 1.2376 / 10a81-mnr-sccg-5-Decay-0.0-13.00
* Peak Reactivity for 10a82 at mnu: 1.2408 / 10a82-mnu-sccg-5-Decay-0.0-13.50
* Peak Reactivity for 10a82 at mnr: 1.2527 / 10a82-mnr-sccg-5-Decay-0.0-12.50
* Peak Reactivity for 10a82 at mxu: 1.2304 / 10a82-mxu-sccg-5-Decay-0.0-15.50
* Peak Reactivity for 10a82 at mxr: 1.2347 / 10a82-mxr-sccg-5-Decay-0.0-16.50
* Final Peak Reactivity for 10a82: 1.2527 / 10a82-mnr-sccg-5-Decay-0.0-12.50
* Peak Reactivity for 10a83 at mnu: 1.2389 / 10a83-mnu-sccg-5-Decay-0.0-13.00
* Peak Reactivity for 10a83 at mnr: 1.2508 / 10a83-mnr-sccg-5-Decay-0.0-12.50
* Peak Reactivity for 10a83 at mxu: 1.2277 / 10a83-mxu-sccg-5-Decay-0.0-15.50
* Peak Reactivity for 10a83 at mxr: 1.2325 / 10a83-mxr-sccg-5-Decay-0.0-16.50
* Final Peak Reactivity for 10a83: 1.2508 / 10a83-mnr-sccg-5-Decay-0.0-12.50
* Peak Reactivity for 10a84 at mnu: 1.2332 / 10a84-mnu-sccg-5-Decay-0.0-13.00
* Peak Reactivity for 10a84 at mnr: 1.2407 / 10a84-mnr-sccg-5-Decay-0.0-12.00
* Peak Reactivity for 10a84 at mxu: 1.2262 / 10a84-mxu-sccg-5-Decay-0.0-15.00
* Peak Reactivity for 10a84 at mxr: 1.2261 / 10a84-mxr-sccg-5-Decay-0.0-16.00
* Final Peak Reactivity for 10a84: 1.2407 / 10a84-mnr-sccg-5-Decay-0.0-12.00
* Peak Reactivity for 10a85 at mnu: 1.2255 / 10a85-mnu-sccg-5-Decay-0.0-12.50
* Peak Reactivity for 10a85 at mnr: 1.2328 / 10a85-mnr-sccg-5-Decay-0.0-12.00
* Peak Reactivity for 10a85 at mxu: 1.2199 / 10a85-mxu-sccg-5-Decay-0.0-15.00
* Peak Reactivity for 10a85 at mxr: 1.2205 / 10a85-mxr-sccg-5-Decay-0.0-16.00
* Final Peak Reactivity for 10a85: 1.2328 / 10a85-mnr-sccg-5-Decay-0.0-12.00
* Peak Reactivity for 10a91 at mnu: 1.2178 / 10a91-mnu-sccg-5-Decay-0.0-14.50
* Peak Reactivity for 10a91 at mnr: 1.2197 / 10a91-mnr-sccg-5-Decay-0.0-15.00
* Peak Reactivity for 10a91 at mxu: 1.2084 / 10a91-mxu-sccg-5-Decay-0.0-17.00
* Peak Reactivity for 10a91 at mxr: 1.2015 / 10a91-mxr-sccg-5-Decay-0.0-19.00

* Final Peak Reactivity for 10a91: 1.2197 / 10a91-mnr-sccg-5-Decay-0.0-15.00
* Peak Reactivity for 10a92 at mnu: 1.2299 / 10a92-mnu-sccg-5-Decay-0.0-13.50
* Peak Reactivity for 10a92 at mnr: 1.2338 / 10a92-mnr-sccg-5-Decay-0.0-14.00
* Peak Reactivity for 10a92 at mxu: 1.2215 / 10a92-mxu-sccg-5-Decay-0.0-16.00
* Peak Reactivity for 10a92 at mxr: 1.2161 / 10a92-mxr-sccg-5-Decay-0.0-18.50
* Final Peak Reactivity for 10a92: 1.2338 / 10a92-mnr-sccg-5-Decay-0.0-14.00
* Peak Reactivity for 10a93 at mnu: 1.2272 / 10a93-mnu-sccg-5-Decay-0.0-13.50
* Peak Reactivity for 10a93 at mnr: 1.2319 / 10a93-mnr-sccg-5-Decay-0.0-13.50
* Peak Reactivity for 10a93 at mxu: 1.2185 / 10a93-mxu-sccg-5-Decay-0.0-16.00
* Peak Reactivity for 10a93 at mxr: 1.2140 / 10a93-mxr-sccg-5-Decay-0.0-18.00
* Final Peak Reactivity for 10a93: 1.2319 / 10a93-mnr-sccg-5-Decay-0.0-13.50
* Peak Reactivity for 10a94 at mnu: 1.2217 / 10a94-mnu-sccg-5-Decay-0.0-13.00
* Peak Reactivity for 10a94 at mnr: 1.2205 / 10a94-mnr-sccg-5-Decay-0.0-13.50
* Peak Reactivity for 10a94 at mxu: 1.2161 / 10a94-mxu-sccg-5-Decay-0.0-15.00
* Peak Reactivity for 10a94 at mxr: 1.2052 / 10a94-mxr-sccg-5-Decay-0.0-18.50
* Final Peak Reactivity for 10a94: 1.2217 / 10a94-mnu-sccg-5-Decay-0.0-13.00
* Peak Reactivity for 10a95 at mnu: 1.2144 / 10a95-mnu-sccg-5-Decay-0.0-13.00
* Peak Reactivity for 10a95 at mnr: 1.2164 / 10a95-mnr-sccg-5-Decay-0.0-13.50
* Peak Reactivity for 10a95 at mxu: 1.2099 / 10a95-mxu-sccg-5-Decay-0.0-15.00
* Peak Reactivity for 10a95 at mxr: 1.2006 / 10a95-mxr-sccg-5-Decay-0.0-18.50
* Final Peak Reactivity for 10a95: 1.2164 / 10a95-mnr-sccg-5-Decay-0.0-13.50

Table A.3
Post Processing Summary for CASMO In-rack (no cell blocker included) COP Screening Calculations[2]

* Peak Reactivity for 07a00 at mnu: 0.9013 / 07a00-mnu-bfx-5-Decay-0.0-0.00
* Peak Reactivity for 07a00 at mnr: 0.9013 / 07a00-mnr-bfx-5-Decay-0.0-0.00
* Peak Reactivity for 07a00 at mxu: 0.9013 / 07a00-mxu-bfx-5-Decay-0.0-0.00
* Peak Reactivity for 07a00 at mxr: 0.9013 / 07a00-mxr-bfx-5-Decay-0.0-0.00
* Final Peak Reactivity for 07a00: 0.9013 / 07a00-mxr-bfx-5-Decay-0.0-0.00
* Peak Reactivity for 07b10 at mnu: 0.9053 / 07b10-mnu-bfx-5-Decay-0.0-3.50
* Peak Reactivity for 07b10 at mnr: 0.9140 / 07b10-mnr-bfx-5-Decay-0.0-3.50
* Peak Reactivity for 07b10 at mxu: 0.9076 / 07b10-mxu-bfx-5-Decay-0.0-4.00
* Peak Reactivity for 07b10 at mxr: 0.9237 / 07b10-mxr-bfx-5-Decay-0.0-6.00
* Final Peak Reactivity for 07b10: 0.9237 / 07b10-mxr-bfx-5-Decay-0.0-6.00
* Peak Reactivity for 07b20 at mnu: 0.8518 / 07b20-mnu-bfx-5-Decay-0.0-6.50
* Peak Reactivity for 07b20 at mnr: 0.8668 / 07b20-mnr-bfx-5-Decay-0.0-6.00
* Peak Reactivity for 07b20 at mxu: 0.8647 / 07b20-mxu-bfx-5-Decay-0.0-8.00
* Peak Reactivity for 07b20 at mxr: 0.8924 / 07b20-mxr-bfx-5-Decay-0.0-10.50
* Final Peak Reactivity for 07b20: 0.8924 / 07b20-mxr-bfx-5-Decay-0.0-10.50
* Peak Reactivity for 07c00 at mnu: 0.8861 / 07c00-mnu-bfx-5-Decay-0.0-4.50
* Peak Reactivity for 07c00 at mnr: 0.8903 / 07c00-mnr-bfx-5-Decay-0.0-5.00
* Peak Reactivity for 07c00 at mxu: 0.8911 / 07c00-mxu-bfx-5-Decay-0.0-6.00
* Peak Reactivity for 07c00 at mxr: 0.9057 / 07c00-mxr-bfx-5-Decay-0.0-9.00
* Final Peak Reactivity for 07c00: 0.9057 / 07c00-mxr-bfx-5-Decay-0.0-9.00
* Peak Reactivity for 08a10 at mnu: 0.9016 / 08a10-mnu-bfx-5-Decay-0.0-4.00
* Peak Reactivity for 08a10 at mnr: 0.9071 / 08a10-mnr-bfx-5-Decay-0.0-4.00
* Peak Reactivity for 08a10 at mxu: 0.9065 / 08a10-mxu-bfx-5-Decay-0.0-5.00
* Peak Reactivity for 08a10 at mxr: 0.9177 / 08a10-mxr-bfx-5-Decay-0.0-6.50
* Final Peak Reactivity for 08a10: 0.9177 / 08a10-mxr-bfx-5-Decay-0.0-6.50
* Peak Reactivity for 08a20 at mnu: 0.8918 / 08a20-mnu-bfx-5-Decay-0.0-4.00
* Peak Reactivity for 08a20 at mnr: 0.8972 / 08a20-mnr-bfx-5-Decay-0.0-4.00
* Peak Reactivity for 08a20 at mxu: 0.8974 / 08a20-mxu-bfx-5-Decay-0.0-5.00
* Peak Reactivity for 08a20 at mxr: 0.9098 / 08a20-mxr-bfx-5-Decay-0.0-6.50
* Final Peak Reactivity for 08a20: 0.9098 / 08a20-mxr-bfx-5-Decay-0.0-6.50
* Peak Reactivity for 08a30 at mnu: 0.9008 / 08a30-mnu-bfx-5-Decay-0.0-5.00
* Peak Reactivity for 08a30 at mnr: 0.8992 / 08a30-mnr-bfx-5-Decay-0.0-5.50
* Peak Reactivity for 08a30 at mxu: 0.9064 / 08a30-mxu-bfx-5-Decay-0.0-6.50
* Peak Reactivity for 08a30 at mxr: 0.9120 / 08a30-mxr-bfx-5-Decay-0.0-9.00
* Final Peak Reactivity for 08a30: 0.9120 / 08a30-mxr-bfx-5-Decay-0.0-9.00
* Peak Reactivity for 08a40 at mnu: 0.8834 / 08a40-mnu-bfx-5-Decay-0.0-7.00
* Peak Reactivity for 08a40 at mnr: 0.8815 / 08a40-mnr-bfx-5-Decay-0.0-7.00
* Peak Reactivity for 08a40 at mxu: 0.8927 / 08a40-mxu-bfx-5-Decay-0.0-8.00
* Peak Reactivity for 08a40 at mxr: 0.9004 / 08a40-mxr-bfx-5-Decay-0.0-11.00

[2] The data in this table is used solely for screening lattices. The reactivity of the lattices using CASMO-5 is not used for the design basis analysis.

* Final Peak Reactivity for 08a40: 0.9004 / 08a40-mxr-bfx-5-Decay-0.0-11.50
* Peak Reactivity for 08b11 at mnu: 0.8806 / 08b11-mnu-bfx-5-Decay-0.0-0.00
* Peak Reactivity for 08b11 at mnr: 0.8806 / 08b11-mnr-bfx-5-Decay-0.0-0.00
* Peak Reactivity for 08b11 at mxu: 0.8806 / 08b11-mxu-bfx-5-Decay-0.0-0.00
* Peak Reactivity for 08b11 at mxr: 0.8823 / 08b11-mxr-bfx-5-Decay-0.0-3.00
* Final Peak Reactivity for 08b11: 0.8823 / 08b11-mxr-bfx-5-Decay-0.0-3.50
* Peak Reactivity for 08b12 at mnu: 0.8845 / 08b12-mnu-bfx-5-Decay-0.0-7.50
* Peak Reactivity for 08b12 at mnr: 0.8851 / 08b12-mnr-bfx-5-Decay-0.0-7.00
* Peak Reactivity for 08b12 at mxu: 0.8882 / 08b12-mxu-bfx-5-Decay-0.0-9.50
* Peak Reactivity for 08b12 at mxr: 0.9010 / 08b12-mxr-bfx-5-Decay-0.0-11.50
* Final Peak Reactivity for 08b12: 0.9010 / 08b12-mxr-bfx-5-Decay-0.0-11.50
* Peak Reactivity for 08b13 at mnu: 0.8872 / 08b13-mnu-bfx-5-Decay-0.0-7.50
* Peak Reactivity for 08b13 at mnr: 0.8897 / 08b13-mnr-bfx-5-Decay-0.0-7.00
* Peak Reactivity for 08b13 at mxu: 0.8934 / 08b13-mxu-bfx-5-Decay-0.0-9.00
* Peak Reactivity for 08b13 at mxr: 0.9067 / 08b13-mxr-bfx-5-Decay-0.0-11.00
* Final Peak Reactivity for 08b13: 0.9067 / 08b13-mxr-bfx-5-Decay-0.0-11.50
* Peak Reactivity for 08b20 at mnu: 0.8916 / 08b20-mnu-bfx-5-Decay-0.0-9.50
* Peak Reactivity for 08b20 at mnr: 0.8920 / 08b20-mnr-bfx-5-Decay-0.0-10.00
* Peak Reactivity for 08b20 at mxu: 0.8968 / 08b20-mxu-bfx-5-Decay-0.0-11.50
* Peak Reactivity for 08b20 at mxr: 0.9082 / 08b20-mxr-bfx-5-Decay-0.0-15.50
* Final Peak Reactivity for 08b20: 0.9082 / 08b20-mxr-bfx-5-Decay-0.0-15.50
* Peak Reactivity for 08c11 at mnu: 0.8867 / 08c11-mnu-bfx-5-Decay-0.0-12.50
* Peak Reactivity for 08c11 at mnr: 0.8914 / 08c11-mnr-bfx-5-Decay-0.0-13.50
* Peak Reactivity for 08c11 at mxu: 0.8933 / 08c11-mxu-bfx-5-Decay-0.0-14.50
* Peak Reactivity for 08c11 at mxr: 0.9059 / 08c11-mxr-bfx-5-Decay-0.0-18.50
* Final Peak Reactivity for 08c11: 0.9059 / 08c11-mxr-bfx-5-Decay-0.0-18.50
* Peak Reactivity for 08c12 at mnu: 0.9047 / 08c12-mnu-bfx-5-Decay-0.0-10.50
* Peak Reactivity for 08c12 at mnr: 0.9087 / 08c12-mnr-bfx-5-Decay-0.0-11.50
* Peak Reactivity for 08c12 at mxu: 0.9082 / 08c12-mxu-bfx-5-Decay-0.0-12.50
* Peak Reactivity for 08c12 at mxr: 0.9180 / 08c12-mxr-bfx-5-Decay-0.0-16.00
* Final Peak Reactivity for 08c12: 0.9180 / 08c12-mxr-bfx-5-Decay-0.0-16.00
* Peak Reactivity for 08c21 at mnu: 0.8980 / 08c21-mnu-bfx-5-Decay-0.0-13.00
* Peak Reactivity for 08c21 at mnr: 0.8905 / 08c21-mnr-bfx-5-Decay-0.0-14.00
* Peak Reactivity for 08c21 at mxu: 0.9019 / 08c21-mxu-bfx-5-Decay-0.0-15.00
* Peak Reactivity for 08c21 at mxr: 0.9029 / 08c21-mxr-bfx-5-Decay-0.0-19.50
* Final Peak Reactivity for 08c21: 0.9029 / 08c21-mxr-bfx-5-Decay-0.0-19.50
* Peak Reactivity for 08c22 at mnu: 0.9161 / 08c22-mnu-bfx-5-Decay-0.0-11.00
* Peak Reactivity for 08c22 at mnr: 0.9089 / 08c22-mnr-bfx-5-Decay-0.0-12.50
* Peak Reactivity for 08c22 at mxu: 0.9171 / 08c22-mxu-bfx-5-Decay-0.0-13.00
* Peak Reactivity for 08c22 at mxr: 0.9161 / 08c22-mxr-bfx-5-Decay-0.0-17.50
* Final Peak Reactivity for 08c22: 0.9171 / 08c22-mxu-bfx-5-Decay-0.0-13.00
* Peak Reactivity for 08c23 at mnu: 0.9004 / 08c23-mnu-bfx-5-Decay-0.0-12.50
* Peak Reactivity for 08c23 at mnr: 0.8977 / 08c23-mnr-bfx-5-Decay-0.0-13.50
* Peak Reactivity for 08c23 at mxu: 0.8976 / 08c23-mxu-bfx-5-Decay-0.0-15.50
* Peak Reactivity for 08c23 at mxr: 0.9005 / 08c23-mxr-bfx-5-Decay-0.0-20.00
* Final Peak Reactivity for 08c23: 0.9005 / 08c23-mxr-bfx-5-Decay-0.0-20.50

* Peak Reactivity for 09a11 at mnu: 0.8927 / 09a11-mnu-bfx-5-Decay-0.0-12.00
* Peak Reactivity for 09a11 at mnr: 0.8938 / 09a11-mnr-bfx-5-Decay-0.0-12.50
* Peak Reactivity for 09a11 at mxu: 0.8987 / 09a11-mxu-bfx-5-Decay-0.0-14.50
* Peak Reactivity for 09a11 at mxr: 0.9048 / 09a11-mxr-bfx-5-Decay-0.0-16.50
* Final Peak Reactivity for 09a11: 0.9048 / 09a11-mxr-bfx-5-Decay-0.0-17.00
* Peak Reactivity for 09a12 at mnu: 0.8984 / 09a12-mnu-bfx-5-Decay-0.0-12.00
* Peak Reactivity for 09a12 at mnr: 0.8932 / 09a12-mnr-bfx-5-Decay-0.0-12.50
* Peak Reactivity for 09a12 at mxu: 0.9052 / 09a12-mxu-bfx-5-Decay-0.0-13.50
* Peak Reactivity for 09a12 at mxr: 0.9058 / 09a12-mxr-bfx-5-Decay-0.0-16.50
* Final Peak Reactivity for 09a12: 0.9058 / 09a12-mxr-bfx-5-Decay-0.0-16.50
* Peak Reactivity for 09a13 at mnu: 0.8978 / 09a13-mnu-bfx-5-Decay-0.0-11.50
* Peak Reactivity for 09a13 at mnr: 0.8893 / 09a13-mnr-bfx-5-Decay-0.0-12.00
* Peak Reactivity for 09a13 at mxu: 0.9044 / 09a13-mxu-bfx-5-Decay-0.0-13.50
* Peak Reactivity for 09a13 at mxr: 0.9038 / 09a13-mxr-bfx-5-Decay-0.0-16.00
* Final Peak Reactivity for 09a13: 0.9044 / 09a13-mxu-bfx-5-Decay-0.0-13.50
* Peak Reactivity for 09a21 at mnu: 0.8901 / 09a21-mnu-bfx-5-Decay-0.0-14.50
* Peak Reactivity for 09a21 at mnr: 0.8965 / 09a21-mnr-bfx-5-Decay-0.0-15.50
* Peak Reactivity for 09a21 at mxu: 0.8974 / 09a21-mxu-bfx-5-Decay-0.0-17.00
* Peak Reactivity for 09a21 at mxr: 0.9031 / 09a21-mxr-bfx-5-Decay-0.0-20.50
* Final Peak Reactivity for 09a21: 0.9031 / 09a21-mxr-bfx-5-Decay-0.0-20.50
* Peak Reactivity for 09a22 at mnu: 0.8902 / 09a22-mnu-bfx-5-Decay-0.0-14.00
* Peak Reactivity for 09a22 at mnr: 0.9050 / 09a22-mnr-bfx-5-Decay-0.0-14.50
* Peak Reactivity for 09a22 at mxu: 0.8982 / 09a22-mxu-bfx-5-Decay-0.0-16.00
* Peak Reactivity for 09a22 at mxr: 0.9116 / 09a22-mxr-bfx-5-Decay-0.0-20.00
* Final Peak Reactivity for 09a22: 0.9116 / 09a22-mxr-bfx-5-Decay-0.0-20.00
* Peak Reactivity for 09a23 at mnu: 0.8901 / 09a23-mnu-bfx-5-Decay-0.0-14.00
* Peak Reactivity for 09a23 at mnr: 0.9070 / 09a23-mnr-bfx-5-Decay-0.0-14.50
* Peak Reactivity for 09a23 at mxu: 0.8979 / 09a23-mxu-bfx-5-Decay-0.0-16.50
* Peak Reactivity for 09a23 at mxr: 0.9128 / 09a23-mxr-bfx-5-Decay-0.0-20.00
* Final Peak Reactivity for 09a23: 0.9128 / 09a23-mxr-bfx-5-Decay-0.0-20.00
* Peak Reactivity for 09b11 at mnu: 0.8882 / 09b11-mnu-bfx-5-Decay-0.0-14.50
* Peak Reactivity for 09b11 at mnr: 0.8947 / 09b11-mnr-bfx-5-Decay-0.0-15.50
* Peak Reactivity for 09b11 at mxu: 0.8950 / 09b11-mxu-bfx-5-Decay-0.0-17.00
* Peak Reactivity for 09b11 at mxr: 0.9008 / 09b11-mxr-bfx-5-Decay-0.0-21.00
* Final Peak Reactivity for 09b11: 0.9008 / 09b11-mxr-bfx-5-Decay-0.0-21.00
* Peak Reactivity for 09b12 at mnu: 0.8881 / 09b12-mnu-bfx-5-Decay-0.0-14.00
* Peak Reactivity for 09b12 at mnr: 0.9031 / 09b12-mnr-bfx-5-Decay-0.0-14.50
* Peak Reactivity for 09b12 at mxu: 0.8958 / 09b12-mxu-bfx-5-Decay-0.0-16.50
* Peak Reactivity for 09b12 at mxr: 0.9091 / 09b12-mxr-bfx-5-Decay-0.0-20.00
* Final Peak Reactivity for 09b12: 0.9091 / 09b12-mxr-bfx-5-Decay-0.0-20.00
* Peak Reactivity for 09b13 at mnu: 0.8880 / 09b13-mnu-bfx-5-Decay-0.0-14.00
* Peak Reactivity for 09b13 at mnr: 0.9047 / 09b13-mnr-bfx-5-Decay-0.0-14.50
* Peak Reactivity for 09b13 at mxu: 0.8953 / 09b13-mxu-bfx-5-Decay-0.0-17.00
* Peak Reactivity for 09b13 at mxr: 0.9100 / 09b13-mxr-bfx-5-Decay-0.0-20.00
* Final Peak Reactivity for 09b13: 0.9100 / 09b13-mxr-bfx-5-Decay-0.0-20.50
* Peak Reactivity for 09b21 at mnu: 0.8846 / 09b21-mnu-bfx-5-Decay-0.0-15.50

* Peak Reactivity for 09b21 at mnr: 0.8824 / 09b21-mnr-bfx-5-Decay-0.0-15.50
* Peak Reactivity for 09b21 at mxu: 0.8905 / 09b21-mxu-bfx-5-Decay-0.0-18.50
* Peak Reactivity for 09b21 at mxr: 0.8920 / 09b21-mxr-bfx-5-Decay-0.0-21.50
* Final Peak Reactivity for 09b21: 0.8920 / 09b21-mxr-bfx-5-Decay-0.0-22.00
* Peak Reactivity for 09b22 at mnu: 0.8887 / 09b22-mnu-bfx-5-Decay-0.0-15.00
* Peak Reactivity for 09b22 at mnr: 0.8816 / 09b22-mnr-bfx-5-Decay-0.0-15.50
* Peak Reactivity for 09b22 at mxu: 0.8961 / 09b22-mxu-bfx-5-Decay-0.0-18.00
* Peak Reactivity for 09b22 at mxr: 0.8928 / 09b22-mxr-bfx-5-Decay-0.0-21.50
* Final Peak Reactivity for 09b22: 0.8961 / 09b22-mxu-bfx-5-Decay-0.0-18.00
* Peak Reactivity for 09b23 at mnu: 0.8881 / 09b23-mnu-bfx-5-Decay-0.0-14.50
* Peak Reactivity for 09b23 at mnr: 0.8784 / 09b23-mnr-bfx-5-Decay-0.0-16.00
* Peak Reactivity for 09b23 at mxu: 0.8969 / 09b23-mxu-bfx-5-Decay-0.0-17.00
* Peak Reactivity for 09b23 at mxr: 0.8908 / 09b23-mxr-bfx-5-Decay-0.0-21.50
* Final Peak Reactivity for 09b23: 0.8969 / 09b23-mxu-bfx-5-Decay-0.0-17.00
* Peak Reactivity for 09b31 at mnu: 0.8910 / 09b31-mnu-bfx-5-Decay-0.0-16.50
* Peak Reactivity for 09b31 at mnr: 0.8928 / 09b31-mnr-bfx-5-Decay-0.0-16.50
* Peak Reactivity for 09b31 at mxu: 0.8939 / 09b31-mxu-bfx-5-Decay-0.0-19.50
* Peak Reactivity for 09b31 at mxr: 0.8969 / 09b31-mxr-bfx-5-Decay-0.0-23.00
* Final Peak Reactivity for 09b31: 0.8969 / 09b31-mxr-bfx-5-Decay-0.0-23.00
* Peak Reactivity for 09b32 at mnu: 0.8966 / 09b32-mnu-bfx-5-Decay-0.0-16.00
* Peak Reactivity for 09b32 at mnr: 0.8922 / 09b32-mnr-bfx-5-Decay-0.0-16.50
* Peak Reactivity for 09b32 at mxu: 0.9005 / 09b32-mxu-bfx-5-Decay-0.0-19.00
* Peak Reactivity for 09b32 at mxr: 0.8980 / 09b32-mxr-bfx-5-Decay-0.0-22.50
* Final Peak Reactivity for 09b32: 0.9005 / 09b32-mxu-bfx-5-Decay-0.0-19.00
* Peak Reactivity for 09b33 at mnu: 0.8970 / 09b33-mnu-bfx-5-Decay-0.0-15.50
* Peak Reactivity for 09b33 at mnr: 0.8906 / 09b33-mnr-bfx-5-Decay-0.0-16.50
* Peak Reactivity for 09b33 at mxu: 0.9022 / 09b33-mxu-bfx-5-Decay-0.0-18.50
* Peak Reactivity for 09b33 at mxr: 0.8974 / 09b33-mxr-bfx-5-Decay-0.0-22.50
* Final Peak Reactivity for 09b33: 0.9022 / 09b33-mxu-bfx-5-Decay-0.0-18.50
* Peak Reactivity for 09b41 at mnu: 0.9024 / 09b41-mnu-bfx-5-Decay-0.0-17.00
* Peak Reactivity for 09b41 at mnr: 0.9020 / 09b41-mnr-bfx-5-Decay-0.0-17.00
* Peak Reactivity for 09b41 at mxu: 0.9042 / 09b41-mxu-bfx-5-Decay-0.0-20.00
* Peak Reactivity for 09b41 at mxr: 0.9041 / 09b41-mxr-bfx-5-Decay-0.0-23.00
* Final Peak Reactivity for 09b41: 0.9042 / 09b41-mxu-bfx-5-Decay-0.0-20.00
* Peak Reactivity for 09b42 at mnu: 0.9086 / 09b42-mnu-bfx-5-Decay-0.0-15.50
* Peak Reactivity for 09b42 at mnr: 0.9006 / 09b42-mnr-bfx-5-Decay-0.0-17.00
* Peak Reactivity for 09b42 at mxu: 0.9129 / 09b42-mxu-bfx-5-Decay-0.0-18.50
* Peak Reactivity for 09b42 at mxr: 0.9052 / 09b42-mxr-bfx-5-Decay-0.0-22.50
* Final Peak Reactivity for 09b42: 0.9129 / 09b42-mxu-bfx-5-Decay-0.0-18.50
* Peak Reactivity for 09b51 at mnu: 0.9024 / 09b51-mnu-bfx-5-Decay-0.0-17.00
* Peak Reactivity for 09b51 at mnr: 0.9020 / 09b51-mnr-bfx-5-Decay-0.0-17.00
* Peak Reactivity for 09b51 at mxu: 0.9042 / 09b51-mxu-bfx-5-Decay-0.0-20.00
* Peak Reactivity for 09b51 at mxr: 0.9041 / 09b51-mxr-bfx-5-Decay-0.0-23.00
* Final Peak Reactivity for 09b51: 0.9042 / 09b51-mxu-bfx-5-Decay-0.0-20.00
* Peak Reactivity for 09b52 at mnu: 0.9116 / 09b52-mnu-bfx-5-Decay-0.0-15.50
* Peak Reactivity for 09b52 at mnr: 0.9003 / 09b52-mnr-bfx-5-Decay-0.0-17.00

* Peak Reactivity for 09b52 at mxu: 0.9182 / 09b52-mxu-bfx-5-Decay-0.0-18.00
* Peak Reactivity for 09b52 at mxr: 0.9059 / 09b52-mxr-bfx-5-Decay-0.0-22.00
* Final Peak Reactivity for 09b52: 0.9182 / 09b52-mxu-bfx-5-Decay-0.0-18.00
* Peak Reactivity for 09b61 at mnu: 0.9055 / 09b61-mnu-bfx-5-Decay-0.0-17.00
* Peak Reactivity for 09b61 at mnr: 0.9030 / 09b61-mnr-bfx-5-Decay-0.0-17.00
* Peak Reactivity for 09b61 at mxu: 0.9053 / 09b61-mxu-bfx-5-Decay-0.0-20.50
* Peak Reactivity for 09b61 at mxr: 0.9029 / 09b61-mxr-bfx-5-Decay-0.0-23.00
* Final Peak Reactivity for 09b61: 0.9055 / 09b61-mnu-bfx-5-Decay-0.0-17.00
* Peak Reactivity for 09b62 at mnu: 0.9156 / 09b62-mnu-bfx-5-Decay-0.0-16.00
* Peak Reactivity for 09b62 at mnr: 0.9079 / 09b62-mnr-bfx-5-Decay-0.0-15.50
* Peak Reactivity for 09b62 at mxu: 0.9146 / 09b62-mxu-bfx-5-Decay-0.0-19.00
* Peak Reactivity for 09b62 at mxr: 0.9079 / 09b62-mxr-bfx-5-Decay-0.0-21.50
* Final Peak Reactivity for 09b62: 0.9156 / 09b62-mnu-bfx-5-Decay-0.0-16.00
* Peak Reactivity for 09b63 at mnu: 0.9195 / 09b63-mnu-bfx-5-Decay-0.0-15.00
* Peak Reactivity for 09b63 at mnr: 0.9047 / 09b63-mnr-bfx-5-Decay-0.0-16.50
* Peak Reactivity for 09b63 at mxu: 0.9215 / 09b63-mxu-bfx-5-Decay-0.0-18.00
* Peak Reactivity for 09b63 at mxr: 0.9075 / 09b63-mxr-bfx-5-Decay-0.0-21.50
* Final Peak Reactivity for 09b63: 0.9215 / 09b63-mxu-bfx-5-Decay-0.0-18.00
* Peak Reactivity for 09b71 at mnu: 0.9049 / 09b71-mnu-bfx-5-Decay-0.0-17.00
* Peak Reactivity for 09b71 at mnr: 0.9026 / 09b71-mnr-bfx-5-Decay-0.0-17.00
* Peak Reactivity for 09b71 at mxu: 0.9048 / 09b71-mxu-bfx-5-Decay-0.0-20.50
* Peak Reactivity for 09b71 at mxr: 0.9026 / 09b71-mxr-bfx-5-Decay-0.0-23.00
* Final Peak Reactivity for 09b71: 0.9049 / 09b71-mnu-bfx-5-Decay-0.0-17.00
* Peak Reactivity for 09b72 at mnu: 0.9117 / 09b72-mnu-bfx-5-Decay-0.0-16.00
* Peak Reactivity for 09b72 at mnr: 0.9087 / 09b72-mnr-bfx-5-Decay-0.0-16.00
* Peak Reactivity for 09b72 at mxu: 0.9127 / 09b72-mxu-bfx-5-Decay-0.0-19.00
* Peak Reactivity for 09b72 at mxr: 0.9083 / 09b72-mxr-bfx-5-Decay-0.0-22.00
* Final Peak Reactivity for 09b72: 0.9127 / 09b72-mxu-bfx-5-Decay-0.0-19.50
* Peak Reactivity for 09b73 at mnu: 0.9157 / 09b73-mnu-bfx-5-Decay-0.0-15.00
* Peak Reactivity for 09b73 at mnr: 0.9052 / 09b73-mnr-bfx-5-Decay-0.0-16.00
* Peak Reactivity for 09b73 at mxu: 0.9222 / 09b73-mxu-bfx-5-Decay-0.0-18.00
* Peak Reactivity for 09b73 at mxr: 0.9092 / 09b73-mxr-bfx-5-Decay-0.0-21.50
* Final Peak Reactivity for 09b73: 0.9222 / 09b73-mxu-bfx-5-Decay-0.0-18.00
* Peak Reactivity for 09b81 at mnu: 0.9203 / 09b81-mnu-bfx-5-Decay-0.0-15.00
* Peak Reactivity for 09b81 at mnr: 0.9190 / 09b81-mnr-bfx-5-Decay-0.0-15.50
* Peak Reactivity for 09b81 at mxu: 0.9165 / 09b81-mxu-bfx-5-Decay-0.0-18.50
* Peak Reactivity for 09b81 at mxr: 0.9138 / 09b81-mxr-bfx-5-Decay-0.0-21.50
* Final Peak Reactivity for 09b81: 0.9203 / 09b81-mnu-bfx-5-Decay-0.0-15.00
* Peak Reactivity for 09b82 at mnu: 0.9212 / 09b82-mnu-bfx-5-Decay-0.0-15.00
* Peak Reactivity for 09b82 at mnr: 0.9307 / 09b82-mnr-bfx-5-Decay-0.0-14.50
* Peak Reactivity for 09b82 at mxu: 0.9183 / 09b82-mxu-bfx-5-Decay-0.0-18.00
* Peak Reactivity for 09b82 at mxr: 0.9220 / 09b82-mxr-bfx-5-Decay-0.0-21.00
* Final Peak Reactivity for 09b82: 0.9307 / 09b82-mnr-bfx-5-Decay-0.0-15.00
* Peak Reactivity for 09b83 at mnu: 0.9273 / 09b83-mnu-bfx-5-Decay-0.0-14.00
* Peak Reactivity for 09b83 at mnr: 0.9309 / 09b83-mnr-bfx-5-Decay-0.0-14.00
* Peak Reactivity for 09b83 at mxu: 0.9272 / 09b83-mxu-bfx-5-Decay-0.0-16.50

* Peak Reactivity for 09b83 at mxr: 0.9258 / 09b83-mxr-bfx-5-Decay-0.0-20.00
* Final Peak Reactivity for 09b83: 0.9309 / 09b83-mnr-bfx-5-Decay-0.0-14.00
* Peak Reactivity for 09b91 at mnu: 0.8865 / 09b91-mnu-bfx-5-Decay-0.0-19.00
* Peak Reactivity for 09b91 at mnr: 0.8899 / 09b91-mnr-bfx-5-Decay-0.0-18.50
* Peak Reactivity for 09b91 at mxu: 0.8891 / 09b91-mxu-bfx-5-Decay-0.0-22.00
* Peak Reactivity for 09b91 at mxr: 0.8927 / 09b91-mxr-bfx-5-Decay-0.0-25.00
* Final Peak Reactivity for 09b91: 0.8927 / 09b91-mxr-bfx-5-Decay-0.0-25.00
* Peak Reactivity for 09b92 at mnu: 0.9030 / 09b92-mnu-bfx-5-Decay-0.0-17.00
* Peak Reactivity for 09b92 at mnr: 0.9159 / 09b92-mnr-bfx-5-Decay-0.0-16.50
* Peak Reactivity for 09b92 at mxu: 0.9031 / 09b92-mxu-bfx-5-Decay-0.0-20.00
* Peak Reactivity for 09b92 at mxr: 0.9107 / 09b92-mxr-bfx-5-Decay-0.0-23.00
* Final Peak Reactivity for 09b92: 0.9159 / 09b92-mnr-bfx-5-Decay-0.0-16.50
* Peak Reactivity for 09b93 at mnu: 0.9058 / 09b93-mnu-bfx-5-Decay-0.0-16.00
* Peak Reactivity for 09b93 at mnr: 0.9163 / 09b93-mnr-bfx-5-Decay-0.0-16.00
* Peak Reactivity for 09b93 at mxu: 0.9089 / 09b93-mxu-bfx-5-Decay-0.0-19.00
* Peak Reactivity for 09b93 at mxr: 0.9147 / 09b93-mxr-bfx-5-Decay-0.0-22.50
* Final Peak Reactivity for 09b93: 0.9163 / 09b93-mnr-bfx-5-Decay-0.0-16.00
* Peak Reactivity for 09ba1 at mnu: 0.9024 / 09ba1-mnu-bfx-5-Decay-0.0-17.00
* Peak Reactivity for 09ba1 at mnr: 0.9020 / 09ba1-mnr-bfx-5-Decay-0.0-17.00
* Peak Reactivity for 09ba1 at mxu: 0.9042 / 09ba1-mxu-bfx-5-Decay-0.0-20.00
* Peak Reactivity for 09ba1 at mxr: 0.9042 / 09ba1-mxr-bfx-5-Decay-0.0-23.00
* Final Peak Reactivity for 09ba1: 0.9042 / 09ba1-mxr-bfx-5-Decay-0.0-23.00
* Peak Reactivity for 09ba2 at mnu: 0.9137 / 09ba2-mnu-bfx-5-Decay-0.0-14.50
* Peak Reactivity for 09ba2 at mnr: 0.9236 / 09ba2-mnr-bfx-5-Decay-0.0-14.50
* Peak Reactivity for 09ba2 at mxu: 0.9211 / 09ba2-mxu-bfx-5-Decay-0.0-17.00
* Peak Reactivity for 09ba2 at mxr: 0.9245 / 09ba2-mxr-bfx-5-Decay-0.0-20.50
* Final Peak Reactivity for 09ba2: 0.9245 / 09ba2-mxr-bfx-5-Decay-0.0-20.50
* Peak Reactivity for 10a11 at mnu: 0.9187 / 10a11-mnu-bfx-5-Decay-0.0-16.50
* Peak Reactivity for 10a11 at mnr: 0.9109 / 10a11-mnr-bfx-5-Decay-0.0-16.00
* Peak Reactivity for 10a11 at mxu: 0.9170 / 10a11-mxu-bfx-5-Decay-0.0-19.00
* Peak Reactivity for 10a11 at mxr: 0.9062 / 10a11-mxr-bfx-5-Decay-0.0-21.50
* Final Peak Reactivity for 10a11: 0.9187 / 10a11-mnu-bfx-5-Decay-0.0-16.50
* Peak Reactivity for 10a12 at mnu: 0.9182 / 10a12-mnu-bfx-5-Decay-0.0-15.50
* Peak Reactivity for 10a12 at mnr: 0.9141 / 10a12-mnr-bfx-5-Decay-0.0-15.50
* Peak Reactivity for 10a12 at mxu: 0.9146 / 10a12-mxu-bfx-5-Decay-0.0-18.50
* Peak Reactivity for 10a12 at mxr: 0.9077 / 10a12-mxr-bfx-5-Decay-0.0-21.50
* Final Peak Reactivity for 10a12: 0.9182 / 10a12-mnu-bfx-5-Decay-0.0-15.50
* Peak Reactivity for 10a13 at mnu: 0.9215 / 10a13-mnu-bfx-5-Decay-0.0-15.50
* Peak Reactivity for 10a13 at mnr: 0.9173 / 10a13-mnr-bfx-5-Decay-0.0-15.00
* Peak Reactivity for 10a13 at mxu: 0.9185 / 10a13-mxu-bfx-5-Decay-0.0-18.50
* Peak Reactivity for 10a13 at mxr: 0.9114 / 10a13-mxr-bfx-5-Decay-0.0-21.00
* Final Peak Reactivity for 10a13: 0.9215 / 10a13-mnu-bfx-5-Decay-0.0-15.50
* Peak Reactivity for 10a14 at mnu: 0.9068 / 10a14-mnu-bfx-5-Decay-0.0-14.50
* Peak Reactivity for 10a14 at mnr: 0.9007 / 10a14-mnr-bfx-5-Decay-0.0-15.50
* Peak Reactivity for 10a14 at mxu: 0.9079 / 10a14-mxu-bfx-5-Decay-0.0-17.00
* Peak Reactivity for 10a14 at mxr: 0.9016 / 10a14-mxr-bfx-5-Decay-0.0-18.50

* Final Peak Reactivity for 10a14: 0.9079 / 10a14-mxu-bfx-5-Decay-0.0-17.00
* Peak Reactivity for 10a15 at mnu: 0.9058 / 10a15-mnu-bfx-5-Decay-0.0-14.00
* Peak Reactivity for 10a15 at mnr: 0.9022 / 10a15-mnr-bfx-5-Decay-0.0-15.00
* Peak Reactivity for 10a15 at mxu: 0.9070 / 10a15-mxu-bfx-5-Decay-0.0-17.00
* Peak Reactivity for 10a15 at mxr: 0.9009 / 10a15-mxr-bfx-5-Decay-0.0-18.50
* Final Peak Reactivity for 10a15: 0.9070 / 10a15-mxu-bfx-5-Decay-0.0-17.00
* Peak Reactivity for 10a21 at mnu: 0.9199 / 10a21-mnu-bfx-5-Decay-0.0-16.50
* Peak Reactivity for 10a21 at mnr: 0.9238 / 10a21-mnr-bfx-5-Decay-0.0-15.50
* Peak Reactivity for 10a21 at mxu: 0.9194 / 10a21-mxu-bfx-5-Decay-0.0-19.50
* Peak Reactivity for 10a21 at mxr: 0.9203 / 10a21-mxr-bfx-5-Decay-0.0-20.50
* Final Peak Reactivity for 10a21: 0.9238 / 10a21-mnr-bfx-5-Decay-0.0-16.00
* Peak Reactivity for 10a22 at mnu: 0.9186 / 10a22-mnu-bfx-5-Decay-0.0-16.00
* Peak Reactivity for 10a22 at mnr: 0.9348 / 10a22-mnr-bfx-5-Decay-0.0-15.00
* Peak Reactivity for 10a22 at mxu: 0.9187 / 10a22-mxu-bfx-5-Decay-0.0-18.50
* Peak Reactivity for 10a22 at mxr: 0.9251 / 10a22-mxr-bfx-5-Decay-0.0-21.00
* Final Peak Reactivity for 10a22: 0.9348 / 10a22-mnr-bfx-5-Decay-0.0-15.00
* Peak Reactivity for 10a23 at mnu: 0.9220 / 10a23-mnu-bfx-5-Decay-0.0-15.50
* Peak Reactivity for 10a23 at mnr: 0.9386 / 10a23-mnr-bfx-5-Decay-0.0-14.50
* Peak Reactivity for 10a23 at mxu: 0.9221 / 10a23-mxu-bfx-5-Decay-0.0-18.00
* Peak Reactivity for 10a23 at mxr: 0.9290 / 10a23-mxr-bfx-5-Decay-0.0-20.50
* Final Peak Reactivity for 10a23: 0.9386 / 10a23-mnr-bfx-5-Decay-0.0-15.00
* Peak Reactivity for 10a24 at mnu: 0.9199 / 10a24-mnu-bfx-5-Decay-0.0-13.50
* Peak Reactivity for 10a24 at mnr: 0.9278 / 10a24-mnr-bfx-5-Decay-0.0-13.00
* Peak Reactivity for 10a24 at mxu: 0.9202 / 10a24-mxu-bfx-5-Decay-0.0-15.50
* Peak Reactivity for 10a24 at mxr: 0.9200 / 10a24-mxr-bfx-5-Decay-0.0-18.00
* Final Peak Reactivity for 10a24: 0.9278 / 10a24-mnr-bfx-5-Decay-0.0-13.00
* Peak Reactivity for 10a25 at mnu: 0.9185 / 10a25-mnu-bfx-5-Decay-0.0-13.50
* Peak Reactivity for 10a25 at mnr: 0.9263 / 10a25-mnr-bfx-5-Decay-0.0-13.00
* Peak Reactivity for 10a25 at mxu: 0.9194 / 10a25-mxu-bfx-5-Decay-0.0-15.50
* Peak Reactivity for 10a25 at mxr: 0.9193 / 10a25-mxr-bfx-5-Decay-0.0-18.00
* Final Peak Reactivity for 10a25: 0.9263 / 10a25-mnr-bfx-5-Decay-0.0-13.00
* Peak Reactivity for 10a31 at mnu: 0.9186 / 10a31-mnu-bfx-5-Decay-0.0-16.50
* Peak Reactivity for 10a31 at mnr: 0.9127 / 10a31-mnr-bfx-5-Decay-0.0-16.50
* Peak Reactivity for 10a31 at mxu: 0.9164 / 10a31-mxu-bfx-5-Decay-0.0-19.00
* Peak Reactivity for 10a31 at mxr: 0.9054 / 10a31-mxr-bfx-5-Decay-0.0-22.00
* Final Peak Reactivity for 10a31: 0.9186 / 10a31-mnu-bfx-5-Decay-0.0-16.50
* Peak Reactivity for 10a32 at mnu: 0.9182 / 10a32-mnu-bfx-5-Decay-0.0-15.50
* Peak Reactivity for 10a32 at mnr: 0.9141 / 10a32-mnr-bfx-5-Decay-0.0-15.50
* Peak Reactivity for 10a32 at mxu: 0.9146 / 10a32-mxu-bfx-5-Decay-0.0-18.50
* Peak Reactivity for 10a32 at mxr: 0.9077 / 10a32-mxr-bfx-5-Decay-0.0-21.50
* Final Peak Reactivity for 10a32: 0.9182 / 10a32-mnu-bfx-5-Decay-0.0-15.50
* Peak Reactivity for 10a33 at mnu: 0.9215 / 10a33-mnu-bfx-5-Decay-0.0-15.50
* Peak Reactivity for 10a33 at mnr: 0.9173 / 10a33-mnr-bfx-5-Decay-0.0-15.00
* Peak Reactivity for 10a33 at mxu: 0.9185 / 10a33-mxu-bfx-5-Decay-0.0-18.50
* Peak Reactivity for 10a33 at mxr: 0.9114 / 10a33-mxr-bfx-5-Decay-0.0-21.00
* Final Peak Reactivity for 10a33: 0.9215 / 10a33-mnu-bfx-5-Decay-0.0-15.50

* Peak Reactivity for 10a34 at mnu: 0.9068 / 10a34-mnu-bfx-5-Decay-0.0-14.50
* Peak Reactivity for 10a34 at mnr: 0.9007 / 10a34-mnr-bfx-5-Decay-0.0-15.50
* Peak Reactivity for 10a34 at mxu: 0.9079 / 10a34-mxu-bfx-5-Decay-0.0-17.00
* Peak Reactivity for 10a34 at mxr: 0.9016 / 10a34-mxr-bfx-5-Decay-0.0-18.50
* Final Peak Reactivity for 10a34: 0.9079 / 10a34-mxu-bfx-5-Decay-0.0-17.00
* Peak Reactivity for 10a35 at mnu: 0.9058 / 10a35-mnu-bfx-5-Decay-0.0-14.00
* Peak Reactivity for 10a35 at mnr: 0.9022 / 10a35-mnr-bfx-5-Decay-0.0-15.00
* Peak Reactivity for 10a35 at mxu: 0.9070 / 10a35-mxu-bfx-5-Decay-0.0-17.00
* Peak Reactivity for 10a35 at mxr: 0.9009 / 10a35-mxr-bfx-5-Decay-0.0-18.50
* Final Peak Reactivity for 10a35: 0.9070 / 10a35-mxu-bfx-5-Decay-0.0-17.00
* Peak Reactivity for 10a41 at mnu: 0.9199 / 10a41-mnu-bfx-5-Decay-0.0-16.50
* Peak Reactivity for 10a41 at mnr: 0.9238 / 10a41-mnr-bfx-5-Decay-0.0-15.50
* Peak Reactivity for 10a41 at mxu: 0.9194 / 10a41-mxu-bfx-5-Decay-0.0-19.50
* Peak Reactivity for 10a41 at mxr: 0.9203 / 10a41-mxr-bfx-5-Decay-0.0-20.50
* Final Peak Reactivity for 10a41: 0.9238 / 10a41-mnr-bfx-5-Decay-0.0-16.00
* Peak Reactivity for 10a42 at mnu: 0.9183 / 10a42-mnu-bfx-5-Decay-0.0-16.00
* Peak Reactivity for 10a42 at mnr: 0.9299 / 10a42-mnr-bfx-5-Decay-0.0-15.50
* Peak Reactivity for 10a42 at mxu: 0.9179 / 10a42-mxu-bfx-5-Decay-0.0-18.50
* Peak Reactivity for 10a42 at mxr: 0.9205 / 10a42-mxr-bfx-5-Decay-0.0-21.00
* Final Peak Reactivity for 10a42: 0.9299 / 10a42-mnr-bfx-5-Decay-0.0-15.50
* Peak Reactivity for 10a43 at mnu: 0.9218 / 10a43-mnu-bfx-5-Decay-0.0-15.50
* Peak Reactivity for 10a43 at mnr: 0.9336 / 10a43-mnr-bfx-5-Decay-0.0-15.00
* Peak Reactivity for 10a43 at mxu: 0.9214 / 10a43-mxu-bfx-5-Decay-0.0-18.50
* Peak Reactivity for 10a43 at mxr: 0.9244 / 10a43-mxr-bfx-5-Decay-0.0-21.00
* Final Peak Reactivity for 10a43: 0.9336 / 10a43-mnr-bfx-5-Decay-0.0-15.00
* Peak Reactivity for 10a44 at mnu: 0.9203 / 10a44-mnu-bfx-5-Decay-0.0-13.50
* Peak Reactivity for 10a44 at mnr: 0.9209 / 10a44-mnr-bfx-5-Decay-0.0-13.00
* Peak Reactivity for 10a44 at mxu: 0.9198 / 10a44-mxu-bfx-5-Decay-0.0-15.50
* Peak Reactivity for 10a44 at mxr: 0.9147 / 10a44-mxr-bfx-5-Decay-0.0-18.00
* Final Peak Reactivity for 10a44: 0.9209 / 10a44-mnr-bfx-5-Decay-0.0-13.00
* Peak Reactivity for 10a45 at mnu: 0.9189 / 10a45-mnu-bfx-5-Decay-0.0-13.50
* Peak Reactivity for 10a45 at mnr: 0.9194 / 10a45-mnr-bfx-5-Decay-0.0-13.00
* Peak Reactivity for 10a45 at mxu: 0.9191 / 10a45-mxu-bfx-5-Decay-0.0-15.50
* Peak Reactivity for 10a45 at mxr: 0.9140 / 10a45-mxr-bfx-5-Decay-0.0-18.00
* Final Peak Reactivity for 10a45: 0.9194 / 10a45-mnr-bfx-5-Decay-0.0-13.50
* Peak Reactivity for 10a51 at mnu: 0.9100 / 10a51-mnu-bfx-5-Decay-0.0-15.50
* Peak Reactivity for 10a51 at mnr: 0.9087 / 10a51-mnr-bfx-5-Decay-0.0-16.50
* Peak Reactivity for 10a51 at mxu: 0.9094 / 10a51-mxu-bfx-5-Decay-0.0-18.50
* Peak Reactivity for 10a51 at mxr: 0.9022 / 10a51-mxr-bfx-5-Decay-0.0-22.00
* Final Peak Reactivity for 10a51: 0.9100 / 10a51-mnu-bfx-5-Decay-0.0-15.50
* Peak Reactivity for 10a52 at mnu: 0.9131 / 10a52-mnu-bfx-5-Decay-0.0-14.50
* Peak Reactivity for 10a52 at mnr: 0.9142 / 10a52-mnr-bfx-5-Decay-0.0-15.00
* Peak Reactivity for 10a52 at mxu: 0.9099 / 10a52-mxu-bfx-5-Decay-0.0-17.50
* Peak Reactivity for 10a52 at mxr: 0.9079 / 10a52-mxr-bfx-5-Decay-0.0-21.00
* Final Peak Reactivity for 10a52: 0.9142 / 10a52-mnr-bfx-5-Decay-0.0-15.00
* Peak Reactivity for 10a53 at mnu: 0.9167 / 10a53-mnu-bfx-5-Decay-0.0-14.00

* Peak Reactivity for 10a53 at mnr: 0.9175 / 10a53-mnr-bfx-5-Decay-0.0-15.00
* Peak Reactivity for 10a53 at mxu: 0.9138 / 10a53-mxu-bfx-5-Decay-0.0-17.50
* Peak Reactivity for 10a53 at mxr: 0.9118 / 10a53-mxr-bfx-5-Decay-0.0-20.50
* Final Peak Reactivity for 10a53: 0.9175 / 10a53-mnr-bfx-5-Decay-0.0-15.00
* Peak Reactivity for 10a54 at mnu: 0.8999 / 10a54-mnu-bfx-5-Decay-0.0-14.00
* Peak Reactivity for 10a54 at mnr: 0.9018 / 10a54-mnr-bfx-5-Decay-0.0-14.50
* Peak Reactivity for 10a54 at mxu: 0.9003 / 10a54-mxu-bfx-5-Decay-0.0-16.50
* Peak Reactivity for 10a54 at mxr: 0.9007 / 10a54-mxr-bfx-5-Decay-0.0-19.00
* Final Peak Reactivity for 10a54: 0.9018 / 10a54-mnr-bfx-5-Decay-0.0-14.50
* Peak Reactivity for 10a55 at mnu: 0.8987 / 10a55-mnu-bfx-5-Decay-0.0-14.00
* Peak Reactivity for 10a55 at mnr: 0.9020 / 10a55-mnr-bfx-5-Decay-0.0-14.50
* Peak Reactivity for 10a55 at mxu: 0.8993 / 10a55-mxu-bfx-5-Decay-0.0-16.50
* Peak Reactivity for 10a55 at mxr: 0.9001 / 10a55-mxr-bfx-5-Decay-0.0-19.00
* Final Peak Reactivity for 10a55: 0.9020 / 10a55-mnr-bfx-5-Decay-0.0-14.50
* Peak Reactivity for 10a61 at mnu: 0.9276 / 10a61-mnu-bfx-5-Decay-0.0-14.50
* Peak Reactivity for 10a61 at mnr: 0.9431 / 10a61-mnr-bfx-5-Decay-0.0-13.50
* Peak Reactivity for 10a61 at mxu: 0.9273 / 10a61-mxu-bfx-5-Decay-0.0-16.50
* Peak Reactivity for 10a61 at mxr: 0.9399 / 10a61-mxr-bfx-5-Decay-0.0-17.50
* Final Peak Reactivity for 10a61: 0.9431 / 10a61-mnr-bfx-5-Decay-0.0-13.50
* Peak Reactivity for 10a62 at mnu: 0.9276 / 10a62-mnu-bfx-5-Decay-0.0-14.00
* Peak Reactivity for 10a62 at mnr: 0.9453 / 10a62-mnr-bfx-5-Decay-0.0-13.00
* Peak Reactivity for 10a62 at mxu: 0.9253 / 10a62-mxu-bfx-5-Decay-0.0-16.50
* Peak Reactivity for 10a62 at mxr: 0.9392 / 10a62-mxr-bfx-5-Decay-0.0-18.00
* Final Peak Reactivity for 10a62: 0.9453 / 10a62-mnr-bfx-5-Decay-0.0-13.00
* Peak Reactivity for 10a63 at mnu: 0.9311 / 10a63-mnu-bfx-5-Decay-0.0-13.50
* Peak Reactivity for 10a63 at mnr: 0.9490 / 10a63-mnr-bfx-5-Decay-0.0-12.50
* Peak Reactivity for 10a63 at mxu: 0.9289 / 10a63-mxu-bfx-5-Decay-0.0-16.50
* Peak Reactivity for 10a63 at mxr: 0.9429 / 10a63-mxr-bfx-5-Decay-0.0-17.50
* Final Peak Reactivity for 10a63: 0.9490 / 10a63-mnr-bfx-5-Decay-0.0-12.50
* Peak Reactivity for 10a64 at mnu: 0.9139 / 10a64-mnu-bfx-5-Decay-0.0-13.50
* Peak Reactivity for 10a64 at mnr: 0.9291 / 10a64-mnr-bfx-5-Decay-0.0-12.50
* Peak Reactivity for 10a64 at mxu: 0.9141 / 10a64-mxu-bfx-5-Decay-0.0-15.50
* Peak Reactivity for 10a64 at mxr: 0.9256 / 10a64-mxr-bfx-5-Decay-0.0-17.00
* Final Peak Reactivity for 10a64: 0.9291 / 10a64-mnr-bfx-5-Decay-0.0-12.50
* Peak Reactivity for 10a65 at mnu: 0.9123 / 10a65-mnu-bfx-5-Decay-0.0-13.00
* Peak Reactivity for 10a65 at mnr: 0.9269 / 10a65-mnr-bfx-5-Decay-0.0-12.50
* Peak Reactivity for 10a65 at mxu: 0.9131 / 10a65-mxu-bfx-5-Decay-0.0-15.50
* Peak Reactivity for 10a65 at mxr: 0.9246 / 10a65-mxr-bfx-5-Decay-0.0-17.00
* Final Peak Reactivity for 10a65: 0.9269 / 10a65-mnr-bfx-5-Decay-0.0-12.50
* Peak Reactivity for 10a71 at mnu: 0.9181 / 10a71-mnu-bfx-5-Decay-0.0-14.50
* Peak Reactivity for 10a71 at mnr: 0.9317 / 10a71-mnr-bfx-5-Decay-0.0-15.00
* Peak Reactivity for 10a71 at mxu: 0.9161 / 10a71-mxu-bfx-5-Decay-0.0-17.00
* Peak Reactivity for 10a71 at mxr: 0.9240 / 10a71-mxr-bfx-5-Decay-0.0-20.50
* Final Peak Reactivity for 10a71: 0.9317 / 10a71-mnr-bfx-5-Decay-0.0-15.00
* Peak Reactivity for 10a72 at mnu: 0.9150 / 10a72-mnu-bfx-5-Decay-0.0-14.50
* Peak Reactivity for 10a72 at mnr: 0.9314 / 10a72-mnr-bfx-5-Decay-0.0-14.00

* Peak Reactivity for 10a72 at mxu: 0.9113 / 10a72-mxu-bfx-5-Decay-0.0-17.50
* Peak Reactivity for 10a72 at mxr: 0.9234 / 10a72-mxr-bfx-5-Decay-0.0-20.00
* Final Peak Reactivity for 10a72: 0.9314 / 10a72-mnr-bfx-5-Decay-0.0-14.00
* Peak Reactivity for 10a73 at mnu: 0.9189 / 10a73-mnu-bfx-5-Decay-0.0-14.50
* Peak Reactivity for 10a73 at mnr: 0.9353 / 10a73-mnr-bfx-5-Decay-0.0-13.50
* Peak Reactivity for 10a73 at mxu: 0.9149 / 10a73-mxu-bfx-5-Decay-0.0-17.50
* Peak Reactivity for 10a73 at mxr: 0.9275 / 10a73-mxr-bfx-5-Decay-0.0-19.50
* Final Peak Reactivity for 10a73: 0.9353 / 10a73-mnr-bfx-5-Decay-0.0-13.50
* Peak Reactivity for 10a74 at mnu: 0.9028 / 10a74-mnu-bfx-5-Decay-0.0-14.00
* Peak Reactivity for 10a74 at mnr: 0.9159 / 10a74-mnr-bfx-5-Decay-0.0-13.50
* Peak Reactivity for 10a74 at mxu: 0.9017 / 10a74-mxu-bfx-5-Decay-0.0-16.50
* Peak Reactivity for 10a74 at mxr: 0.9102 / 10a74-mxr-bfx-5-Decay-0.0-19.00
* Final Peak Reactivity for 10a74: 0.9159 / 10a74-mnr-bfx-5-Decay-0.0-13.50
* Peak Reactivity for 10a75 at mnu: 0.9008 / 10a75-mnu-bfx-5-Decay-0.0-13.50
* Peak Reactivity for 10a75 at mnr: 0.9159 / 10a75-mnr-bfx-5-Decay-0.0-13.50
* Peak Reactivity for 10a75 at mxu: 0.9006 / 10a75-mxu-bfx-5-Decay-0.0-16.50
* Peak Reactivity for 10a75 at mxr: 0.9097 / 10a75-mxr-bfx-5-Decay-0.0-19.00
* Final Peak Reactivity for 10a75: 0.9159 / 10a75-mnr-bfx-5-Decay-0.0-13.50
* Peak Reactivity for 10a81 at mnu: 0.9304 / 10a81-mnu-bfx-5-Decay-0.0-14.50
* Peak Reactivity for 10a81 at mnr: 0.9370 / 10a81-mnr-bfx-5-Decay-0.0-13.50
* Peak Reactivity for 10a81 at mxu: 0.9304 / 10a81-mxu-bfx-5-Decay-0.0-16.50
* Peak Reactivity for 10a81 at mxr: 0.9350 / 10a81-mxr-bfx-5-Decay-0.0-17.50
* Final Peak Reactivity for 10a81: 0.9370 / 10a81-mnr-bfx-5-Decay-0.0-13.50
* Peak Reactivity for 10a82 at mnu: 0.9331 / 10a82-mnu-bfx-5-Decay-0.0-13.50
* Peak Reactivity for 10a82 at mnr: 0.9442 / 10a82-mnr-bfx-5-Decay-0.0-13.00
* Peak Reactivity for 10a82 at mxu: 0.9310 / 10a82-mxu-bfx-5-Decay-0.0-16.00
* Peak Reactivity for 10a82 at mxr: 0.9393 / 10a82-mxr-bfx-5-Decay-0.0-17.50
* Final Peak Reactivity for 10a82: 0.9442 / 10a82-mnr-bfx-5-Decay-0.0-13.00
* Peak Reactivity for 10a83 at mnu: 0.9374 / 10a83-mnu-bfx-5-Decay-0.0-13.00
* Peak Reactivity for 10a83 at mnr: 0.9485 / 10a83-mnr-bfx-5-Decay-0.0-12.50
* Peak Reactivity for 10a83 at mxu: 0.9346 / 10a83-mxu-bfx-5-Decay-0.0-15.50
* Peak Reactivity for 10a83 at mxr: 0.9430 / 10a83-mxr-bfx-5-Decay-0.0-17.00
* Final Peak Reactivity for 10a83: 0.9485 / 10a83-mnr-bfx-5-Decay-0.0-12.50
* Peak Reactivity for 10a84 at mnu: 0.9212 / 10a84-mnu-bfx-5-Decay-0.0-13.00
* Peak Reactivity for 10a84 at mnr: 0.9287 / 10a84-mnr-bfx-5-Decay-0.0-12.50
* Peak Reactivity for 10a84 at mxu: 0.9215 / 10a84-mxu-bfx-5-Decay-0.0-15.00
* Peak Reactivity for 10a84 at mxr: 0.9258 / 10a84-mxr-bfx-5-Decay-0.0-16.50
* Final Peak Reactivity for 10a84: 0.9287 / 10a84-mnr-bfx-5-Decay-0.0-12.50
* Peak Reactivity for 10a85 at mnu: 0.9194 / 10a85-mnu-bfx-5-Decay-0.0-12.50
* Peak Reactivity for 10a85 at mnr: 0.9265 / 10a85-mnr-bfx-5-Decay-0.0-12.00
* Peak Reactivity for 10a85 at mxu: 0.9204 / 10a85-mxu-bfx-5-Decay-0.0-15.00
* Peak Reactivity for 10a85 at mxr: 0.9248 / 10a85-mxr-bfx-5-Decay-0.0-16.50
* Final Peak Reactivity for 10a85: 0.9265 / 10a85-mnr-bfx-5-Decay-0.0-12.00
* Peak Reactivity for 10a91 at mnu: 0.9204 / 10a91-mnu-bfx-5-Decay-0.0-15.00
* Peak Reactivity for 10a91 at mnr: 0.9235 / 10a91-mnr-bfx-5-Decay-0.0-15.00
* Peak Reactivity for 10a91 at mxu: 0.9196 / 10a91-mxu-bfx-5-Decay-0.0-17.50

* Peak Reactivity for 10a91 at mxr: 0.9191 / 10a91-mxr-bfx-5-Decay-0.0-20.00
* Final Peak Reactivity for 10a91: 0.9235 / 10a91-mnr-bfx-5-Decay-0.0-15.00
* Peak Reactivity for 10a92 at mnu: 0.9248 / 10a92-mnu-bfx-5-Decay-0.0-13.50
* Peak Reactivity for 10a92 at mnr: 0.9297 / 10a92-mnr-bfx-5-Decay-0.0-14.00
* Peak Reactivity for 10a92 at mxu: 0.9247 / 10a92-mxu-bfx-5-Decay-0.0-16.00
* Peak Reactivity for 10a92 at mxr: 0.9257 / 10a92-mxr-bfx-5-Decay-0.0-19.00
* Final Peak Reactivity for 10a92: 0.9297 / 10a92-mnr-bfx-5-Decay-0.0-14.00
* Peak Reactivity for 10a93 at mnu: 0.9285 / 10a93-mnu-bfx-5-Decay-0.0-13.50
* Peak Reactivity for 10a93 at mnr: 0.9336 / 10a93-mnr-bfx-5-Decay-0.0-13.50
* Peak Reactivity for 10a93 at mxu: 0.9281 / 10a93-mxu-bfx-5-Decay-0.0-16.00
* Peak Reactivity for 10a93 at mxr: 0.9294 / 10a93-mxr-bfx-5-Decay-0.0-19.00
* Final Peak Reactivity for 10a93: 0.9336 / 10a93-mnr-bfx-5-Decay-0.0-13.50
* Peak Reactivity for 10a94 at mnu: 0.9125 / 10a94-mnu-bfx-5-Decay-0.0-13.00
* Peak Reactivity for 10a94 at mnr: 0.9132 / 10a94-mnr-bfx-5-Decay-0.0-13.50
* Peak Reactivity for 10a94 at mxu: 0.9141 / 10a94-mxu-bfx-5-Decay-0.0-15.00
* Peak Reactivity for 10a94 at mxr: 0.9108 / 10a94-mxr-bfx-5-Decay-0.0-19.00
* Final Peak Reactivity for 10a94: 0.9141 / 10a94-mxu-bfx-5-Decay-0.0-15.00
* Peak Reactivity for 10a95 at mnu: 0.9110 / 10a95-mnu-bfx-5-Decay-0.0-13.00
* Peak Reactivity for 10a95 at mnr: 0.9137 / 10a95-mnr-bfx-5-Decay-0.0-13.50
* Peak Reactivity for 10a95 at mxu: 0.9131 / 10a95-mxu-bfx-5-Decay-0.0-15.00
* Peak Reactivity for 10a95 at mxr: 0.9102 / 10a95-mxr-bfx-5-Decay-0.0-18.50
* Final Peak Reactivity for 10a95: 0.9137 / 10a95-mnr-bfx-5-Decay-0.0-13.50

Appendix B

Analysis Results

Appendix B contains results and other analysis information for the following:

Table B.1

MCNP SCCG Results for COP Screening with 7 Most Reactive Lattices

"mnu' COP			"mnr" COP			"mxu" COP			"mxr" COP		
Lattice	bu	kclac	Lattice	bu	kclac	Lattice	bu	kclac	Lattice	bu	kclac
	120	1.2152		120	1.2398		150	1.2152		150	1.2247
	130	1.2216		130	1.2435		160	1.2173		160	1.2263
10a61	140	1.2258	10a61	140	1.2438	10a61	170	1.2163	10a61	170	1.2279
	150	1.2248		150	1.2398		180	1.2149		180	1.2279
	160	1.2207		160	1.2351		190	1.2120		190	1.2261
max		1.2258	max		1.2438	max		1.2173	max		1.2279
	120	1.2240		120	1.2500		150	1.2183		150	1.2271
	130	1.2299		130	1.2529		160	1.2204		160	1.2309
10a62	140	1.2316	10a62	140	1.2504	10a62	170	1.2206	10a62	170	1.2327
	150	1.2294		150	1.2450		180	1.2184		180	1.2318
	160	1.2232		160	1.2379		190	1.2149		190	1.2309
max		1.2316	max		1.2529	max		1.2206	max		1.2327
	120	1.2234		110	1.2416		150	1.2163		150	1.2253
	130	1.2278		120	1.2487		160	1.2179		160	1.2296
10a63	140	1.2287	10a63	130	1.2492	10a63	170	1.2174	10a63	170	1.2298
	150	1.2245		140	1.2458		180	1.2149		180	1.2296
	160	1.2187		150	1.2397		190	1.2102		190	1.2270
max		1.2287	max		1.2492	max		1.2179	max		1.2298
	120	1.2160		110	1.2331		150	1.2143		150	1.2207
	130	1.2217		120	1.2390		160	1.2150		160	1.2234
10a64	140	1.2214	10a64	130	1.2392	10a64	170	1.2120	10a64	170	1.2243
	150	1.2165		140	1.2354		180	1.2076		180	1.2228
	160	1.2084		150	1.2290		190	1.2024		190	1.2198
max		1.2217	max		1.2392	max		1.2150	max		1.2243
	120	1.2341		110	1.2453		150	1.2286		150	1.2315
	130	1.2397		120	1.2507		160	1.2295		160	1.2328
10a82	140	1.2384	10a82	130	1.2509	10a82	170	1.2274	10a82	170	1.2334
	150	1.2327		140	1.2485		180	1.2235		180	1.2325
	160	1.2244		150	1.2427		190	1.2181		190	1.2307
max		1.2397	max		1.2509	max		1.2295	max		1.2334
	120	1.2337		110	1.2449		140	1.2225		150	1.2285
	130	1.2377		120	1.2491		150	1.2259		160	1.2300
10a83	140	1.2349	10a83	130	1.2482	10a83	160	1.2258	10a83	170	1.2305
	150	1.2282		140	1.2439		170	1.2229		180	1.2295
	160	1.2189		150	1.2374		180	1.2188		190	1.2273
max		1.2377	max		1.2491	max		1.2259	max		1.2305
	120	1.2303		110	1.2358		140	1.2231		150	1.2240
	130	1.2321		120	1.2394		150	1.2246		160	1.2241
10a84	140	1.2281	10a84	130	1.2385	10a84	160	1.2223	10a84	170	1.2240
	150	1.2197		140	1.2344		170	1.2184		180	1.2221
	160	1.2096		150	1.2278		180	1.2116		190	1.2197
max		1.2321	max		1.2394	max		1.2246	max		1.2241

Table B.2

MCNP In-rack with No Cell Blocker Results for COP Screening with 7 Most Reactive Lattices

"mnu' COP			"mnr" COP			"mxu" COP			"mxr" COP		
Lattice	bu	kclac	Lattice	bu	kclac	Lattice	bu	kclac	Lattice	bu	kclac
	120	0.9077		120	0.9277		150	0.9128		150	0.9235
	130	0.9124		130	0.9309		160	0.9146		160	0.9252
10a61	140	0.9153	10a61	140	0.9303	10a61	170	0.9142	10a61	170	0.9253
	150	0.9147		150	0.9282		180	0.9126		180	0.9270
	160	0.9123		160	0.9242		190	0.9103		190	0.9244
max		0.9153	max		0.9309	max		0.9146	max		0.9270
	120	0.9099		120	0.9309		150	0.9107		160	0.9236
	130	0.9153		130	0.9328		160	0.9127		170	0.9252
10a62	140	0.9158	10a62	140	0.9318	10a62	170	0.9126	10a62	180	0.9255
	150	0.9146		150	0.9273		180	0.9115		190	0.9242
	160	0.9100		160	0.9223		190	0.9086		200	0.9233
max		0.9158	max		0.9328	max		0.9127	max		0.9255
	120	0.9156		120	0.9364		150	0.9146		150	0.9244
	130	0.9205		130	0.9368		160	0.9170		160	0.9280
10a63	140	0.9198	10a63	140	0.9340	10a63	170	0.9168	10a63	170	0.9287
	150	0.9168		150	0.9294		180	0.9140		180	0.9294
	160	0.9121		160	0.9243		190	0.9106		190	0.9283
max		0.9205	max		0.9368	max		0.9170	max		0.9294
	120	0.8989		120	0.9170		150	0.9015		150	0.9089
	130	0.9028		130	0.9171		160	0.9022		160	0.9110
10a64	140	0.9023	10a64	140	0.9133	10a64	170	0.9002	10a64	170	0.9130
	150	0.8987		150	0.9089		180	0.8971		180	0.9115
	160	0.8923		160	0.9034		190	0.8935		190	0.9102
max		0.9028	max		0.9171	max		0.9022	max		0.9130
	120	0.9172		120	0.9312		150	0.9173		150	0.9228
	130	0.9210		130	0.9313		160	0.9185		160	0.9245
10a82	140	0.9211	10a82	140	0.9305	10a82	170	0.9173	10a82	170	0.9254
	150	0.9162		150	0.9253		180	0.9146		180	0.9254
	160	0.9097		160	0.9204		190	0.9099		190	0.9242
max		0.9211	max		0.9313	max		0.9185	max		0.9254
	120	0.9241		110	0.9331		150	0.9224		150	0.9274
	130	0.9265		120	0.9358		160	0.9226		160	0.9288
10a83	140	0.9249	10a83	130	0.9350	10a83	170	0.9200	10a83	170	0.9300
	150	0.9190		140	0.9333		180	0.9173		180	0.9290
	160	0.9127		150	0.9276		190	0.9128		190	0.9279
max		0.9265	max		0.9358	max		0.9226	max		0.9300
	120	0.9091		110	0.9140		140	0.9080		150	0.9110
	130	0.9105		120	0.9170		150	0.9094		160	0.9123
10a84	140	0.9070	10a84	130	0.9163	10a84	160	0.9076	10a84	170	0.9122
	150	0.9009		140	0.9130		170	0.9046		180	0.9113
	160	0.8932		150	0.9079		180	0.8995		190	0.9096
max		0.9105	max		0.9170	max		0.9094	max		0.9123

Table B.3

MCNP In-rack with Cell Blocker Results (Design Basis Model with Empty Cell) for Bounding COP with 7 Most Reactive Lattices

Lattice	bu	kclac	Lattice	bu	kclac
10a61	120	0.8076	10a82	120	0.8099
	130	0.8100		130	0.8119
	140	0.8102		140	0.8093
	150	0.8082		150	0.8055
	160	0.8051		160	0.8015
	peak	0.8102		peak	0.8119
10a62	120	0.8108	10a83	120	0.8196
	130	0.8125		130	0.8198
	140	0.8107		140	0.8167
	150	0.8066		150	0.8117
	160	0.8026		160	0.8074
	peak	0.8125		peak	0.8198
10a63	120	0.8195	10a84	110	0.7989
	130	0.8200		120	0.8013
	140	0.8182		130	0.8000
	150	0.8137		140	0.7979
	160	0.8090		150	0.7939
	peak	0.8200		peak	0.8013
10a64	120	0.8016			
	130	0.8017			
	140	0.7991			
	150	0.7947			
	160	0.7904			
	peak	0.8017			

max 0.8200

Table B.4

MCNP SCCG Results for the 7 Super Lattices with Bounding COP

gd loading	30			35		40		45	
Lattice		bu	sccg	bu	sccg	bu	sccg	bu	sccg
10a61		080	1.3063	100	1.3030	100	1.2856	100	1.2684
		085	1.3108	105	1.3052	105	1.2899	105	1.2720
		090	1.3148	110	1.3062	110	1.2922	110	1.2761
		095	1.3162	115	1.3063	115	1.2950	115	1.2794
		100	1.3174	120	1.3054	120	1.2952	120	1.2828
		105	1.3178	125	1.3042	125	1.2955	125	1.2837
		110	1.3166	130	1.3019	130	1.2943	130	1.2847
		115	1.3148	135	1.2988	135	1.2930	135	1.2847
		120	1.3126	140	1.2962	140	1.2905	140	1.2836
	max		1.3178		1.3063		1.2955		1.2847
							Interpolated gd to 1.31		3.34
10a62		080	1.3127	100	1.3104	100	1.2941	120	1.2914
		085	1.3181	105	1.3122	105	1.2981	125	1.2924
		090	1.3211	110	1.3119	110	1.3004	130	1.2916
		095	1.3229	115	1.3113	115	1.3019	135	1.2910
		100	1.3229	120	1.3093	120	1.3017	140	1.2892
		105	1.3221	125	1.3064	125	1.3012	145	1.2863
		110	1.3197	130	1.3032	130	1.2994	150	1.2835
		115	1.3170	135	1.2996	135	1.2965	155	1.2808
		120	1.3146	140	1.2961	140	1.2935	160	1.2761
	max		1.3229		1.3122		1.3019		1.2924
							Interpolated gd to 1.31		3.61
10a63		080	1.3117	100	1.3079	100	1.2920	120	1.2884
		085	1.3157	105	1.3089	105	1.2961	125	1.2891
		090	1.3183	110	1.3074	110	1.2982	130	1.2885
		095	1.3191	115	1.3064	115	1.2984	135	1.2867
		100	1.3186	120	1.3044	120	1.2973	140	1.2841
		105	1.3163	125	1.3013	125	1.2961	145	1.2806
		110	1.3145	130	1.2979	130	1.2940	150	1.2777
		115	1.3116	135	1.2945	135	1.2912	155	1.2747
		120	1.3083	140	1.2904	140	1.2880	160	1.2706
	max		1.3191		1.3089		1.2984		1.2891
							Interpolated gd to 1.31		3.45
10a64		080	1.3034	100	1.3000	100	1.2849	120	1.2812
		085	1.3078	105	1.3009	105	1.2884	125	1.2815
		090	1.3107	110	1.3000	110	1.2902	130	1.2802
		095	1.3114	115	1.2983	115	1.2906	135	1.2785
		100	1.3107	120	1.2959	120	1.2904	140	1.2762
		105	1.3095	125	1.2936	125	1.2882	145	1.2727
		110	1.3067	130	1.2897	130	1.2860	150	1.2693
		115	1.3039	135	1.2863	135	1.2831	155	1.2660
		120	1.3009	140	1.2828	140	1.2800	160	1.2631
	max		1.3114		1.3009		1.2906		1.2815
							Interpolated gd to 1.31		3.07
10a82		080	1.3122	100	1.3095	100	1.2922	120	1.2908
		085	1.3166	105	1.3115	105	1.2970	125	1.2922
		090	1.3204	110	1.3120	110	1.2996	130	1.2918
		095	1.3223	115	1.3117	115	1.3019	135	1.2906
		100	1.3230	120	1.3099	120	1.3025	140	1.2892
		105	1.3212	125	1.3062	125	1.3005	145	1.2866

		110	1.3197	130	1.3040	130	1.2985	150	1.2833
		115	1.3166	135	1.3004	135	1.2967	155	1.2804
		120	1.3132	140	1.2965	140	1.2934	160	1.2765
	max		1.3230		1.3120		1.3025		1.2922
							Interpolated gd to 1.31		3.61
10a83		080	1.3103	100	1.3075	100	1.2928	100	1.2727
		085	1.3149	105	1.3092	105	1.2967	105	1.2793
		090	1.3184	110	1.3079	110	1.2988	110	1.2838
		095	1.3196	115	1.3064	115	1.2991	115	1.2874
		100	1.3183	120	1.3044	120	1.2983	120	1.2888
		105	1.3166	125	1.3010	125	1.2960	125	1.2891
		110	1.3143	130	1.2979	130	1.2940	130	1.2886
		115	1.3118	135	1.2944	135	1.2914	135	1.2866
		120	1.3076	140	1.2909	140	1.2878	140	1.2837
	max		1.3196		1.3092		1.2991		1.2891
							Interpolated gd to 1.31		3.46
10a84		080	1.3044	095	1.2984	100	1.2865	100	1.2673
		085	1.3083	100	1.3007	105	1.2899	105	1.2737
		090	1.3113	105	1.3006	110	1.2910	110	1.2783
		095	1.3114	110	1.3003	115	1.2914	115	1.2809
		100	1.3105	115	1.2989	120	1.2904	120	1.2815
		105	1.3091	120	1.2960	125	1.2882	125	1.2816
		110	1.3064	125	1.2933	130	1.2860	130	1.2805
		115	1.3036	130	1.2897	135	1.2833	135	1.2788
		120	1.3001	135	1.2862	140	1.2798	140	1.2761
	max		1.3114		1.3007		1.2914		1.2816
							Interpolated gd to 1.31		3.07

Table B.5

MCNP In-rack with Cell Blocker (Design Basis Model with Empty Cell) Results for the 7 Super Lattices with Bounding COP

gd loading	30		35		40	
Lattice	bu	kcalc	bu	kcalc	bu	kcalc
10a61	080	0.8528	100	0.8510	100	0.8390
	085	0.8562	105	0.8527	105	0.8412
	090	0.8587	110	0.8530	110	0.8434
	095	0.8601	115	0.8536	115	0.8447
	100	0.8602	120	0.8527	120	0.8456
	105	0.8602	125	0.8518	125	0.8461
	110	0.8599	130	0.8511	130	0.8458
	115	0.8589	135	0.8487	135	0.8442
	120	0.8575	140	0.8466	140	0.8433
		0.8602		0.8536		0.8461
	Interpolation of kcalc to interpolated Gd to sccg 1.31 (Table B.4)			0.8557		
10a62	080	0.8529	100	0.8520	100	0.8401
	085	0.8560	105	0.8528	105	0.8432
	090	0.8587	110	0.8529	110	0.8452
	095	0.8601	115	0.8525	115	0.8456
	100	0.8603	120	0.8507	120	0.8466
	105	0.8592	125	0.8497	125	0.8456
	110	0.8577	130	0.8471	130	0.8447
	115	0.8567	135	0.8458	135	0.8422
	120	0.8546	140	0.8424	140	0.8410
		0.8603		0.8529		0.8466
	Interpolation of kcalc to interpolated Gd to sccg 1.31 (Table B.4)			0.8516		
10a63	080	0.8624	100	0.8605	100	0.8507
	085	0.8654	105	0.8609	105	0.8529
	090	0.8668	110	0.8607	110	0.8542
	095	0.8679	115	0.8591	115	0.8542
	100	0.8677	120	0.8574	120	0.8537
	105	0.8662	125	0.8561	125	0.8524
	110	0.8648	130	0.8536	130	0.8514
	115	0.8630	135	0.8503	135	0.8485
	120	0.8596	140	0.8481	140	0.8469
		0.8679		0.8609		0.8542
	Interpolation of kcalc to interpolated Gd to sccg 1.31 (Table B.4)			0.8617		
10a64	080	0.8450	095	0.8418	100	0.8331
	085	0.8482	100	0.8432	105	0.8355
	090	0.8493	105	0.8440	110	0.8362
	095	0.8495	110	0.8429	115	0.8371
	100	0.8501	115	0.8423	120	0.8363
	105	0.8491	120	0.8398	125	0.8345
	110	0.8472	125	0.8382	130	0.8325
	115	0.8455	130	0.8366	135	0.8309
	120	0.8434	135	0.8342	140	0.8290
		0.8501		0.8440		0.8371
	Interpolation of kcalc to interpolated Gd to sccg 1.31 (Table B.4)			0.8493		
10a82	080	0.8513	100	0.8512	100	0.8398
	085	0.8555	105	0.8530	105	0.8426
	090	0.8585	110	0.8521	110	0.8448
	095	0.8592	115	0.8515	115	0.8458
	100	0.8603	120	0.8512	120	0.8470

	105	0.8595	125	0.8498	125	0.8462
	110	0.8580	130	0.8474	130	0.8444
	115	0.8567	135	0.8451	135	0.8434
	120	0.8546	140	0.8425	140	0.8403
		0.8603		0.8530		0.8470
	Interpolation of kcalc to interpolated Gd to sccg 1.31 (Table B.4)			0.8515		
10a83	080	0.8617	095	0.8591	100	0.8495
	085	0.8656	100	0.8605	105	0.8525
	090	0.8669	105	0.8607	110	0.8539
	095	0.8677	110	0.8605	115	0.8543
	100	0.8677	115	0.8593	120	0.8536
	105	0.8659	120	0.8586	125	0.8533
	110	0.8644	125	0.8562	130	0.8508
	115	0.8626	130	0.8534	135	0.8490
	120	0.8602	135	0.8506	140	0.8475
		0.8677		0.8607		0.8543
	Interpolation of kcalc to interpolated Gd to sccg 1.31 (Table B.4)			0.8612		
10a84	080	0.8459	095	0.8419	100	0.8331
	085	0.8478	100	0.8438	105	0.8353
	090	0.8507	105	0.8441	110	0.8372
	095	0.8497	110	0.8429	115	0.8370
	100	0.8503	115	0.8424	120	0.8356
	105	0.8486	120	0.8404	125	0.8351
	110	0.8469	125	0.8381	130	0.8328
	115	0.8448	130	0.8356	135	0.8304
	120	0.8422	135	0.8336	140	0.8289
		0.8507		0.8441		0.8372
	Interpolation of kcalc to interpolated Gd to sccg 1.31 (Table B.4)			0.8498		

Table B.6

MCNP SCCG Results with the Bounding Super Lattice to Confirm the Gd Loading Interpolation

gd loading	33		34		35	
	bu	kcalc	bu	kcalc	bu	kcalc
Lattice 10a63	090	1.3092	090	1.3050	090	1.3014
	095	1.3112	095	1.3087	095	1.3057
	100	1.3131	100	1.3100	100	1.3079
	105	1.3124	105	1.3106	105	1.3089
	110	1.3106	110	1.3100	110	1.3074
		1.3131		1.3106		1.3089
					Interpolated to 1.31	3.42
					Table B.4 Interpolated to 1.31	3.45

Table B.7

MCNP In-rack with Cell Blocker (Empty Cell) Results with the Bounding Super Lattice to Confirm the Gd Loading Interpolation

gd loading	33		34		35	
Lattice	bu	kcalc	bu	kcalc	bu	kcalc
10a63	090	0.8609	085	0.8556	090	0.8560
	095	0.8627	090	0.8583	095	0.8586
	100	0.8635	095	0.8612	100	0.8605
	105	0.8635	100	0.8624	105	0.8609
	110	0.8617	105	0.8621	110	0.8607
		0.8635		0.8624		0.8609
					Interpolated to Table B.5 interpolated Gd	0.8617
					Table B.7 Interpolation	0.8617

Table B.8

MCNP In-rack with Cell Blocker (Empty Cell) Results for the SFP Temperature Evaluation (Lattice 10a63)

SFP Temperature Study, Case 20

bu	kcalc	bu	kcalc	bu	kcalc	peak
090	0.8523	095	0.8533	100	0.8527	0.8533

SFP Temperature Study, Case 21

bu	kcalc	bu	kcalc	bu	kcalc	peak
090	0.8523	095	0.8538	100	0.8532	0.8538

SFP Temperature Study, Case 22

bu	kcalc	bu	kcalc	bu	kcalc	peak
090	0.8561	095	0.8567	100	0.8563	0.8567

SFP Temperature Study, Case 23

bu	kcalc	bu	kcalc	bu	kcalc	peak
095	0.8636	100	0.8637	105	0.8621	0.8637

SFP Temperature Study, Case 24

bu	kcalc	bu	kcalc	bu	kcalc	peak
090	0.8649	095	0.8658	100	0.8656	0.8658

SFP Temperature Study, Case 25

bu	kcalc	bu	kcalc	bu	kcalc	peak
095	0.8677	100	0.8677	105	0.8658	0.8677

Table B.9

MCNP In-rack with Cell Blocker (Empty Cell) Results for Eccentric Positioning and Fuel Channel Impact (Lattice 10a63)

Channeled, Full Rack, Cell Centered, Case 10

bu	kcalc	bu	kcalc	bu	kcalc	peak	Delta kcalc tmp 25
090	0.8599	095	0.8609	100	0.8603	0.8609	-0.0068

Channeled, Full Rack, Eccentric to Rack Center, Case 11

bu	kcalc	bu	kcalc	bu	kcalc	peak	Delta kcalc Case 10
090	0.8669	095	0.8680	100	0.8679	0.8680	0.0071

Channeled, Full Rack, Eccentric to Rack Exterior, Case 12

bu	kcalc	bu	kcalc	bu	kcalc	peak	Delta kcalc Case 10
090	0.8573	095	0.8587	100	0.8577	0.8587	-0.0022

Channeled, Full Rack, Eccentric 2x2 Blocks In, Case 13

bu	kcalc	bu	kcalc	bu	kcalc	peak	Delta kcalc Case 10
095	0.8567	100	0.8576	105	0.8558	0.8576	-0.0033

No Channel, Full Rack, Cell Centered, Case 00

bu	kcalc	bu	kcalc	bu	kcalc	peak	Delta kcalc tmp 25
085	0.8598	090	0.8611	095	0.8611	0.8611	0.0002

No Channel, Full Rack, Eccentric to Rack Center, Case 01

bu	kcalc	bu	kcalc	bu	kcalc	peak	Delta kcalc Case 00
085	0.8762	090	0.8793	095	0.8789	0.8793	0.0182

No Channel, Full Rack, Eccentric to Rack Exterior, Case 02

bu	kcalc	bu	kcalc	bu	kcalc	peak	Delta kcalc Case 00
085	0.8571	090	0.8593	095	0.8589	0.8593	-0.0018

No Channel, Full Rack, Eccentric 2x2 Blocks In, Case 03

bu	kcalc	bu	kcalc	bu	kcalc	peak	Delta kcalc Case 00
095	0.8496	100	0.8501	105	0.8491	0.8501	-0.0110

Eccentric Bias	0.0182

Table B.10

MCNP In-rack with Cell Blocker (Empty Cell) Results for Assembly Rotation (Lattice 10a63)

Full Rack, Assembly Rotation Case 00 (reference)

bu	kcalc	bu	kcalc	bu	kcalc	peak	delta k case tmp 25
090	0.8609	095	0.8609	100	0.8603	0.8609	-0.0068

Full Rack, Assembly Rotation Case 01

bu	kcalc	bu	kcalc	bu	kcalc	peak	Delta kcalc Case 00
090	0.8607	095	0.8612	100	0.8609	0.8612	0.0003

Full Rack, Assembly Rotation Case 02

bu	kcalc	bu	kcalc	bu	kcalc	peak	Delta kcalc Case 00
095	0.8609	100	0.8611	105	0.8597	0.8611	0.0002

Full Rack, Assembly Rotation Case 03

bu	kcalc	bu	kcalc	bu	kcalc	peak	Delta kcalc Case 00
090	0.8606	095	0.8609	100	0.8603	0.8609	0.0000

Full Rack, Assembly Rotation Case 04

bu	kcalc	bu	kcalc	bu	kcalc	peak	Delta kcalc Case 00
090	0.8604	095	0.8616	100	0.8615	0.8616	0.0007
						bias	0.0007

Table B.11

MCNP In-rack with Cell Blocker (Empty Cell) Results for Fuel Manufacturing Tolerances (Lattice 10a63)

Fuel Tolerance Calculations, Case 00

bu	kcalc	bu	kcalc	bu	kcalc	peak kcalc	Delta kcalc tmp 25	
090	0.8668	095	0.8679	100	0.8677	0.8679	0.0002	

Increase Clad ID and Decrease Clad OD Tolerance Calculations, Case 01

bu	kcalc	bu	kcalc	bu	kcalc	peak kcalc	Delta kcalc	95/95 unc
090	0.8682	095	0.8691	100	0.8684	0.8691	0.0012	0.0023

Decrease Clad ID and Increase Clad OD Tolerance Calculations, Case 02

bu	kcalc	bu	kcalc	bu	kcalc	peak kcalc	Delta kcalc	95/95 unc
090	0.8660	095	0.8665	100	0.8661	0.8665	-0.0014	-0.0003

Decrease Fuel Rod Pitch Tolerance Calculations, Case 03

bu	kcalc	bu	kcalc	bu	kcalc	peak kcalc	Delta kcalc	95/95 unc
090	0.8163	095	0.8183	100	0.8181	0.8183	-0.0496	-0.0485

Decrease Water Rod Thickness Tolerance Calculations, Case 05

bu	kcalc	bu	kcalc	bu	kcalc	peak kcalc	Delta kcalc	95/95 unc
090	0.8675	095	0.8684	100	0.8675	0.8684	0.0005	0.0016

Increase Water Rod Thickness Tolerance Calculations, Case 06

bu	kcalc	bu	kcalc	bu	kcalc	peak kcalc	Delta kcalc	95/95 unc
090	0.8669	095	0.8677	100	0.8669	0.8677	-0.0002	0.0009

Decrease Channel Thickness Tolerance Calculations, Case 07

bu	kcalc	bu	kcalc	bu	kcalc	peak kcalc	Delta kcalc	95/95 unc
090	0.8673	095	0.8675	100	0.8675	0.8675	-0.0004	0.0007

Increase Channel Thickness Tolerance Calculations, Case 08

bu	kcalc	bu	kcalc	bu	kcalc	peak kcalc	Delta kcalc	95/95 unc
085	0.8661	090	0.8682	095	0.8675	0.8682	0.0003	0.0014

Decrease channel ID Tolerance Calculations, Case 09

bu	kcalc	bu	kcalc	bu	kcalc	peak kcalc	Delta kcalc	95/95 unc
090	0.8677	095	0.8679	100	0.8678	0.8679	0.0000	0.0011

Increase Channel ID Tolerance Calculations, Case 10

bu	kcalc	bu	kcalc	bu	kcalc	peak kcalc	Delta kcalc	95/95 unc
095	0.8675	100	0.8677	105	0.8662	0.8677	-0.0002	0.0009

Increase Pellet Density Tolerance Calculations, Case 25

bu	kcalc	bu	kcalc	bu	kcalc	peak kcalc	Delta kcalc	95/95 unc
085	0.8667	090	0.8682	095	0.8677	0.8682	0.0003	0.0014

Decrease Pellet OD Tolerance Calculations, Case 26

bu	kcalc	bu	kcalc	bu	kcalc	peak kcalc	Delta kcalc	95/95 unc
085	0.8662	090	0.8683	095	0.8683	0.8683	0.0004	0.0015

Increase Pellet OD Tolerance Calculations, Case 27

bu	kcalc	bu	kcalc	bu	kcalc	peak kcalc	Delta kcalc	95/95 unc
085	0.8660	090	0.8681	095	0.8677	0.8681	0.0002	0.0013

statistical combination of positive calculations 0.0040

Table B.12

MCNP In-rack with Cell Blocker (Empty Cell) Results for BORAFLEX™ rack manufacturing tolerances (Lattice 10a63)

Nominal Rack Calculations, Case 00

bu	kcalc	bu	kcalc	bu	kcalc	peak kcalc	Delta kcalc tmp 25	
090	0.8668	095	0.8679	100	0.8677	0.8679	0.0002	

Minimum Cell ID (NS) Tolerance Calculations, Case 11

bu	kcalc	bu	kcalc	bu	kcalc	peak kcalc	Delta kcalc	95/95 unc
090	0.8679	095	0.8682	100	0.8676	0.8682	0.0003	0.0014

Maximum Cell ID (NS) Tolerance Calculations, Case 12

bu	kcalc	bu	kcalc	bu	kcalc	peak kcalc	Delta kcalc	95/95 unc
090	0.8669	095	0.8676	100	0.8669	0.8676	-0.0003	0.0008

Minimum Cell ID (WE) Tolerance Calculations, Case 13

bu	kcalc	bu	kcalc	bu	kcalc	peak kcalc	Delta kcalc	95/95 unc
095	0.8685	100	0.8690	105	0.8679	0.8690	0.0011	0.0022

Maximum Cell ID (WE) Tolerance Calculations, Case 14

bu	kcalc	bu	kcalc	bu	kcalc	peak kcalc	Delta kcalc	95/95 unc
090	0.8668	095	0.8670	100	0.8668	0.8670	-0.0009	0.0002

Minimum Cell Wall Thickness Tolerance Calculations, Case 15

bu	kcalc	bu	kcalc	bu	kcalc	peak kcalc	Delta kcalc	95/95 unc
095	0.8735	100	0.8745	105	0.8726	0.8745	0.0066	0.0077

Maximum Cell Wall Thickness Tolerance Calculations, Case 16

bu	kcalc	bu	kcalc	bu	kcalc	peak kcalc	Delta kcalc	95/95 unc
095	0.8615	100	0.8624	105	0.8604	0.8624	-0.0055	-0.0044

Minimum Poison Box ID Tolerance Calculations, Case 17

bu	kcalc	bu	kcalc	bu	kcalc	peak kcalc	Delta kcalc	95/95 unc
090	0.8693	095	0.8697	100	0.8687	0.8697	0.0018	0.0029

Maximum Poison Box ID Tolerance Calculations, Case 18

bu	kcalc	bu	kcalc	bu	kcalc	peak kcalc	Delta kcalc	95/95 unc
090	0.8655	095	0.8666	100	0.8660	0.8666	-0.0013	-0.0002

statistical combination of positive calculations 0.0087

Table B.13

MCNP In-rack with Cell Blocker (Empty Cell) Results for the Depletion Related Fuel Geometry Changes (Lattice 10a63)

Nominal Fuel Calculations, Case 00

bu	kcalc	bu	kcalc	bu	kcalc	peak kcalc	Delta kcalc tmp 25
085	0.8654	090	0.8668	095	0.8679	0.8679	0.0002

Fuel Rod Growth and Cladding Creep Calculations, Case cc

bu	kcalc	bu	kcalc	bu	kcalc	peak kcalc	Delta kcalc case 00
085	0.8690	090	0.8710	095	0.8715	0.8715	0.0036

Fuel Channel Bulging and Bowing Calculations, Case cb

bu	kcalc	bu	kcalc	bu	kcalc	peak kcalc	Delta kcalc case 00
090	0.8677	095	0.8673	100	0.8673	0.8677	-0.0002

sum	0.0036
95/95 unc	0.0011

Table B.14

MCNP In-rack with Cell Blocker (Empty Cell) Results for the Depletion Uncertainty

(Lattice 10a63)

Depletion Uncertainty

bu	kcalc	Delta kcalc tmp 25	95/95 unc	5% factor
000	0.9488	0.0811	0.0822	0.0041

Table B.15

MCNP In-rack with Cell Blocker (Empty Cell) Results for the Cooling Time Study Results (Lattice 10a63)

Cooling Time Study, Case 01

bu	kcalc	bu	kcalc	bu	kcalc	peak kcalc	Delta kcalc tmp 25
085	0.8656	090	0.8676	095	0.8672	0.8676	-0.0001

Cooling Time Study, Subcase 02

bu	kcalc	bu	kcalc	bu	kcalc	peak kcalc	Delta kcalc tmp 25
085	0.8655	090	0.8669	090	0.8669	0.8669	-0.0008

Cooling Time Study, Subcase 03

bu	kcalc	bu	kcalc	bu	kcalc	peak kcalc	Delta kcalc tmp 25
085	0.8654	090	0.8676	090	0.8676	0.8676	-0.0001

Cooling Time Study, Subcase 04

bu	kcalc	bu	kcalc	bu	kcalc	peak kcalc	Delta kcalc tmp 25
085	0.8657	090	0.8675	090	0.8675	0.8675	-0.0002

				cooling time bias	0.0000		

Table B.16

MCNP In-rack with Cell Blocker (Empty Cell) Results for the Alternative COP Study

(Lattice 10a63)

COP Study, Maximum Fuel Temperature, Case 01

bu	kcalc	bu	kcalc	bu	kcalc	peak kcalc	Delta kcalc tmp 25
090	0.8672	095	0.8686	100	0.8680	0.8686	0.0009

COP Study, Maximum Moderator Temperature, Case 02

bu	kcalc	bu	kcalc	bu	kcalc	peak kcalc	Delta kcalc tmp 25
085	0.8650	090	0.8661	090	0.8661	0.8661	-0.0016

COP Study, Maximum Void Fraction, Case 02

bu	kcalc	bu	kcalc	bu	kcalc	peak kcalc	Delta kcalc tmp 25
130	0.8544	135	0.8548	140	0.8534	0.8548	-0.0129

Table B.17

MCNP In-rack with Cell Blocker (Empty Cell) Results for the Accident Calculations

(Lattice 10a63)

case	bu	kcalc	bu	kcalc	bu	kcalc	peak kcalc
010	090	0.8624	095	0.8633	100	0.8629	0.8633
011	085	0.8668	090	0.8692	095	0.8683	0.8692
012	095	0.8610	100	0.8628	105	0.8607	0.8628
013	090	0.8620	095	0.8637	100	0.8622	0.8637
014	095	0.8688	100	0.8692	105	0.8667	0.8692
015	095	0.8608	100	0.8616	105	0.8603	0.8616
110	090	0.8642	095	0.8644	100	0.8641	0.8644
111	090	0.8687	095	0.8693	100	0.8691	0.8693
112	090	0.8677	095	0.8679	100	0.8662	0.8679
113	090	0.8625	095	0.8627	100	0.8627	0.8627
114	085	0.8675	090	0.8684	095	0.8683	0.8684
115	090	0.8607	095	0.8624	100	0.8617	0.8624
410	085	0.8614	090	0.8631	095	0.8630	0.8631
411	090	0.8696	095	0.8697	100	0.8691	0.8697
412	090	0.8611	095	0.8623	100	0.8615	0.8623
413	090	0.8628	095	0.8632	100	0.8621	0.8632
414	090	0.8681	095	0.8688	100	0.8684	0.8688
415	085	0.8593	090	0.8620	095	0.8614	0.8620
						max	0.8697

Table B.18

Comparison of the Fuel Vendor SCCG with MCNP SCCG

Parameter	Value
Fuel Vendor Lattice ID	11399
Fuel Vendor SCCG k_{inf} (with 1% bias)	1.2379
MCNP Lattice ID	10a63
MCNP k_{calc}	1.2492
Delta-k MCNP to Vendor SCCG	0.0113

Figure B.1

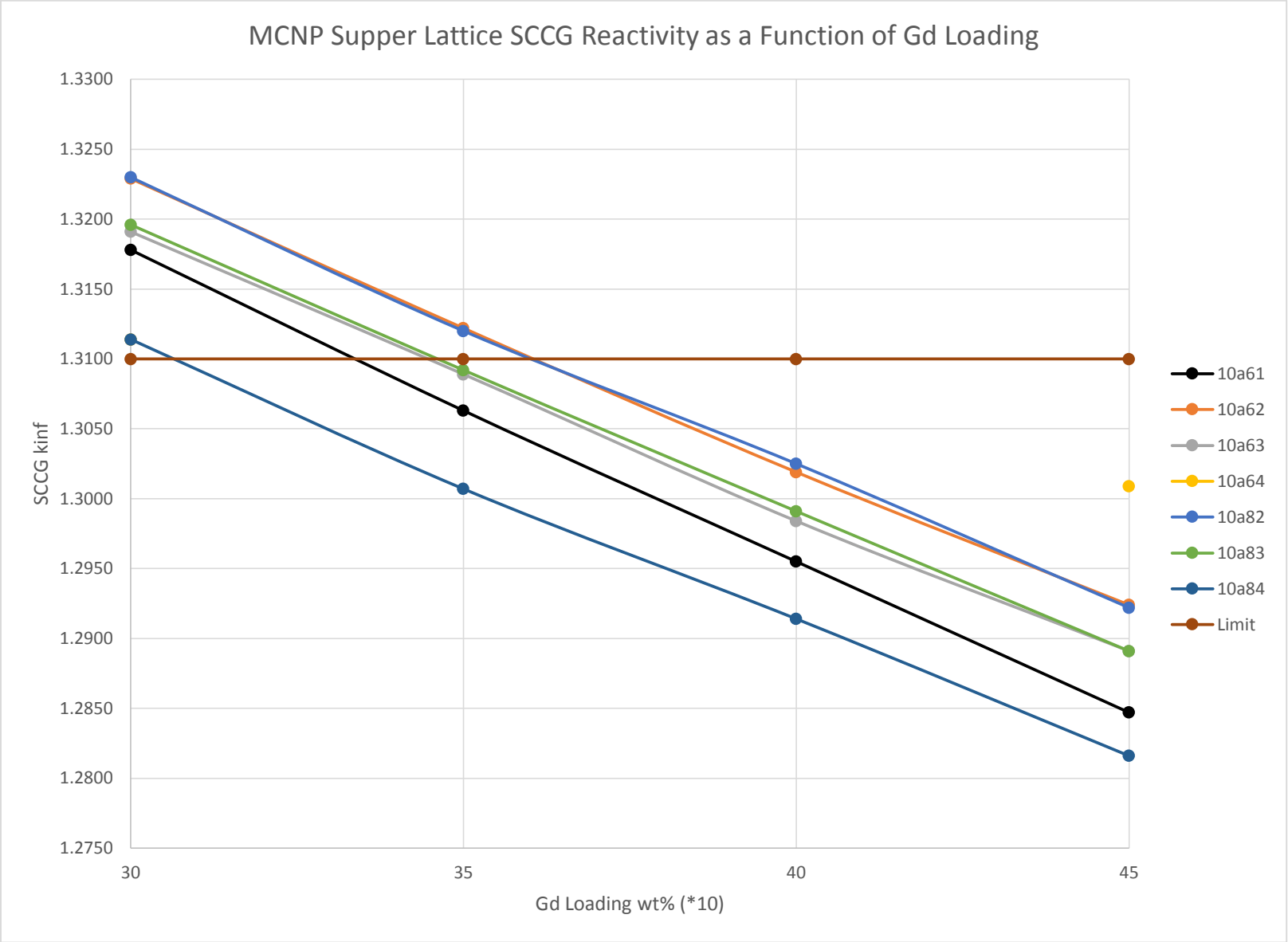
MCNP Supper Lattice SCCG Reactivity as a Function of Gd Loading
SCCG kinf
1.3300
1.3250
1.3200
1.3150
1.3100
1.3050
1.3000
1.2950
1.2900
1.2850
1.2800
1.2750
30
35
40
45
Gd Loading wt% (*10)
10a61
10a62
10a63
10a64
10a82
10a83
10a84
Limit

Figure B.2

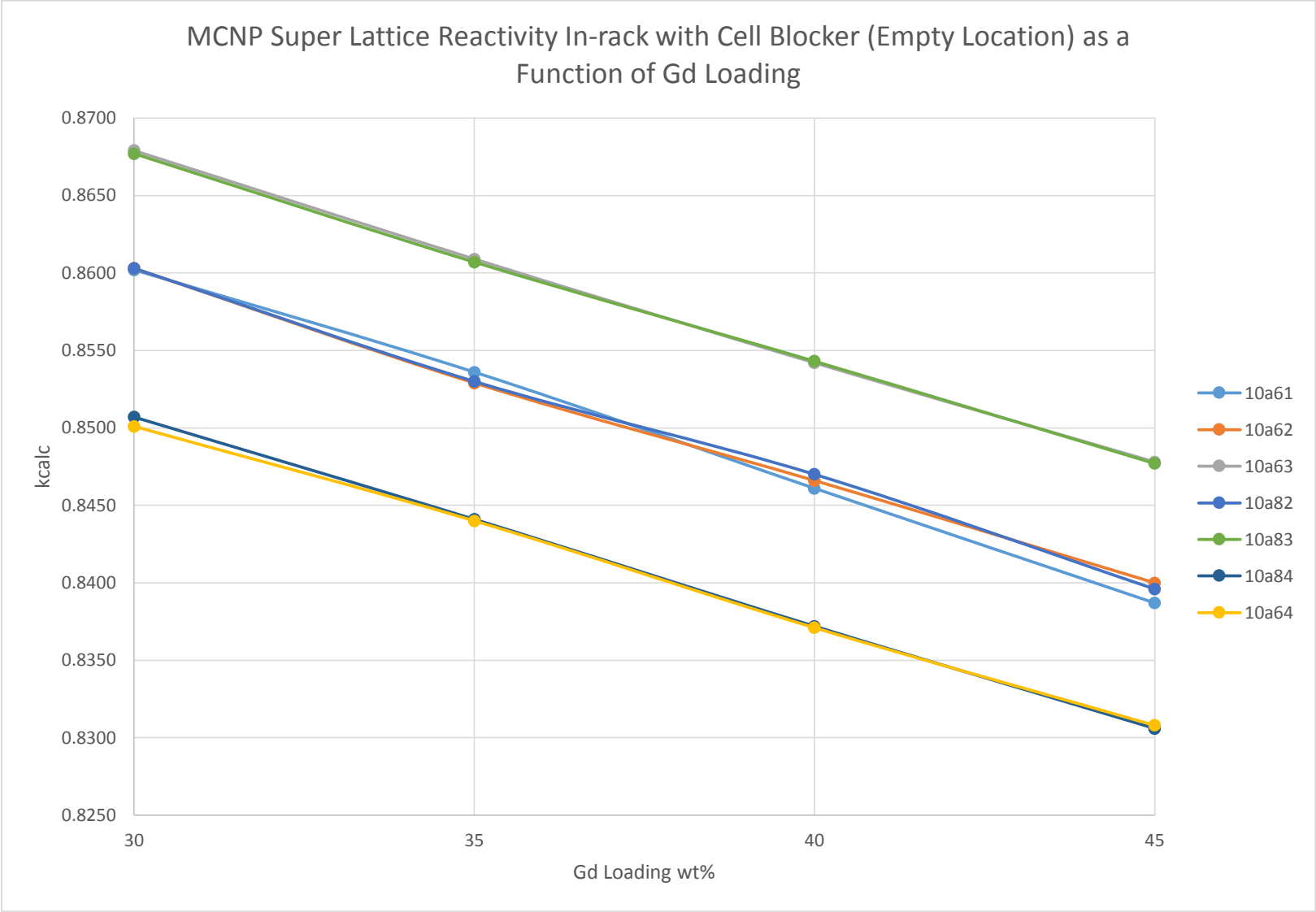
MCNP Super Lattice Reactivity In-rack with Cell Blocker (Empty Location) as a Function of Gd Loading
0.8700
0.8650
0.8600
0.8550
0.8500
0.8450
0.8400
0.8350
0.8300
0.8250
kcalc
30
35
40
45
Gd Loading wt%
10a61
10a62
10a63
10a82
10a83
10a84
10a64

Figure B.3

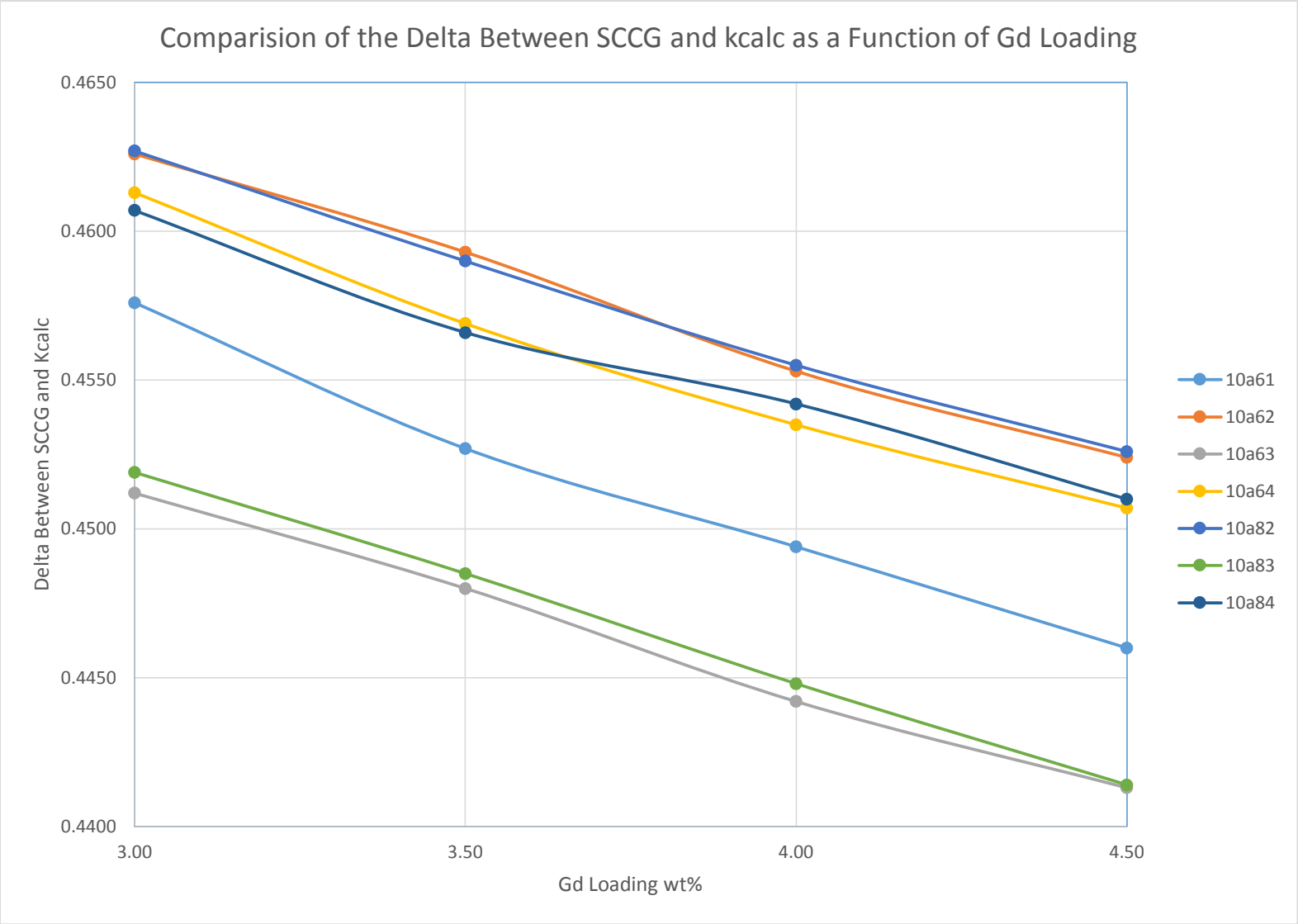
Comparision of the Delta Between SCCG and kcalc as a Function of Gd Loading
Delta Between SCCG and Kcalc
0.4650
0.4600
0.4550
0.4500
0.4450
0.4400
3.00
3.50
4.00
4.50
Gd Loading wt%
10a61
10a62
10a63
10a64
10a82
10a83
10a84

Figure B.4

Eccentric Positioning Case 10 (Reference Case)

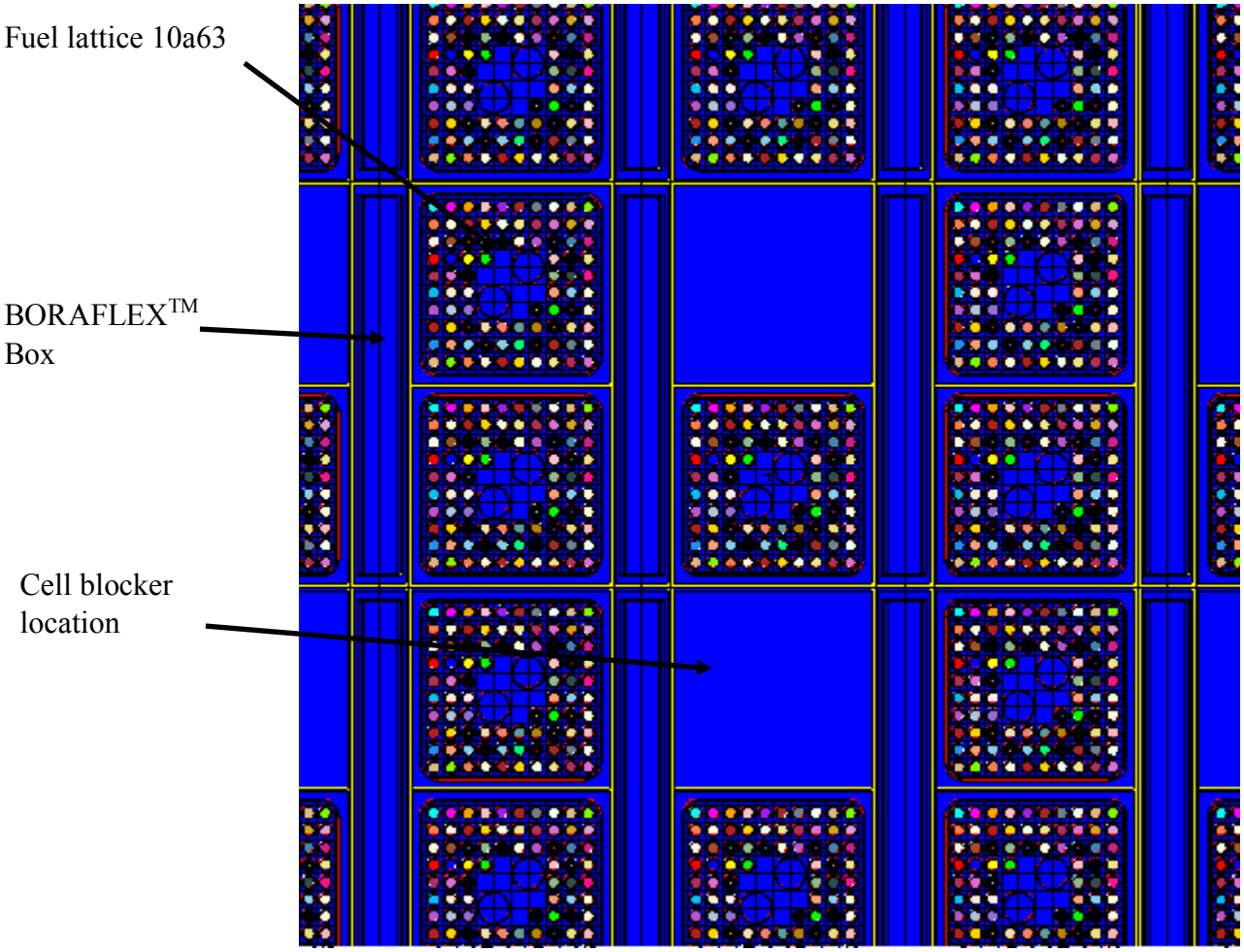

Note: This is a partial 2D representation of the full rack MCNP model.

Figure B.5

Eccentric Positioning Case 11

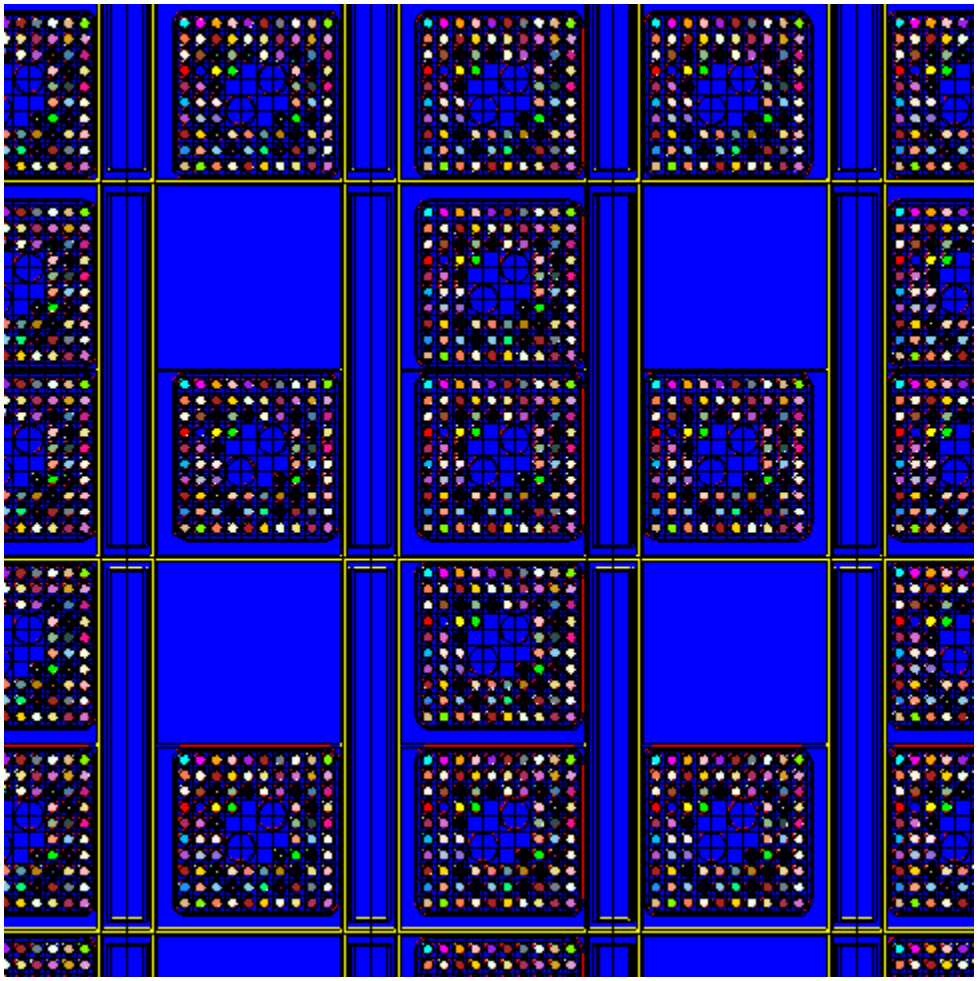

Note: This is a partial 2D representation of the full rack MCNP model.

Figure B.6

Eccentric Positioning Case 12

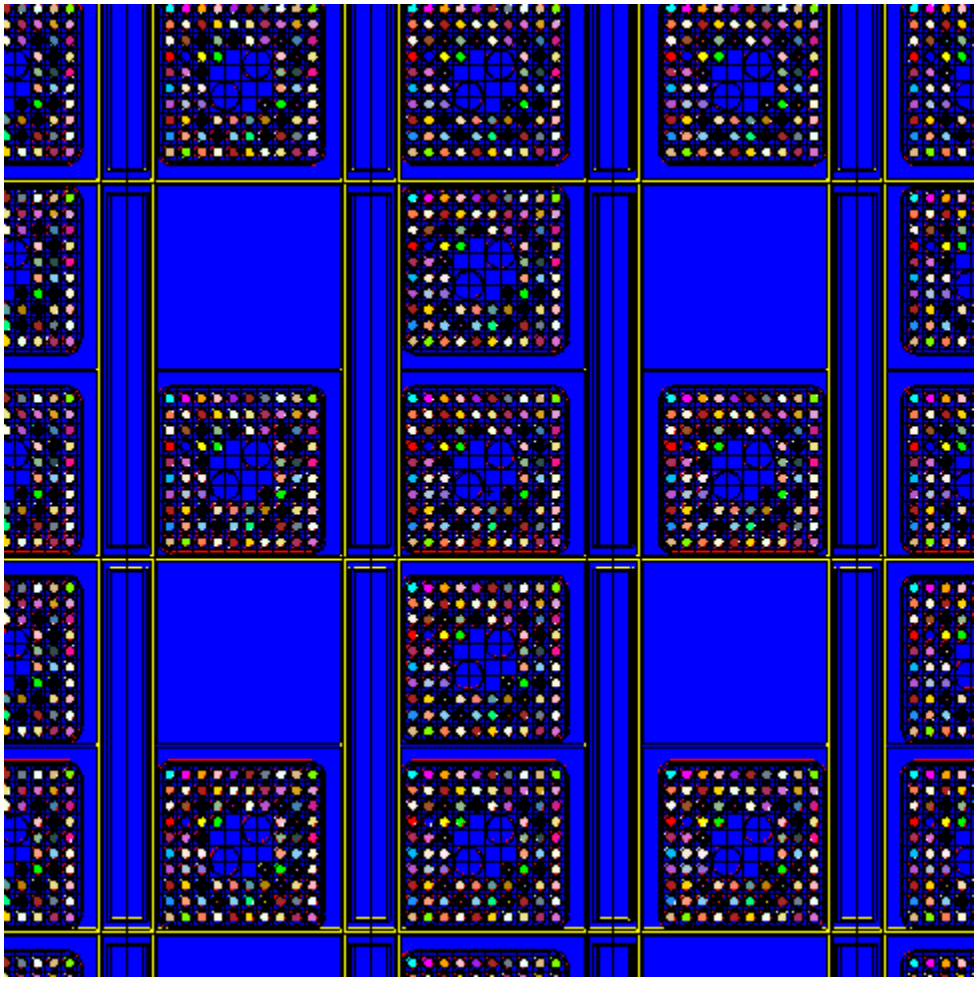

Note: This is a partial 2D representation of the full rack MCNP model.

Figure B.7

Eccentric Positioning Case 13

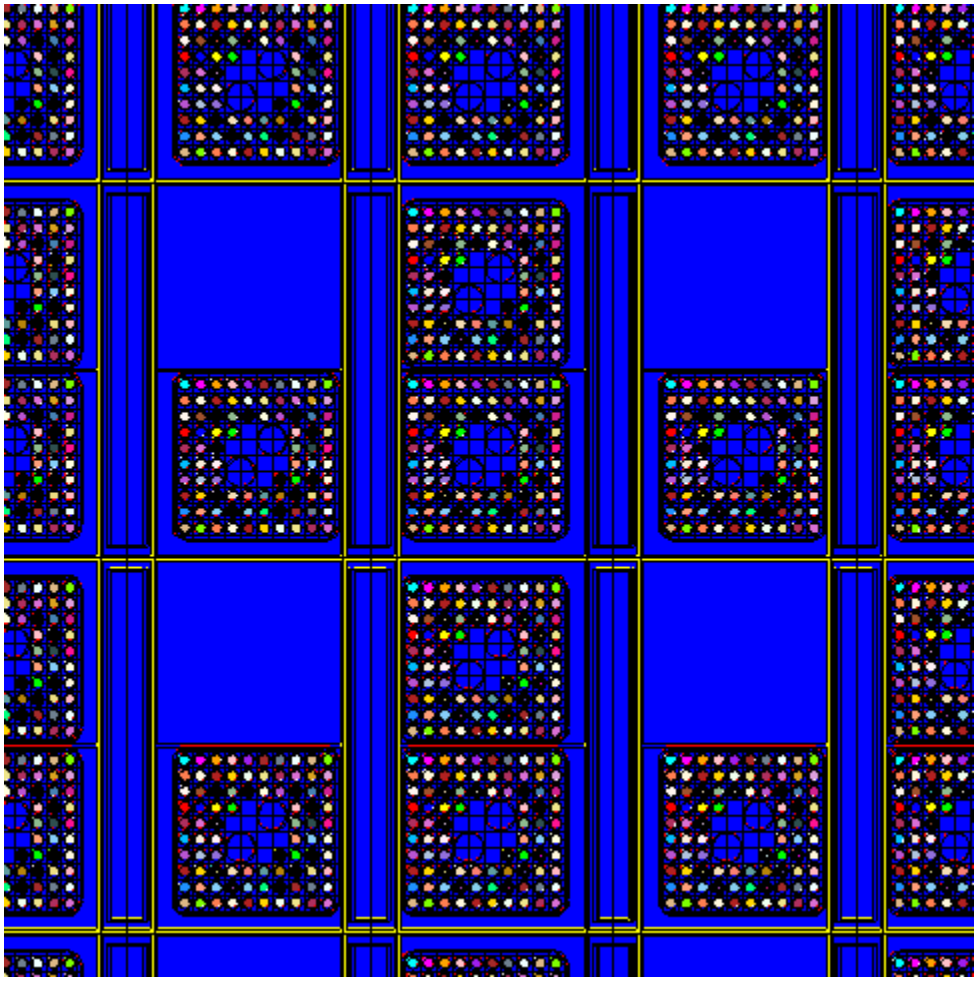

Note: This is a partial 2D representation of the full rack MCNP model.

Figure B.8

Lattice Orientation Case 00 (Reference Case)

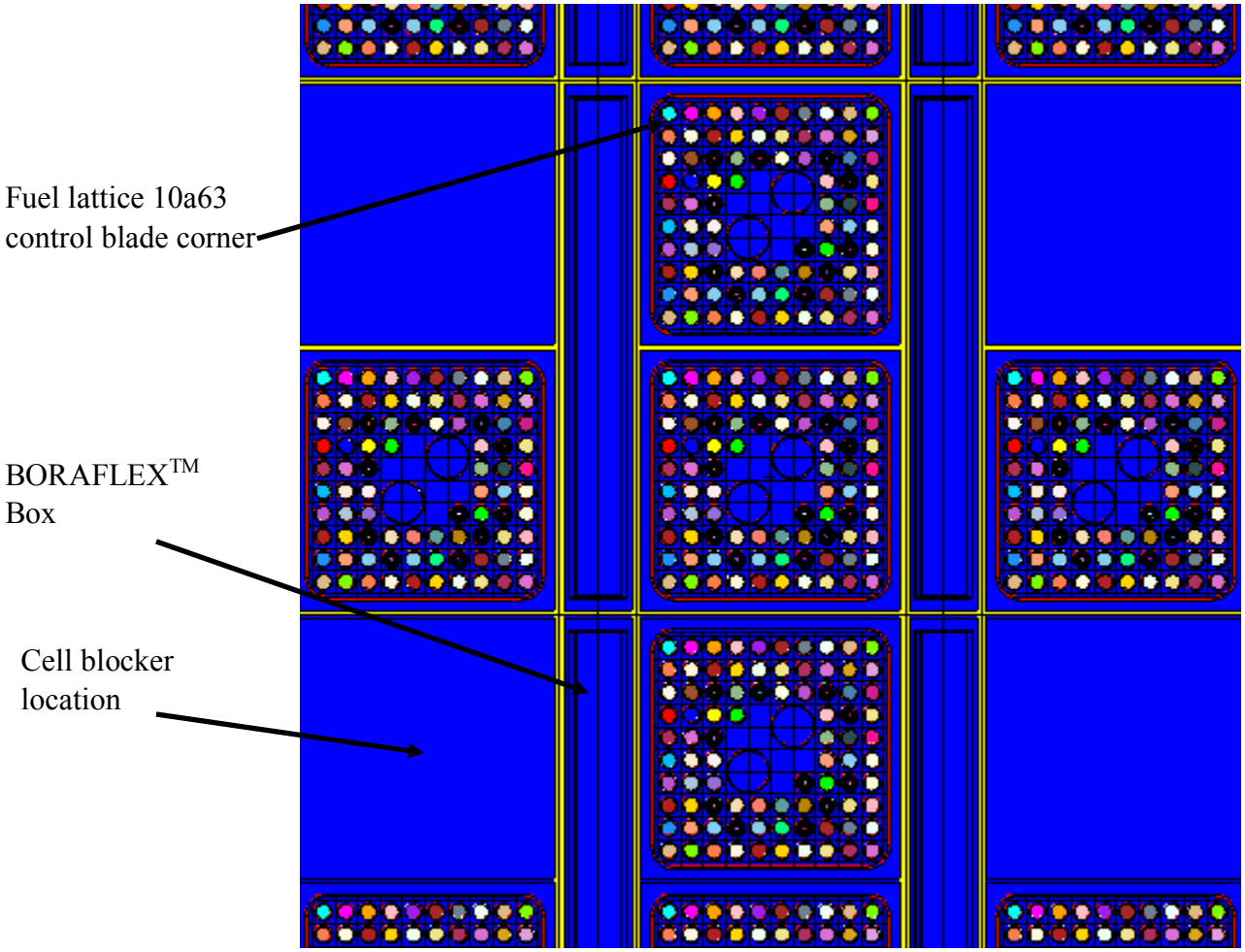

Note: This is a partial 2D representation of the full rack MCNP model.

Figure B.9

Lattice Orientation Case 01

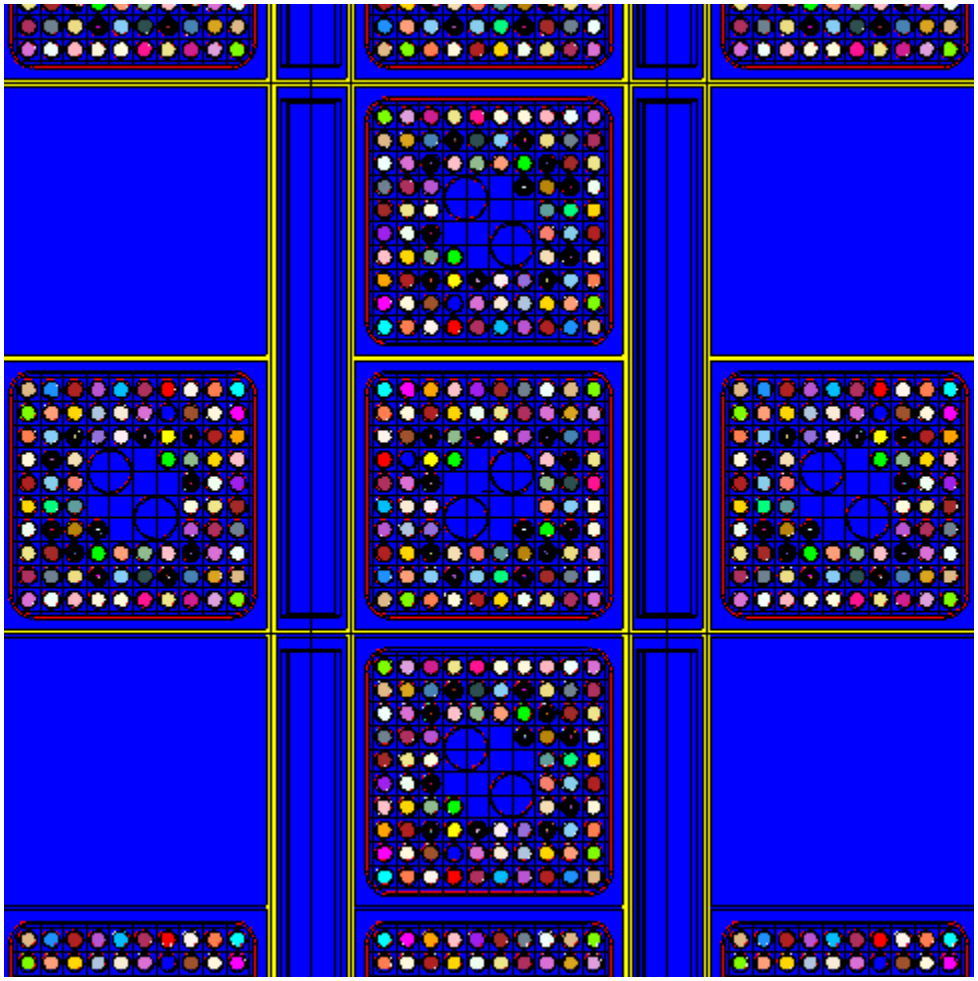

Note: This is a partial 2D representation of the full rack MCNP model.

Figure B.10

Lattice Orientation Case 02

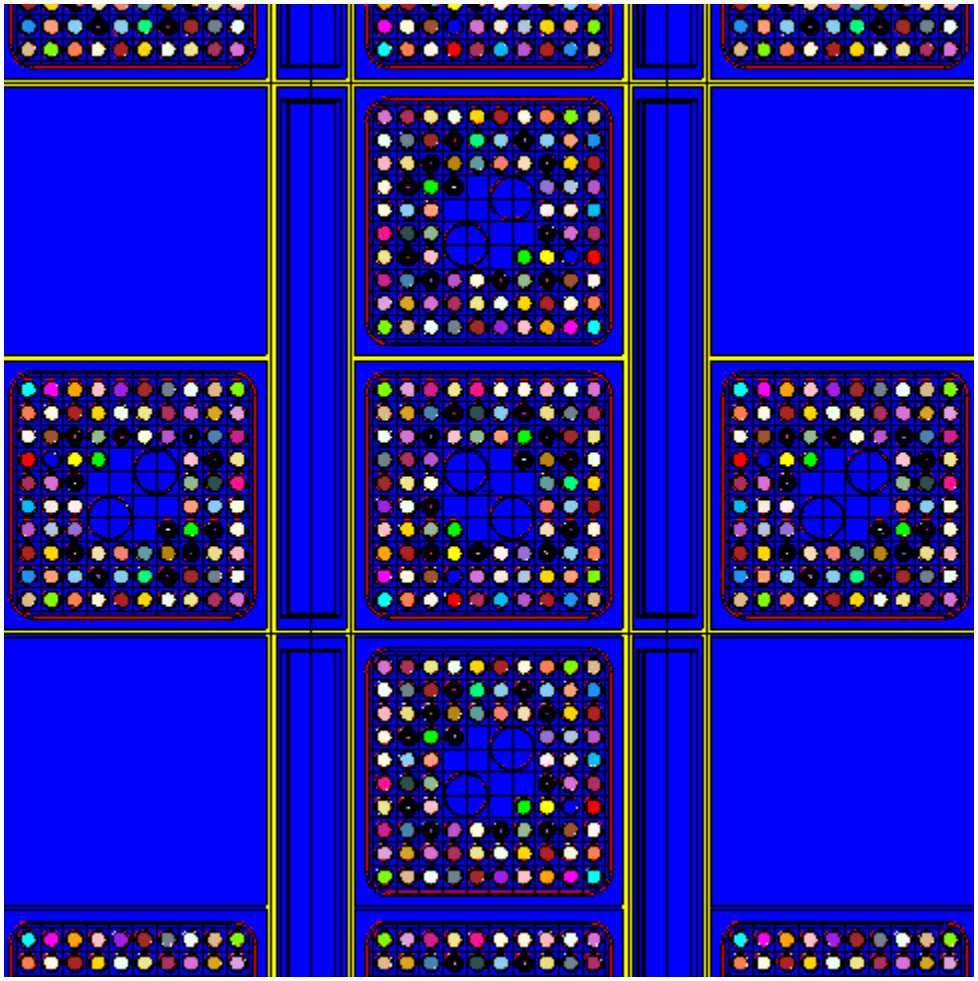

Note: This is a partial 2D representation of the full rack MCNP model.

Figure B.11

Lattice Orientation Case 03

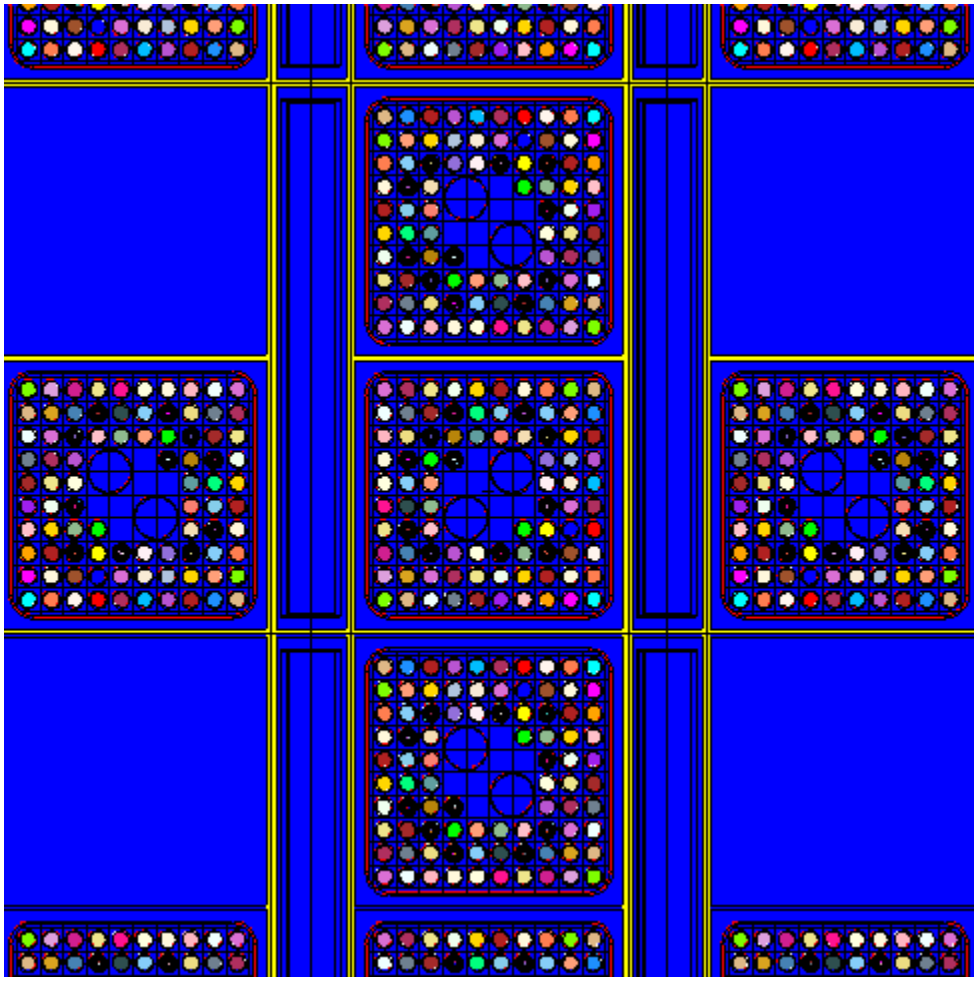

Note: This is a partial 2D representation of the full rack MCNP model.

Figure B.12

Lattice Orientation Case 04

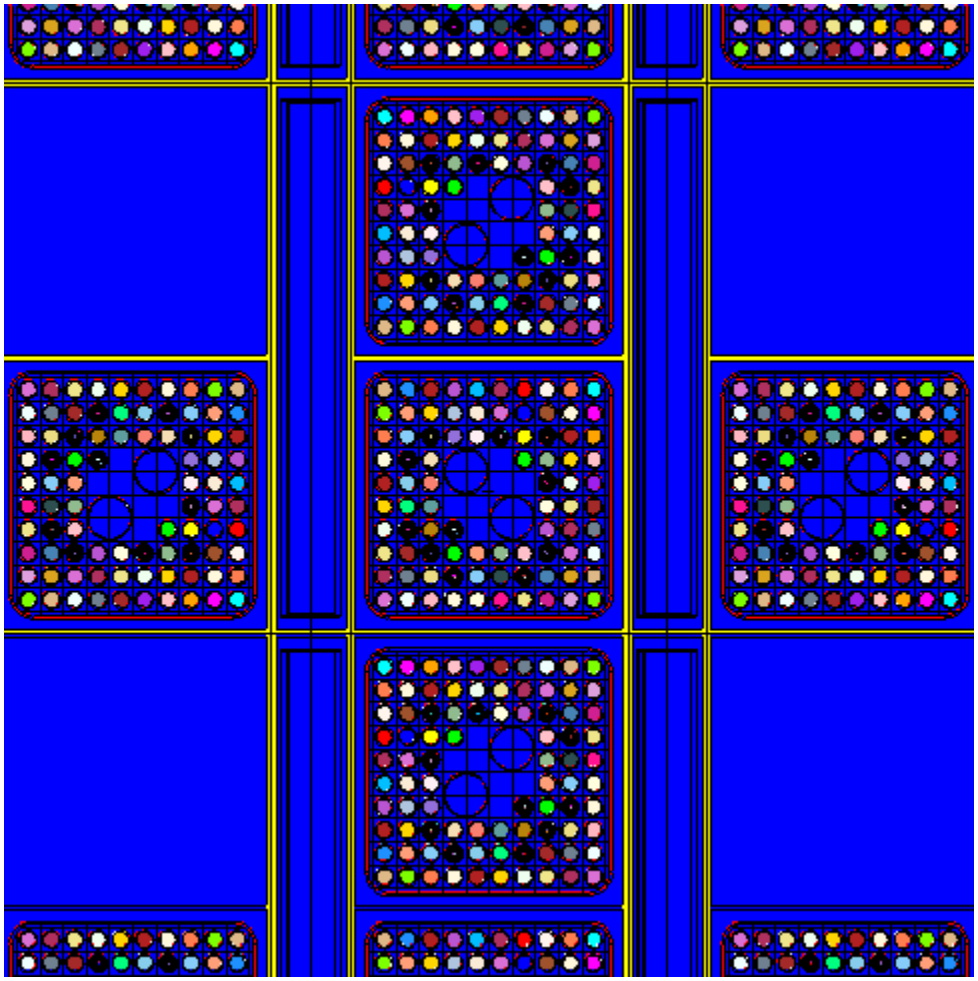

Note: This is a partial 2D representation of the full rack MCNP model.

APPENDIX C: CRITICALITY ANALYSIS CHECKLIST [18]

The criticality analysis checklist is completed by the applicant prior to submittal to the NRC. It provides a useful guide to the applicant to ensure that all the applicable subject areas are addressed in the application, or to provide justification/identification of alternative approaches.

The checklist also assists the NRC reviewer in identifying areas of the analysis that conform or do not conform to the guidance in NEI 12-16. Subsequently, the NRC review can then be more efficiently focused on those areas that deviate from NEI 12-16 and the justification for those deviations.

Subject	Included	Notes / Explanation
1.0 Introduction and Overview		
Purpose of submittal	Remove Boraflex credit from the only two Boraflex racks in NMP1 SFP using cell blockers.	
Changes requested		
Summary of physical changes	Addition of cell blockers.	
Summary of Tech Spec changes	none	
Summary of analytical scope	Criticality analysis to show compliance with Tech Spec limits of SCCG < 1.31 and IMPAE < 4.6 % U-235.	
2.0 Acceptance Criteria and Regulatory Guidance		
Summary of requirements and guidance	**YES**/NO	
Requirements documents referenced	**YES**/NO	
Guidance documents referenced	**YES**/NO	
Acceptance criteria described	**YES**/NO	
3.0 Reactor and Fuel Design Description		
Describe reactor operating parameters	**YES**/NO	
Describe all fuel in pool	**YES**/NO	
Geometric dimensions (Nominal and Tolerances)	**YES**/NO	
Schematic of guide tube patterns	**YES**/NO	
Material compositions	**YES**/NO	
Describe future fuel to be covered	**YES**/NO	Current Tech Spec limits govern future fuel.
Geometric dimensions (Nominal and Tolerances)	**YES**/NO	
Schematic of guide tube patterns	YES/**NO**	
Material compositions	YES/**NO**	
Describe all fuel inserts	YES/**NO**	
Geometric Dimensions (Nominal and Tolerances)	YES/NO	
Schematic (axial/cross-section)	YES/NO	
Material compositions	YES/NO	
Describe non-standard fuel	YES/**NO**	
Geometric dimensions		

Subject	Included	Notes / Explanation
Describe non-fuel items in fuel cells	YES/**NO**	
Nominal and tolerance dimensions	YES/NO	
4.0 Spent Fuel Pool/Storage Rack Description		
New fuel vault & Storage rack description	YES/**NO**	
Nominal and tolerance dimensions	YES/NO	
Schematic (axial/cross-section)	YES/NO	
Material compositions		
Spent fuel pool, Storage rack description	**YES**/NO	Two Boraflex racks.
Nominal and tolerance dimensions	**YES**/NO	
Schematic (axial/cross-section)	**YES**/NO	
Material compositions	**YES**/NO	
Other Reactivity Control Devices (Inserts)		
Nominal and tolerance dimensions		
Schematic (axial/cross-section)		
Material compositions		
5.0 Overview of the Method of Analysis		
New fuel rack analysis description	YES/**NO**	
Storage geometries	YES/NO	
Bounding assembly design(s)	YES/NO	
Integral absorber credit	YES/NO	
Accident analysis	YES/NO	
Spent fuel storage rack analysis description	**YES**/NO	
Storage geometries	**YES**/NO	
Bounding assembly design(s)	**YES**/NO	
Soluble boron credit	YES/**NO**	
Boron dilution analysis	YES/NO	
Burnup credit	YES/**NO**	
Decay/Cooling time credit	YES/**NO**	
Integral absorber credit	YES/**NO**	
Other credit	**YES**/NO	Peak reactivity method
Fixed neutron absorbers	YES/**NO**	Boraflex credit removal using cell blockers
Aging management program	YES/NO	
Accident analysis	**YES**/NO	
Temperature increase	**YES**/NO	
Assembly drop	**YES**/NO	
Single assembly misload		Peak reactivity method precludes a misload accident.
Multiple misload	YES/**NO**	
Boron dilution	YES/**NO**	
Other	**YES**/NO	seismic
Fuel out of rack analysis	YES/**NO**	
Handling	YES/NO	
Movement	YES/NO	
Inspection	YES/NO	
6.0 Computer Codes, Cross Sections and Validation Overview		
Code/Modules Used for Calculation of k_{eff}	**YES**/NO	
Cross section library	**YES**/NO	
Description of nuclides used	**YES**/NO	
Convergence checks	**YES**/NO	
Code/Module Used for Depletion Calculation	**YES**/NO	

Subject	Included	Notes / Explanation
Cross section library	**YES**/NO	
Description of nuclides used	**YES**/NO	
Convergence checks	**YES**/NO	
Validation of Code and Library	**YES**/NO	
Major Actinides and Structural Materials	**YES**/NO	
Minor Actinides and Fission Products	**YES**/NO	
Absorbers Credited	**YES**/NO	
7.0 Criticality Safety Analysis of the New Fuel Rack	**NO**	
Rack model	YES/NO	
Boundary conditions	YES/NO	
Source distribution	YES/NO	
Geometry restrictions	YES/NO	
Limiting fuel design	YES/NO	
Fuel density	YES/NO	
Burnable Poisons	YES/NO	
Fuel dimensions	YES/NO	
Axial blankets	YES/NO	
Limiting rack model	YES/NO	
Storage vault dimensions and materials	YES/NO	
Temperature	YES/NO	
Multiple regions/configurations	YES/NO	
Flooded	YES/NO	
Low density moderator	YES/NO	
Eccentric fuel placement	YES/NO	
Tolerances	YES/NO	
Fuel geometry	YES/NO	
Fuel pin pitch	YES/NO	
Fuel pellet OD	YES/NO	
Fuel clad OD	YES/NO	
Fuel content		
Enrichment	YES/NO	
Density	YES/NO	
Integral absorber		
Rack geometry		
Rack pitch	YES/NO	
Cell wall thickness	YES/NO	
Storage vault dimensions/materials		
Code uncertainty	YES/NO	
Biases		
Temperature	YES/NO	
Code bias	YES/NO	
Moderator Conditions		
Fully flooded and optimum density moderator	YES/NO	

Subject	Included	Notes / Explanation
8.0 Depletion Analysis for Spent Fuel		
Depletion Model Considerations		
Time step verification	**YES**/NO	
Convergence verification	**YES**/NO	
Simplifications	**YES**/NO	
Non-uniform enrichments	**YES**/NO	Pin wise compositions considered
Post Depletion Nuclide Adjustment	**YES**/NO	
Cooling Time	YES/**NO**	
Depletion Parameters		
Burnable Absorbers	**YES**/NO	
Integral Absorbers	**YES**/NO	
Soluble Boron	YES/**NO**	
Fuel and Moderator Temperature	**YES**/NO	
Power (	**YES**/NO	
Control rod insertion	**YES**/NO	
Atypical Cycle Operating History	YES/**NO**	
9.0 Criticality Safety Analysis of Spent Fuel Pool Storage Racks		
Rack model	**YES**/NO	
Boundary conditions	**YES**/NO	
Source distribution	**YES**/NO	
Geometry restrictions	**YES**/NO	Cell blocker configuration restriction.
Design Basis Fuel Description	**YES**/NO	
Fuel density	**YES**/NO	
Burnable Poisons	**YES**/NO	
Fuel assembly inserts	YES/**NO**	
Fuel dimensions	**YES**/NO	
Axial blankets	YES/**NO**	
Configurations considered	**YES**/NO	
Borated	YES/NO	
Unborated	YES/NO	
Multiple rack designs	YES/NO	
Alternate storage geometry	**YES**/NO	
Reactivity Control Devices		
Fuel Assembly Inserts		
Storage Cell Inserts		
Storage Cell Blocking Devices	**YES**	
Axial burnup shapes		
Uniform/Distributed	YES/**NO**	
Nodalization		
Blankets modeled		
Tolerances/Uncertainties		
Fuel geometry		
Fuel rod pin pitch	**YES**/NO	
Fuel pellet OD	**YES**/NO	
Cladding OD	**YES**/NO	
Axial fuel position	YES/**NO**	
Fuel content		
Enrichment	**YES**/NO	
Density	**YES**/NO	

Subject	Included	Notes / Explanation
Assembly insert dimensions and materials		
Rack geometry		
Flux-trap size (width)	**YES**/NO	
Rack cell pitch	**YES**/NO	
Rack wall thickness	**YES**/NO	
Neutron Absorber Dimensions	YES/**NO**	
Rack insert dimensions and materials		
Code validation uncertainty	**YES**/NO	
Criticality case uncertainty	**YES**/NO	
Depletion Uncertainty	**YES**/NO	
Burnup Uncertainty	YES/**NO**	
Biases		
Design Basis Fuel design	**YES**/NO	
Minor actinides and fission product worth	**YES**/NO	
Code bias	**YES**/NO	
Temperature	**YES**/NO	
Eccentric fuel placement	**YES**	
Incore thimble depletion effect	YES/**NO**	
NRC administrative margin	**YES**/NO	
Modeling simplifications		
Identified and described	**YES**/NO	
10.0 Interface Analysis		
Interface configurations analyzed	YES/**NO**	
Between dissimilar racks	YES/NO	
Between storage configurations within a rack	YES/NO	
Interface restrictions	**YES**/NO	Cell blocker configuration controls interface.
11.0 Normal Conditions		
Fuel handling equipment	YES/**NO**	
Administrative controls	**YES**/NO	
Fuel inspection equipment or processes	YES/**NO**	
Fuel reconstitution	**NO**	
12.0 Accident Analysis		
Boron dilution	YES/**NO**	
Normal conditions	YES/NO	
Accident conditions	YES/NO	
Single assembly misload	YES/**NO**	
Fuel assembly misplacement	**YES**	
Neutron Absorber Insert Misload	YES/**NO**	
Multiple fuel misload	YES/**NO**	
Dropped assembly	**YES**/NO	
Temperature	**YES**/NO	
Seismic event/other natural phenomena	**YES**/NO	
13.0 Analysis Results and Conclusions		
Summary of results	**YES**/NO	
Burnup curve(s)	YES/**NO**	
Intermediate Decay time treatment		

Subject	Included	Notes / Explanation
New administrative controls	**YES**/NO	
Technical Specification markups	YES/**NO**	
14.0 References		
Appendix A: Computer Code Validation:		
Code validation methodology and bases	**YES**/NO	
New Fuel	**YES**/NO	
Depleted Fuel	**YES**/NO	
MOX	**YES**/NO	
HTC	**YES**/NO	
Convergence	**YES**/NO	
Trends	**YES**/NO	
Bias and uncertainty	**YES**/NO	
Range of applicability	**YES**/NO	
Analysis of Area of Applicability coverage	**YES**	

Supplement 1

NMP SFP BORAFLEX™ Rack to BORAL™ Rack Engineering Judgement Technical Justification

S1.1 Introduction

The criticality safety analysis in the main report (see Section 2.3.6) uses engineering judgement to conclude that the interface between the BORAFLEX™ racks and BORAL™ racks does not create a more reactive configuration than what has been analyzed for the cell blocker configuration in the BORAFLEX™ racks and the criticality analysis for the BORAL™ racks [S1-1]. The purpose of this Supplement 1 is to provide a more detailed discussion of the technical justification for that engineering judgement.

S1.2 Methodology

The following discussion provides the technical justification to support the engineering judgement that the interface between the BORAFLEX™ racks with cell blockers and the BORAL™ racks does not create a more reactive configuration than what has been evaluated in the main report for the BORAFLEX™ racks with cell blockers and the criticality analysis documented in [S1-1] for the BORAL™ racks.

Background

The NMP SFP has two BORAFLEX™ racks that are adjacent to each other (in N-S direction) in the southwest corner of the SFP. There are BORAL™ racks adjacent to the BORAFLEX™ racks along the east and north. The objective of the current application is to:

- Proactively remove BORAFLEX™ credit from these two BORAFLEX™ racks in a manner that is conservative (installation of cell blockers in one of every four locations to reduce reactivity in the BORAFLEX™ racks).
- Have the SFP in a configuration that applies the same TS as the BORAL™ racks (no changes are being made to the BORAL™ rack criticality analysis or TS) to the BORAFLEX™ racks.
- At the same time, it is desirable to maintain as many usable locations as possible in the BORAFLEX™ racks, therefore, leaving a full row of empty locations (with cell blockers) along the interface of the BORAFLEX™ racks and BORAL™ racks, a common method to separate racks neutronically, would be highly undesirable. Therefore, a specific configuration of cell blockers is evaluated.

The SFP configuration of the interface between the BORAFLEX™ racks and the BORAL™ racks is shown in the diagram below.

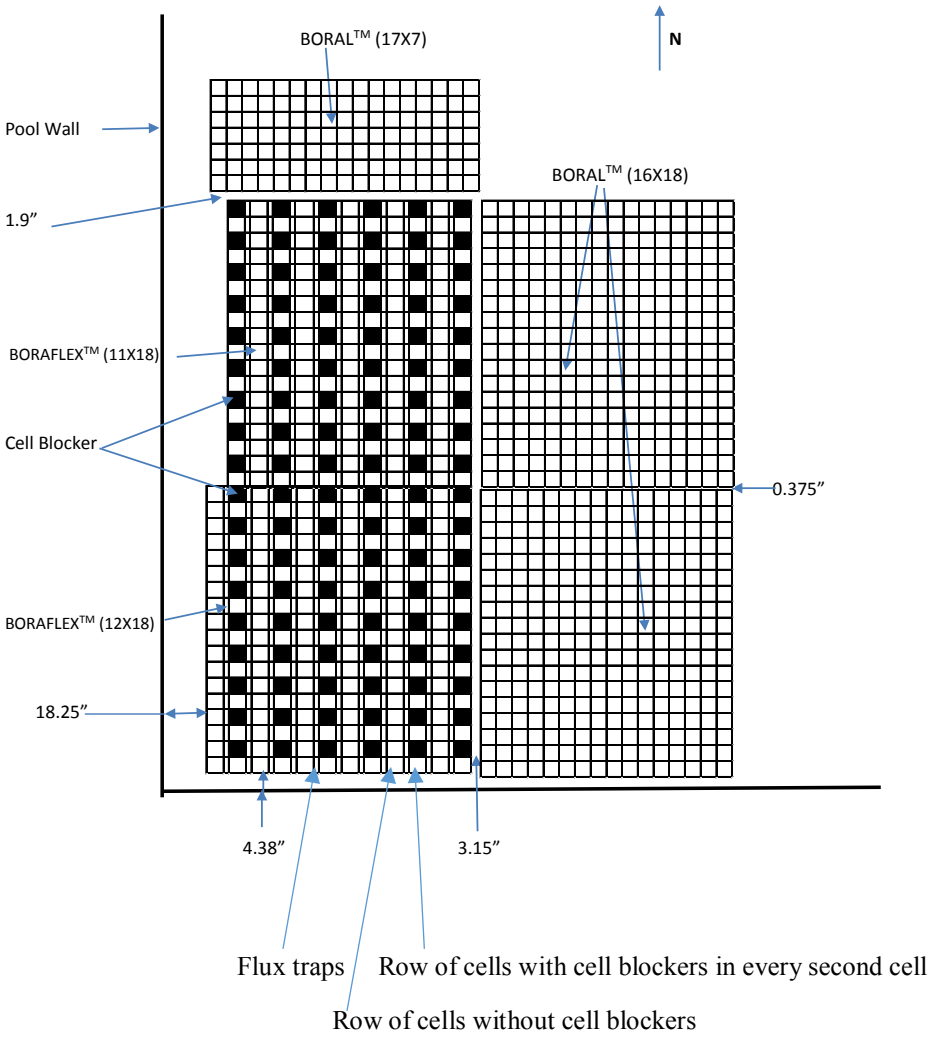

The following parameters are also relevant to the evaluation of the interface:

Parameter	BORAFLEX™ Racks	BORAL™ Racks
Cell ID, inches	5.899 (E-W), 5.87 (N-S)	5.9
Cell Pitch, inches	5.963 (not across flux trap), 7.712 (across flux trap)	6.06
Flux trap, inches	1.72 (includes box walls)	n/a
Poison material	BORAFLEX™ (not credited)	BORAL™
Rack exterior poison	None	poison present on exterior of racks along interface with BORAL™ racks
Reactivity effect of cell blockers.	~10% delta-k	n/a
Maximum k_{eff}[1]	0.9390	0.9348
TS requirement	Maximum enrichment of 4.6 wt% U-235 and SCCG < 1.31	

[1] Includes all analysis biases and uncertainties as well as including the most reactive fuel allowed.

Evaluation of the East-West Interface

The interface of the BORAFLEX™ racks and BORAL™ racks along the East-West interface is evaluated in the following manner:

- The two rack designs share a similar geometry along the interface, i.e. cell ID and cell pitch (as seen when comparing the exterior row from the BORAFLEX™ rack to the exterior row from the BORAL™ rack). Thus, for the purpose of this evaluation, each rack design may be considered an extension of the other along the interface.
- From the perspective of the BORAL™ rack:
    - There is an extra water gap between the exterior row of cells in the BORAL™ rack and the exterior row of cells in the BORAFLEX™ rack, i.e. the rack to rack gap forms a flux trap.
    - Due to the requirement of a cell blocker in every other location in the exterior row of the BORAFLEX™ rack, there is also an empty location in every other cell.
    - Beyond the exterior row the flux traps between rows of cells with and without cell blocker continue.
    - Thus from the viewpoint of the BORAL™ racks, the BORAFLEX™ racks are just a continuation, but with an additional flux trap as a separation, and where the fuel assemblies are separated by empty cells instead of neutron absorbers.
    - The two racks have nearly identically calculated maximum k_{eff} of about 0.94.
    - Hence it can be concluded that along the East-West interface the BORAFLEX™ racks will not increase the reactivity of the BORAL™ racks.
- From the perspective of the BORAFLEX™ racks:
    - There is a poison panel after a large flux trap which is formed by the rack to rack gap (i.e. the rack to rack gap is about twice the size of the BORAFLEX™ flux traps).
    - Due to the requirement of a cell blocker in every other location in the exterior row of the BORAFLEX™ rack, there is also an empty location in every other cell. Thus, the exterior row of the BORAL™ racks may also contain a full row of fuel, similar as if it were a continuation of the BORAFLEX™ racks.
    - Thus from the viewpoint of the BORAFLEX™ racks, the BORAL™ racks are just a continuation, just with a larger flux trap and added neutron absorber.
    - The two racks have nearly identically calculated maximum k_{eff} of about 0.94.
    - Hence it can be concluded that along the East-West interface the BORAL™ racks will not increase the reactivity of the BORAFLEX™ racks.

Evaluation of the North-South Interface

The interface of the BORAFLEX™ racks and BORAL™ racks along the North-South interface is evaluated in the same manner as the East-West interface with the same conclusions while also including the following *additional* consideration:

- The flux traps within the BORAFLEX™ racks creates a much larger pitch, which further reduces reactivity.

- The rack to rack gap along the North-South interface is smaller than the rack to rack gap along the East-West interface, however, it is still larger than the flux trap within the BORAFLEX™ racks.

Additional Considerations

- SFP Moderator Temperature
  - The analysis of the BORAFLEX™ racks with cell blockers considers that the BORAFLEX™ has completely degraded away.
  - The analysis therefore considers the maximum SFP temperature since this yields the most reactive moderator temperature for un-poisoned racks.
  - The reactivity difference between the minimum SFP temperature and maximum SFP temperature is 0.0144 delta-k.
  - The BORAL™ racks consider the minimum SFP temperature to be bounding due to the presence of the BORAL™.
  - Due to the BORAL™ panel along the exterior of the BORAL™ rack, the bounding moderator temperature is the minimum temperature along the interface.
  - Thus, along the interface, it may be concluded that the reactivity of the fuel in the exterior row of the BORAFLEX™ racks is significantly lower than the fuel in the interior of the BORAFLEX™ racks.
- Eccentric Positioning
  - The bounding configuration in the BORAFLEX™ racks with cell blockers is all fuel positioned as close to the center of the rack module as possible.
  - The analysis considers the reactivity effect of the bounding eccentric position of the fuel as a 0.0182 bias (compared to cell centered).
  - The large increase in reactivity for this bias indicates that the maximum reactivity location in the BORAFLEX™ racks is in the center of the rack modules.
  - Therefore, this supports the conclusion that the exterior of the BORAFLEX™ racks are a low reactivity region.

S1.3 References

[S1-1] HI-92793R4, "Fuel Criticality Analysis for Nine Mile Unit 1".

S1.4 Conclusion

The technical evaluation presented in Section S1.2 demonstrate that the geometry of the BORAFLEX™ racks with cell blockers creates a low reactivity configuration along the interface between the BORAFLEX™ racks and BORAL™ racks. Furthermore, the additional considerations discussion further support this evaluation. Therefore, the conclusion can be made that the interface between the BORAFLEX™ racks and BORAL™ racks in the SFP is an area of low reactivity that does not affect the reactivity calculated for each of those rack without any neighbor across the interface. Hence the interface condition is bounded by the evaluations for the individual racks, and no further evaluations are required.

ATTACHMENT 5

License Amendment Request

Nine Mile Point Nuclear Station, Unit 1

Docket No. 50-220

Holtec International Affidavit, Document Number AFF-2698-001 Revision 0,
"Affidavit to Withhold Proprietary HI-2178001."

AFFIDAVIT PURSUANT TO 10 CFR 2.390

I, Kimberly Manzione, being duly sworn, depose and state as follows:

(1) I have reviewed the information described in paragraph (2) which is sought to be withheld, and am authorized to apply for its withholding.

(2) The information sought to be withheld is information provided in Holtec Report HI-2178001R0, which contains Holtec Proprietary information.

(3) In making this application for withholding of proprietary information of which it is the owner, Holtec International relies upon the exemption from disclosure set forth in the Freedom of Information Act ("FOIA"), 5 USC Sec. 552(b)(4) and the Trade Secrets Act, 18 USC Sec. 1905, and NRC regulations 10CFR Part 9.17(a)(4), 2.390(a)(4), and 2.390(b)(1) for "trade secrets and commercial or financial information obtained from a person and privileged or confidential" (Exemption 4). The material for which exemption from disclosure is here sought is all "confidential commercial information", and some portions also qualify under the narrower definition of "trade secret", within the meanings assigned to those terms for purposes of FOIA Exemption 4 in, respectively, Critical Mass Energy Project v. Nuclear Regulatory Commission, 975F2d871 (DC Cir. 1992), and Public Citizen Health Research Group v. FDA, 704F2d1280 (DC Cir. 1983).

AFFIDAVIT PURSUANT TO 10 CFR 2.390

(4) Some examples of categories of information which fit into the definition of proprietary information are:

a. Information that discloses a process, method, or apparatus, including supporting data and analyses, where prevention of its use by Holtec's competitors without license from Holtec International constitutes a competitive economic advantage over other companies;

b. Information which, if used by a competitor, would reduce his expenditure of resources or improve his competitive position in the design, manufacture, shipment, installation, assurance of quality, or licensing of a similar product.

c. Information which reveals cost or price information, production, capacities, budget levels, or commercial strategies of Holtec International, its customers, or its suppliers;

d. Information which reveals aspects of past, present, or future Holtec International customer-funded development plans and programs of potential commercial value to Holtec International;

e. Information which discloses patentable subject matter for which it may be desirable to obtain patent protection.

The information sought to be withheld is considered to be proprietary for the reasons set forth in paragraphs 4.a, 4.b, and 4.e above.

(5) The information sought to be withheld is being submitted to the NRC in confidence. The information (including that compiled from many sources) is of a sort customarily held in confidence by Holtec International, and is in fact so held. The information sought to be withheld has, to the best of my knowledge and belief, consistently been held in confidence by Holtec International. No public disclosure has been made, and it is not available in public sources. All disclosures to third parties, including any required transmittals to the NRC, have been made, or must be made, pursuant to regulatory provisions or proprietary agreements which provide for

AFFIDAVIT PURSUANT TO 10 CFR 2.390

maintenance of the information in confidence. Its initial designation as proprietary information, and the subsequent steps taken to prevent its unauthorized disclosure, are as set forth in paragraphs (6) and (7) following.

(6) Initial approval of proprietary treatment of a document is made by the manager of the originating component, the person most likely to be acquainted with the value and sensitivity of the information in relation to industry knowledge. Access to such documents within Holtec International is limited on a "need to know" basis.

(7) The procedure for approval of external release of such a document typically requires review by the staff manager, project manager, principal scientist or other equivalent authority, by the manager of the cognizant marketing function (or his designee), and by the Legal Operation, for technical content, competitive effect, and determination of the accuracy of the proprietary designation. Disclosures outside Holtec International are limited to regulatory bodies, customers, and potential customers, and their agents, suppliers, and licensees, and others with a legitimate need for the information, and then only in accordance with appropriate regulatory provisions or proprietary agreements.

(8) The information classified as proprietary was developed and compiled by Holtec International at a significant cost to Holtec International. This information is classified as proprietary because it contains detailed descriptions of analytical approaches and methodologies not available elsewhere. This information would provide other parties, including competitors, with information from Holtec International's technical database and the results of evaluations performed by Holtec International. A substantial effort has been expended by Holtec International to develop this information. Release of this information would improve a competitor's position because it would enable Holtec's competitor to copy our technology and offer it for sale in competition with our company, causing us financial injury.

AFFIDAVIT PURSUANT TO 10 CFR 2.390

(9) Public disclosure of the information sought to be withheld is likely to cause substantial harm to Holtec International's competitive position and foreclose or reduce the availability of profit-making opportunities. The information is part of Holtec International's comprehensive spent fuel storage technology base, and its commercial value extends beyond the original development cost. The value of the technology base goes beyond the extensive physical database and analytical methodology, and includes development of the expertise to determine and apply the appropriate evaluation process.

The research, development, engineering, and analytical costs comprise a substantial investment of time and money by Holtec International.

The precise value of the expertise to devise an evaluation process and apply the correct analytical methodology is difficult to quantify, but it clearly is substantial.

Holtec International's competitive advantage will be lost if its competitors are able to use the results of the Holtec International experience to normalize or verify their own process or if they are able to claim an equivalent understanding by demonstrating that they can arrive at the same or similar conclusions.

The value of this information to Holtec International would be lost if the information were disclosed to the public. Making such information available to competitors without their having been required to undertake a similar expenditure of resources would unfairly provide competitors with a windfall, and deprive Holtec International of the opportunity to exercise its competitive advantage to seek an adequate return on its large investment in developing these very valuable analytical tools.

AFFIDAVIT PURSUANT TO 10 CFR 2.390

STATE OF NEW JERSEY)
) ss:
COUNTY OF CAMDEN)

Kimberly Manzione, being duly sworn, deposes and says:

That she has read the foregoing affidavit and the matters stated therein are true and correct to the best of her knowledge, information, and belief.

Executed at Camden, New Jersey, this 22nd day of December, 2017.

Kimberly Manzione
Licensing Manager
Holtec International

Subscribed and sworn before me this 22nd day of December, 2017.

Erika Grandrimo
NOTARY PUBLIC
STATE OF NEW JERSEY
MY COMMISSION EXPIRES January 17, 2022